RELEVANCE OF

COMPOSITION AND LOCALISATION

OF RAW RICE GRAINS

TO TEXTURE OF COOKED RICE

By

Noorhasifah Tengah

BSc, MSc.

Thesis submitted to the University of Nottingham

for the degree of Doctor of Philosophy

Division of Food Sciences

School of Biosciences

University of Nottingham

Loughborough

LE12 5RD

October 2015

ABSTRACT

Previous research has shown that the sticky behaviour of rice may be affected by the composition and structural properties of the rice starch (amylose and amylopectin) as well as the protein and lipid components. Analyses tend to have been based on whole rice grains even though the sticky texture of rice is largely a surface phenomenon; hence, it is essential to develop an understanding of the external composition of rice grains. The objective of this PhD project is to provide an analysis of the internal and external structure of raw rice grains and to investigate how these structure data correlate to the sticky behaviour of cooked rice. The results of Attenuated Total Reflectance – Fourier Transform Infrared spectroscopy show that there is a significant difference in amide and lipid peaks and order of starch between the centre of rice grains and the external regions while X-Ray Diffraction exhibit differences in starch crystallinity. Results of Fourier Transform Infrared microspectroscopy also demonstrated the non-uniformity of amide and lipid peaks across the cross-section of a rice grain. With the aid of chemical analysis, it was concluded that the sticky texture of cooked rice is negatively correlated to the external protein and lipid amount whereas the correlation to the order of starch and starch crystallinity was positive. This is further confirmed as the removal of protein and lipid from the surface of rice grains resulted in a more adhesive cooked rice texture. This project highlights the importance of a surface study when considering rice stickiness.

ACKNOWLEDGEMENT

Firstly, I would like to express my sincere gratitude to my supervisor, Prof Sandra Hill and Assoc Prof. Bettina Wolf for the continuous support of my PhD and related research, for their patience, motivation and immense knowledge. Prof Hill has always encouraged me, never giving up on me, even when I did not believe in myself. I could not imagine having a better advisor and mentor for my PhD study. My sincere thanks also goes to Dr Bill McNaughtan for helping me with the FTIR, XRD and NMR work conducted in this project.

I would like to express my deepest gratitude to my family, my parents, my brothers and sisters, my 9 niece and nephews for supporting me spiritually throughout writing this thesis and my life in general. Mum and dad, thank you for being loving and understanding despite having a daughter who is not married as well as not earning well at 28 years of age.

I would like to thank the My Space Gallery, Brunei staff for my 6 month work while I was tired of writing my thesis, Ms Yuri Aoki, Mr Moh Hack, Ms Vivian Chang, for giving me confidence again and offering me a job for sake of money and sanity.

I would like to thank my friends, Kutz and Yvonne for listening to my complaints, and my friends in food sciences, Deepa, Wenting, Heng, Nicole and Candy. We have drifted apart but I would like to say it goes unnoticed all the years we spent full of laughter, playing sports plus tears.

I would like to acknowledge the locations, Nottingham University, Keyworth library, Brunei Starbucks for giving me the perfect ambience for me to think, as well the therapists that I have seen, Nottingham University counselling team, Brunei counselling and Mr Todd, Riverview Clinic, Brunei.

I would like to thank my future husband, Alistair Grant and my future father-in-law, Iain Grant, for their continuous support and for providing me with food, shelter and care whilst I was struggling with my PhD.

I am very happy to have achieved this far despite all the challenges. Lastly, I would like to thank the Brunei Government (Ministry of Education) for providing me financial back-up for this PhD.

TABLE OF CONTENTS

LIST OF FIGURES

LIST OF TABLES

ABBREVIATIONS

AE	Amylose Equivalent
ATR	Attenuated Total Reflectance
CP-MAS	Cross Polarization - Magic Angle Spinning
DoBS	Dodecyl benzene sulfonate (DoBS)
FTIR	Fourier Transform Infrared Spectroscopy
FTIR-IRS	Fourier Transform Infrared-Internal Reflection Spectroscopy
HA	High Adhesiveness
IGC	Inverse Gas Chromatography
LA	Low Adhesiveness
NMR	Nuclear Magnetic Resonance
NV	Native (rice starch)
RVA	Rapid Visco Analyser
SEM	Scanning Electron Microscopy
SDS	Sodium dodecyl sulphate
SLS	Sodium lauryl sulphate
TA.XT	Texture Analyser XT
TPA	Texture Profile Analysis
WX	Waxy (rice starch)
XRD	X-Ray Diffraction

1. INTRODUCTION

1.1. PROJECT BACKGROUND

1.1.1. SPONSORS

This project was funded by the Ministry of Education, Brunei Darussalam. Independent since 1984 from the United Kingdom, Brunei Darussalam is a full sultanate monarchy country in Southeast Asia which has a high standard of living with a Gross Domestic Product, GDP, per capita of US$ 73 200 (CIA World Factbook, 2014). However, the chief source of the government's revenue is from crude oil and liquefied petroleum exports (70 % of GDP and more than 90 % of exports).

There are concerns that the depletion of oil reserves, or 'peak oil', will eventually damage the country's high standard of living. Therefore, in January 2008, His Majesty Sultan Haji Hassanal Bolkiah, Sultan of Brunei together with the Ministry of Industry and Primary Resources (MiPR) and the Brunei Economic Development Board (BEBD) authorised the launch of Brunei's National Vision 2035 in which one of the main aims is to attain a more dynamic and sustainable economy. In-order to reach this goal, several strategies have been set-up, one of which is food security.

1.1.2. BRUNEI RICE INDUSTRY

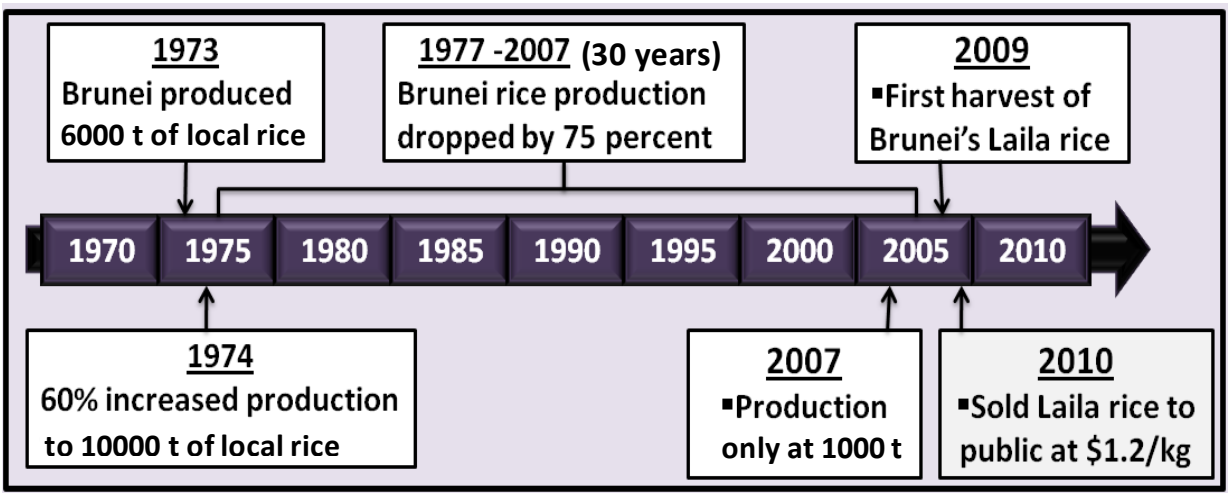

Figure 1. Timeline of Brunei's rice industry from 1970 to 2010.

The staple food of Brunei is rice; hence, Brunei's food security focuses mainly on local production of rice. Over a 30 year period, Brunei's rice production has plummeted from 10 kt in 1977 to 1 kt in 2007 (**Figure 1**). The launch of Brunei's National Vision 2035 prompted Brunei's Department of Agrifood to set a National Rice Production target of 18 000 tonnes, or 60 per cent self-sufficiency by 2015.

However, as of 2015, despite buying new paddy farming equipment and seeking expertise from Thailand, China and Vietnam, Brunei Ministry of Industry and Primary Resources, MiPR disclosed that the Sultanate missed its target of producing its own rice needs (**Figure 2**). The supply of rice in the country is still 3.2 % from local rice production and while an alarming 96.8 % is from imports from Thailand (Brunei Agrifood, 2010).

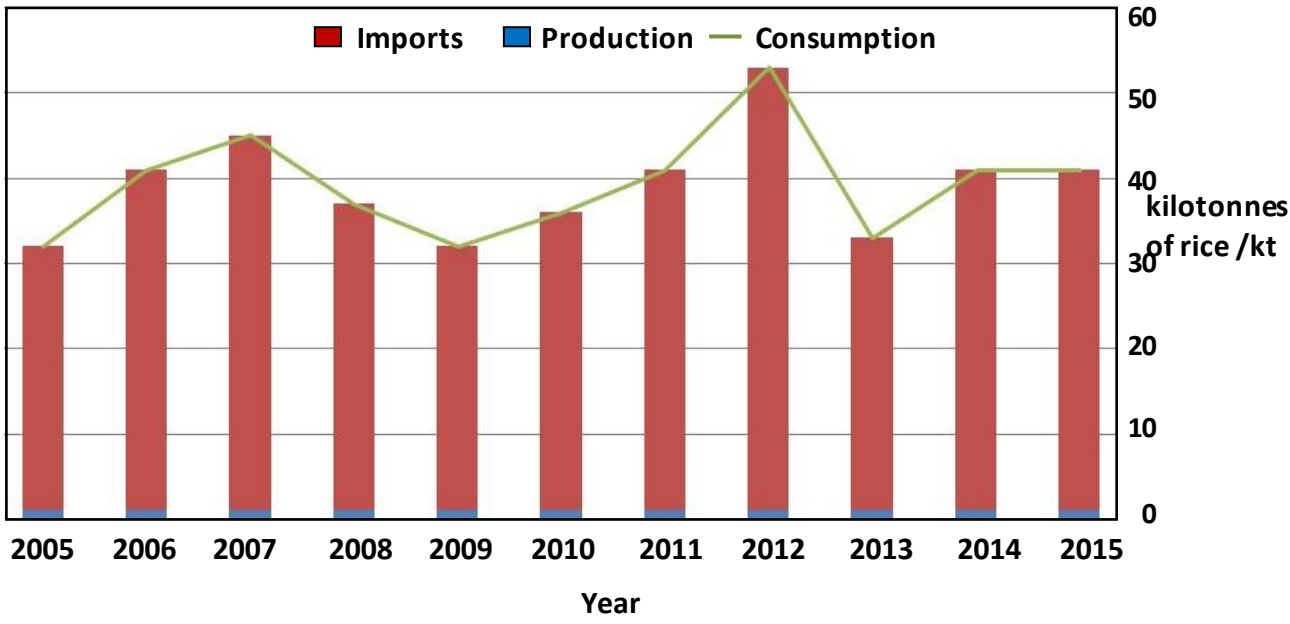

Figure 2. Brunei rice imports, local production and consumption from 2004 to 2015 (USDA, 2015).

Two of the main challenges to meet this goal are (i) shortage of local expertise in rice research and (ii) eating quality of Brunei local rice compared to imported varieties. To increase local expertise, the government has opened up Brunei Rice Farmers Field School (RFFS) as well sending postgraduates abroad to specialise in rice research. Current developments focus on the production of rice hybrids suitable for both growing on local soil and consumption for local consumers hinders mass production of rice. With the help of Assoc Prof. Bettina Wolf and Prof. Sandra Hill, the Brunei Ministry of Education agreed to fund a PhD project which aimed to investigate the eating quality of rice. Brunei's Laila rice, or Brunei Darussalam Rice 1, BDR1, has also been incorporated into this study. Laila rice is the first rice hybrid grown in Brunei and cooked Laila rice has a soft and slightly sticky texture, which is desirable to the Bruneian consumer.

1.2. AIMS AND OBJECTIVES

This PhD project aims to investigate the relevance of composition and localisation of raw rice grains to the sticky texture of cooked rice. This includes:

- Investigating the relationship between components of rice grains and adhesiveness of cooked rice,
- Development of methods to analyse the localisation of components, namely the external and internal components of a rice grain,
- Investigating the relationship between the localisation of starch crystallinity, order of starch, lipid and protein components, and cooked rice texture,
- Development of methods to remove lipid and protein components from the surface of rice grains, and
- Investigating the effect of the removal of protein and lipid from surface of rice kernels on the adhesiveness of cooked rice.

1.3. STRUCTURE OF THESIS

The structure of this thesis is as follows: **Chapter 2** provides a background on rice, its components and published scientific evidence on factors which contributes to texture of cooked rice. **Chapter 3** discusses the preparation of samples and analytical and composition analysis techniques used in this project. **Chapter 4** explains how the evaluation of cooked rice texture was developed in this study and the selection of rice varieties to be used throughout this project. This is followed by **Chapter 5** where the composition of the chosen raw rice varieties was studied, in

relation to their cooked textural properties. **Chapter 6** investigated the localisation of components on the surface and central regions of raw rice grains and its relation to the textural properties of cooked rice. **Chapter 7** confirmed whether alteration of surface properties has any effect on the adhesiveness of the cooked rice grains. Finally, **Chapter 8** includes the general discussion, conclusions and possible future studies that can be followed up from this project.

CHAPTER 2. LITERATURE REVIEW

This chapter aims to provide a background on (i) rice: the rice grain structure, its composition, starch and crystalline structure, and (ii) how the different compositions of raw rice grains contribute to the texture of cooked rice.

2.1. RICE

Rice, *Oryza sativa* L. is a cereal grain which is a rich carbohydrate source and provides over 20 % of the world's kilocalorie supply and 70 % of the daily energy intake in Asia (Fitzgerald *et al*, 2009).

2.1.1. RICE GRAIN STRUCTURE

The structure of a rice grain can be divided into; husk, bran, starch and embryo (**Figure 3**). The husk is the inedible, hard outer coating of the rice grain which is usually used for animal feed and alternative fuel. Removal of the husk after milling exposes the bran, which is the outer layer of brown rice and the removal of bran produces white rice. The starchy endosperm, which is the edible part of the rice grain, mostly consists of starch (90 % of dry matter) while the rest are protein (7 %), lipid (0.5 %), fibre (0.5 %) and ash (0.8 %). Rice starch is the smallest amongst all starch types, such as potato and wheat, with a size range of 3-8 µm (Juliano, 1985).

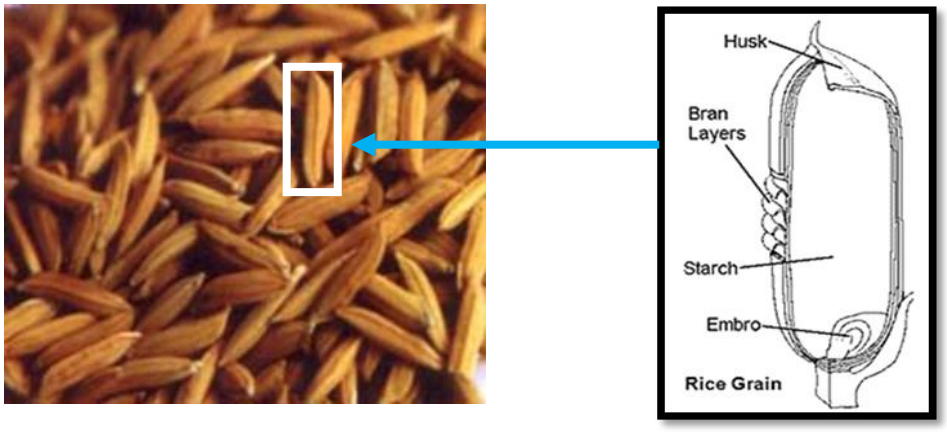

Figure 3. Structure of a rice grain, showing husk, bran, starch and embryo layers (Adapted from International Starch Institute, 2016).

2.2. STARCH

Starch is a storage polysaccharide found in plant tissues and plays an important role in the human diet. The two main components are the polysaccharides amylose and amylopectin. The ratio of the two polymers depends on its source but the typical amylose content of starch is 25 % and amylopectin 75 % (Tomasik, 2003).

2.2.1. AMYLOSE AND AMYLOPECTIN

Amylose is the smaller polysaccharide which is linear and mainly made up of 1 → 4 linked α-D-glucopyranosyl units (Tomasik, 2003). Amylopectin is the larger polysaccharide which is highly branched and contains α (1→4)-linked D-glucopyranosyl units and α (1→6) bonds (**Figure 4**). The α (1→4)-linked D-glucopyranosyl can be classified into A, B and C chains (**Figure 6C**).

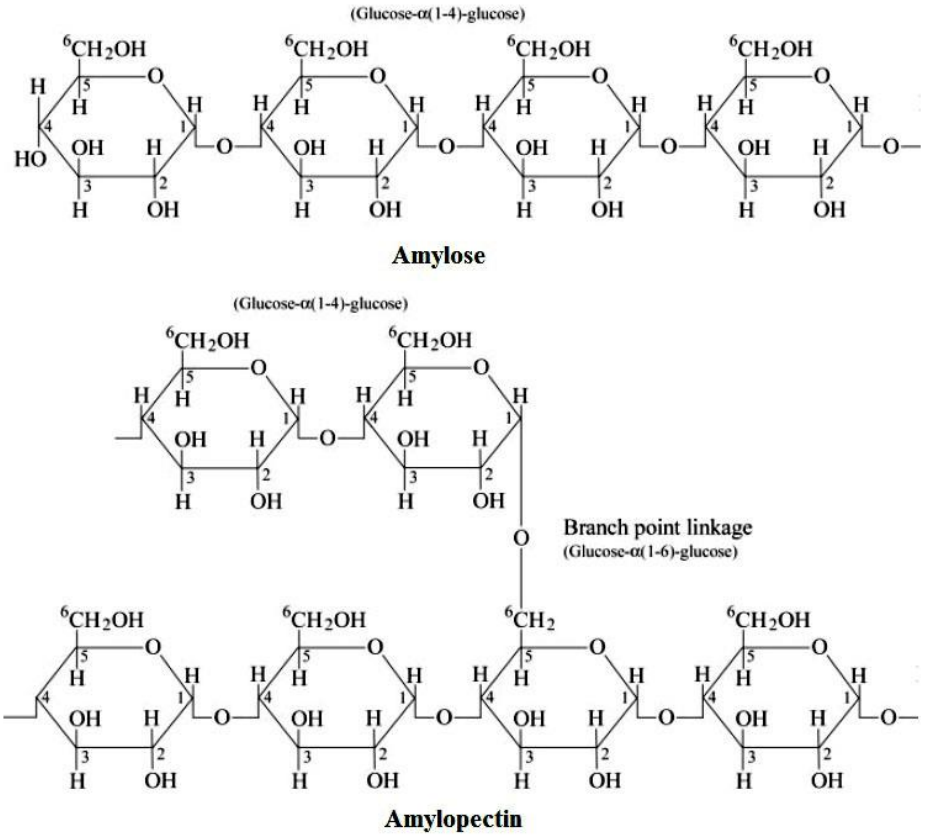

Figure 4. Amylose and amylopectin structure (Buleon *et al*, 1998).

One of the interesting characteristics of amylose is its ability to form complexes with a variety of organic compounds, such as alcohols, lipids and iodine. This is the result of the single helical structure of the amylose molecule, creating an internal helical space where hydrophobic molecules, hydrophobic side chains of molecules can be located as ligands (Obiro *et al*, 2012). Amylose forms a deep blue colour in the presence of Iodine - KI Reagent. Iodine is not very soluble in water; therefore iodine reagent is made by dissolving iodine in water (**Figure 5A**) in the presence of potassium iodide (**Figure 5B**). This makes a linear triiodide ion complex with is soluble. The triiodide ion slips into the coil of the starch causing an intense blue-black colour (**Figure 5C**).

(A)	KI	+	H_2O	→	K^+	+	I_2
	potassium iodide	+	water	→	potassium ion	+	iodine
(B)	I^-	+	I_2	→	I_3		
	iodide ion	+	iodine	→	triiodide ion		
(C)	I_3	+	amylose	→	triiodine-amylose complex		
	triiodide ion	+		→	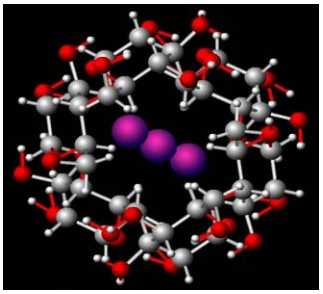		

Figure 5. Principle behind the formation of amylose-iodine complex (Whistler *et al*, 2012).

2.2.2. V-AMYLOSE

Amylose is a single helix which possess a relatively hydrophobic inner surface that holds spiral of water molecules, which is easily lost to be replaced by hydrophobic lipid to form V-type structure, with the helical inclusion complexes generically known as V-amylose (Obiro *et al*, 2012). The V-amylose form compounds with alcohols, fatty acids, potassium hydroxide, iodine, flavour compounds and hydrophobic organic polymers. It is usually used in modification of starch functionality, in this case rice starch/flour texture and pasting properties.

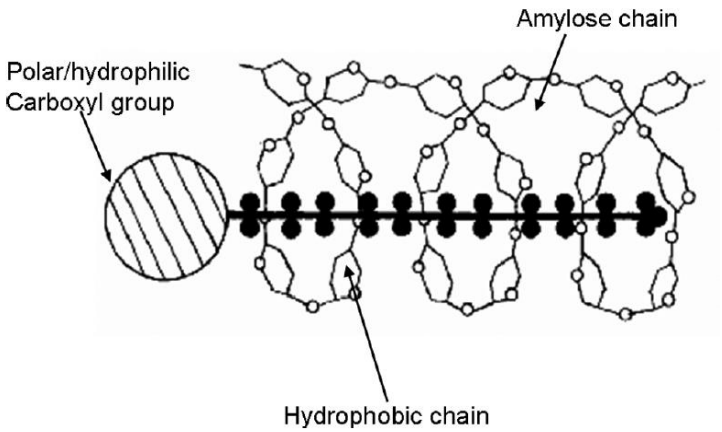

Figure 6. Schematic illustration of monostearin-amylose helical complex with the whole chain inside the helical space (Obiro *et al*, 2012).

2.2.3. DETERMINATION OF AMYLOSE CONTENT

There are several methods to measure amylose content, which includes measuring absorbance of the amylose-iodine complex, concanavalin A binding method, various near infrared (NIR) methods, differential scanning calorimetry, size exclusion chromatography and asymmetric flow field flow fractionation (Fitzgerald *et al*, 2009). A recent review of the different methods by Zhu *et al*, 2008 concluded that the spectrophotometric iodine technique, or amylose leaching, is the most commonly used technique and the rest of the methods are not applicable for routine use and produce different values of amylose content.

Over the decades, there have been several changes made to the amylose leaching method, which includes preparation of samples, standard type (purified amylose or potato amylose) and wavelength (590 - 650 nm) used. The determination of amylose and amylopectin content in this project focuses on Megazyme amylose/amylopectin ratio assay, which utilises the Concanavalin A binding method and soluble starch assay, which is a modified version of amylose leaching.

2.3. STARCH GRANULE ORGANISATION

2.3.1. CONCENTRIC GROWTH RINGS

Starch granule is organised as concentric growth rings which are of 120-400 nm thick (French, 1984). These concentric growth rings can be divided into amorphous and semi-crystalline growth rings (**Figure 6A**).

2.3.2. SEMI-CRYSTALLINE GROWTH RINGS

The semi-crystalline growth rings can then be divided further into amorphous lamellae and crystalline lamellae (**Figure 6B**). It is suggested that crystallinity is mostly due to amylopectin and that the amylopectin were in radial arrangement in the semi-crystalline growth ring (Robin *et al*, 1975).

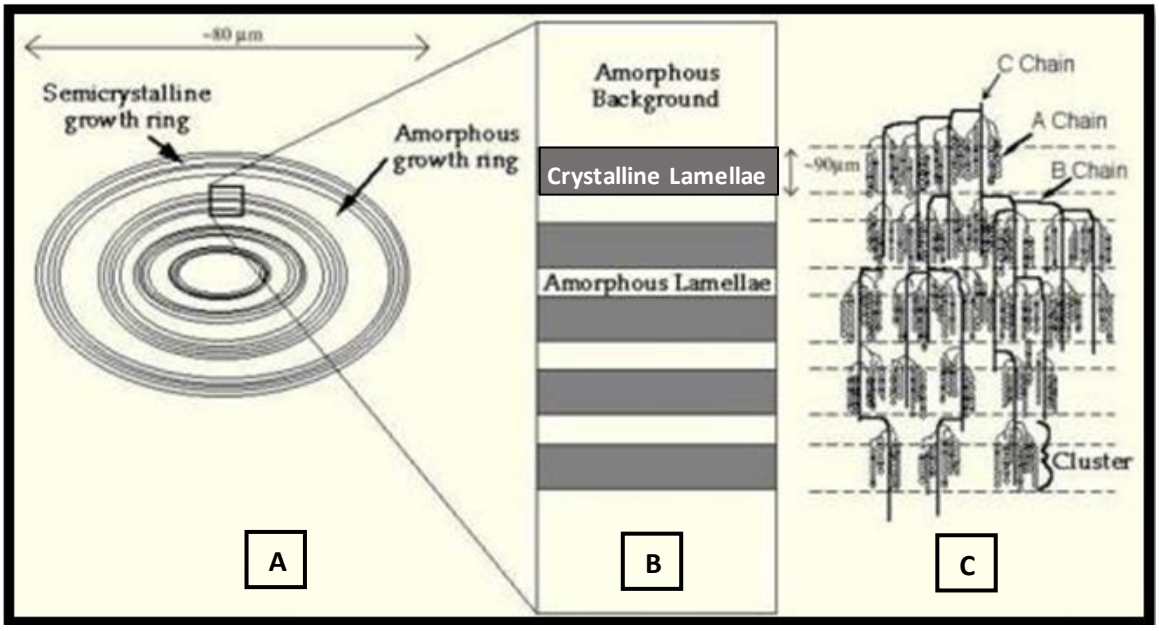

Figure 7. Organisation of the starch granule (Donald *et al*, 1997), showing semi-crystalline and amorphous growth rings, and how it breaks down to crystalline lamellae, amorphous lamellae, and A, B, C chains.

Each amylopectin molecule contains a million or so residues, about 5 % of which form the branch points. Amylopectin chains consists of A-chains, B-chains and C-chains. A-chains are the 'outer' unbranched chains which generally consist of between 13-23 residues. B-chains are the 'inner' branched chains. There are two main fractions of long and short internal B-chains with the longer chains (greater than about 23-35 residues) connecting between clusters and the shorter chains similar in length to the terminal A-chains. C-chain contains a single reducing group.

2.3.3. STARCH CRYSTALLINITY

The degree of starch crystallinity, which is defined as the percentage of the crystalline regions with respect to the total material, has been intensively studied using X-ray diffraction, XRD (Lopez-Rubio *et al*, 2008, Frost *et al*, 2009). Attenuated Total Reflectance Fourier Transform Infrared, ATR-FTIR has been used to determine the order of starch, which is the ratio of the crystalline and amorphous structures (van Soest *et al*, 1994, 1999, Sevenou *et al*, 2002).

2.3.4. STARCH CRYSTALLINE LATTICE

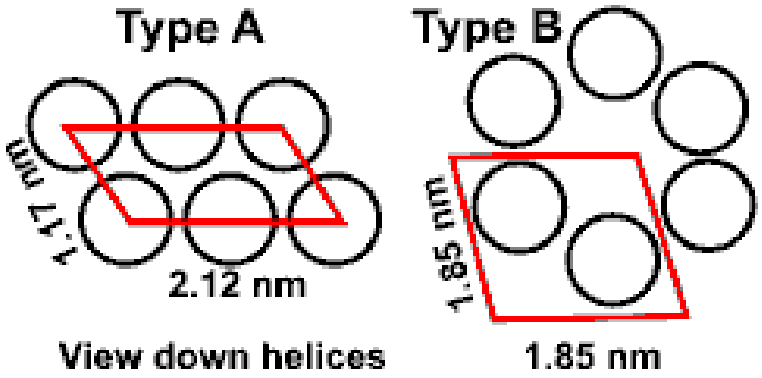

Figure 8. Starch crystalline structure of monoclinic type A and hexagonal type B (Buleon *et al*, 1997)

Starch crystalline can be divided into 3 types; Type A, Type B and Type C crystallites. Type A crystallite (Figure 8) is denser with a staggered monoclinic packing. Type A has unbroken chain lengths of about 23-29 glucose units is found in most cereals, including rice and maize. Type B crystallite is more open hydrated and hexagonal, with slightly longer broken chain length of about 30 – 44 glucose units. Type B is mostly found in tubers such as potato and high amylose cereal starches. Type C structure is a combination of Types A and B and found in peas and beans.

2.4. STARCH CONVERSION

2.4.1. GELATINISATION

When starch is heated above 60 °C in water, water enters the amorphous region of starch, causing starch to swell. This leads to stress on the crystalline region which results in the disruption of the crystalline region. Starch granules burst, the crystalline structure of starch is lost and starch leaches into water. This process is called 'gelatinisation'.

2.4.2. RETROGRADATION

When viscous gelatinised solution is allowed to cool for a certain period of time, the amylose and amylopectin rearrange themselves to form crystalline structure, hence, gel formation, in a process termed as 'retrogradation'.

2.4.3. STARCH PASTING PROPERTIES

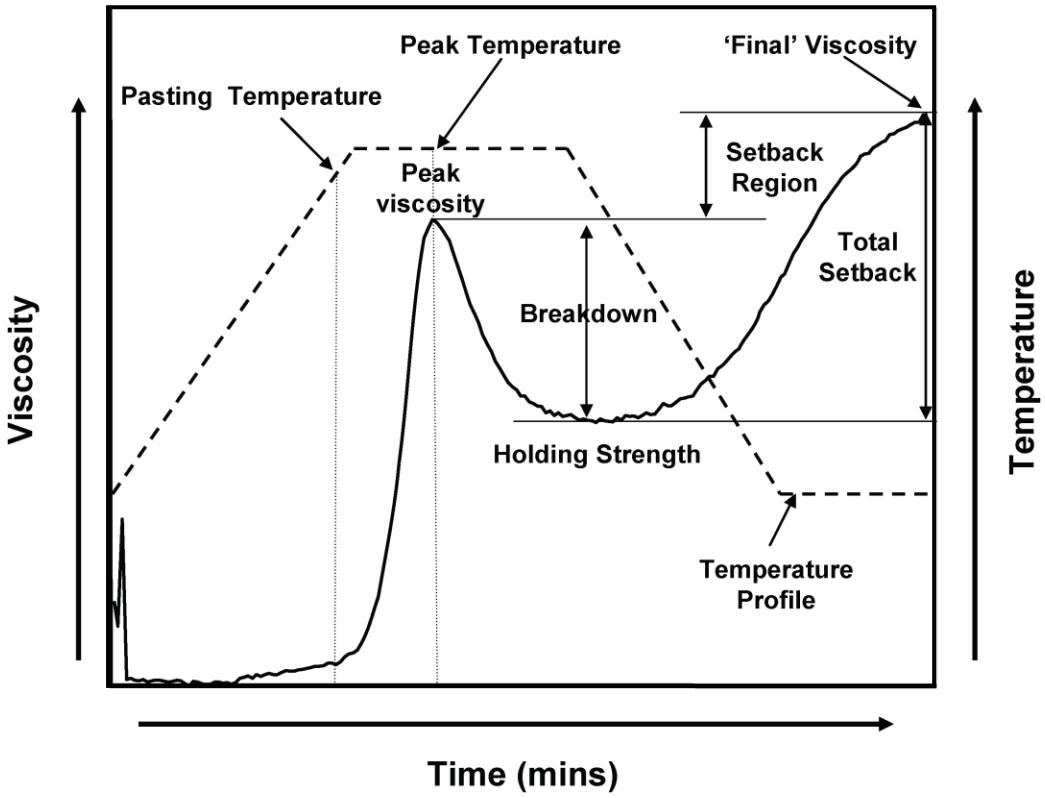

Figure 9. Starch pasting properties, showing pasting temperature, peak viscosity, breakdown, holding strength, final viscosity (Ascheri *et al*, 2012).

As temperature is increased over time, starch is mixed with hot water and swells. At peak temperature, starch granule swells to reach its maximum viscosity, called 'peak viscosity'. This is the highest viscosity achieved by sample during initial heating. It is the equilibrium point between swelling and polymer leaching. After a certain amount of time, starch granule burst and undergoes breakdown until it reaches 'holding strength' which is an indication of how much breakdown the starch can withstand. This results in a decrease in viscosity. This is the minimum

viscosity after peak when sample has leached. This is an indicative of samples ability to withstand heating and shear.

Finally, as starch granule is cooled down, viscosity increases until reaches 'final viscosity'. This possibly involves retrogradation of starch. The difference between final viscosity and holding strength is called 'total setback' as it represents how much viscosity has increased and re-association of starch components (amylose and amylopectin) to form retrograded material.

2.5. RICE EATING QUALITY

Public perception of rice eating quality includes external appearance, colour, flavour, aroma and texture. Rice texture is a principal consideration for consumer acceptability and palatability. There are several attributes that can be used to describe rice texture, this includes hardness, cohesiveness, firmness and stickiness or adhesiveness as well as moistness to touch. The eating quality of cooked rice is most commonly measured by its textural properties; hardness and stickiness (Okabe, 1979). This project only concerns the sticky behaviour of rice.

2.5.1. RICE STICKINESS AND QUANTIFICATION

Stickiness of rice is defined as 'work necessary to overcome the attractive forces between surface of food and the materials with which it comes into contact' (Mestres *et al*, 2011). Stickiness is a difficult attribute to measure and is defined as 'force of adhesion when two surfaces in contact with each other'. There are several terms which can be associated with stickiness which includes 'adhesiveness',

'cohesiveness', 'stringiness' and 'tackiness'. Quantification of rice stickiness has been performed with sensory and instrumental methods. Instrumental methods include the texture analyser (Ayabe *et al*, 2009) and instron tester. The most commonly used instrument is the texture analyser and this study uses texture analysis for measuring rice stickiness.

2.6. ORIGINS OF RICE STICKINESS

There are several hypothesised origins of rice stickiness. This includes amylose and amylopectin content, parboiling and storage of rough rice. Cameron and Wang, 2005 reported the sticky behaviour of rice may be affected by the composition and structural properties of the rice starch (amylose and amylopectin) as well as the protein and lipid components.

2.6.1. AMYLOSE CONTENT AND RICE STICKINESS

In the mid-eighties, it was initially proposed that the most important determinant of the eating quality of rice is the amylose content, or amylose equivalent (AE) (Juliano, 1985). Later, Bhattacharya *et al*, 1982 proposed that 'hot-water-insoluble AE' is the key determinant of rice quality and demonstrated that soluble amylose does not play a role in eating rice quality. Reddy *et al*, 1993 proposed that the fine structure of amylopectin contributes to rice texture and the hot water insoluble AE is the only method to measure this. Further researchers (Ayabe *et al*, 2009, Patindol *et al*, 2010) have concluded that the sticky behavior of cooked rice is solely contributed by amylopectin and not by amylose.

2.6.2. AMYLOPECTIN CONTENT AND RICE STICKINESS

Reddy *et al*, 1993 proposed that the fine structure of amylopectin contributes to rice texture and the insoluble AE is the only method to measure this. Hence, the research on the origin of rice texture has shifted from amylose to amylopectin. Reddy *et al*, 1993 concluded that not only the amount of amylopectin fine structure plays a role, but more specifically, the number of long and short chains in the interior and on the exterior of the molecule. **Table 1** shows a compilation of literature relating to the origins of the sticky behaviour of rice, in terms of amylose-amylopectin content and amount of amylose leached.

A recent study by Ayabe *et al*, 2009 concluded that more short and long amylopectin chains and less amylose content in the surface of cooked rice contribute to rice stickiness. It can be concluded that surface property of the rice starch plays a major role in the sticky texture of rice, in terms of amylose/amylopectin content and position. Hence, it is an area worth investigating. This project focuses on the relevance of the surface properties of rice to its texture.

2.6.3. SURFACE OF STARCH AND RICE STICKINESS

Bielinski *et al*, 2003 started a preliminary study on the surface layer of starch using FTIR-IRS, inverse gas chromatography (IGC) and scanning electron microscopy (SEM). The study concluded that the higher the amylopectin content of starch, the more crystalline it is and the crystallinity of the surface layer is higher than in the bulk of the material. This thesis uses ATR-FTIR for surface analysis because several

authors (Sevenou *et al*, 2002, Bielinski *et al*, 2003) used the technique to study the order of the starch surface.

Table 1. Compilation of literature, relating to the origins of sticky behaviour of rice and amylose-amylopectin content.

Year	Author	Comments
1993	Reddy *et al*	▪ **Fine structure of amylopectin** is key determinant. ▪ **Hot water insoluble Amylose Equivalent, AE** is a reflection of this fine structure, and it is the only index which reflects amylopectin fine structure. ▪ **High Insoluble-AE rice**: Contains a large number of long, unbranched chains in the exterior of the molecule, which leads to strong and elastic starch granules and hence, firm, dry, **non-sticky cooked rice**. ▪ **Low-AE rice**: Contains few long chains, and are mostly in the interior, which leads to weak and fragile granules and hence, soft, moist and **sticky cooked rice**.
2003	Bielinski *et al*	▪ The higher amylopectin content of starch, the more crystalline it is. ▪ The higher amylopectin content leads to more amylose segregation onto the surface of starch. ▪ Crystallinity of the surface layer is higher than in the bulk of the material.
2005	Cameron and Wang	▪ The higher the amount of leached amylose, the harder the rice. ▪ Amylose content does not correlate with cooked rice texture, but the ratio of A and short B chains to long B chains of amylopectin does.
2009	Ayabe *et al*	▪ **More short and long amylopectin** and **less amylose** content in the surface of cooked rice contributes to rice stickiness.
2010	Patindol *et al*	▪ Sticky rice **leached out more amylopectin than amylose** while dry rice leached out more amylose. ▪ Cooked rice **hardness is contributed by amylose** while cooked rice **stickiness is contributed by amylopectin.**

2.6.4. PROTEIN AND RICE TEXTURE

Protein accounts for 7 – 8 % in the milled kernel. Protein in milled rice kernel can be classified into four types: (i) alkali soluble glutelins, which accounts for 80 % of the total rice protein, (ii) salt soluble globulins (7 – 15 %), water soluble albumins (9 - 11%) and alcohol soluble prolamins, which is 2 – 4 % of rice protein (Landers and Hamaker, 1994). Lim *et al*, 1999 used an auto-Kjeldahl system (Kjeltec Auto 1030 Analyzer, Tecator, Sweden) to determine the protein content in rice flours, while the isolated protein was determined by a biuret test, using albumin as the standard.

Several authors (Juliano and Pascual, 1980, Cameron and Wang, 2005) have reported that the protein content of rice is negatively correlated with the stickiness of cooked rice. Chrastil (1992) showed that changes in cooked rice functional properties during storage resulted from the increase in disulphide bonding of rice proteins during storage. Hamaker and Griffin (1990) reported the role of proteins in dictating rice stickiness. Stickiness of cooked rice was increased when rice was cooked in water containing dithiothreitol, a compound known to disrupt proteins. Saleh and Meullenet (2007) concluded that protease treatment decreased the firmness of rice.

Marshall *et al*, 1990 reported that the partial removal of lipid or protein from rice kernels resulted in significant changes in starch gelatinisation. Shibuya and Iwasaki (1982) studied the effect of proteolytic enzymatic treatment on the gelatinisation properties of rice flour in aged and non-aged rice. Enzymatic treatment resulted in softer and stickier rice flour compared with non-treated rice. All of these studies

have suggested a negative correlation between protein content of rice grains and cooked rice texture. This means a decreased amount of rice protein present results in stickier rice texture.

Rice protein in the endosperm is tightly bound to the surface of starch granules and the difficulty in removing the protein makes the starch isolation more costly compared to other starches (Tanaka *et al*, 1980). Heterogeneous large molecules of glutelins exist inside the rice endosperm in the form of protein bodies. These spherically shaped protein bodies bind strongly to the compound starch granules with strong disulphide bonds and/or hydrophobic bonds (Tanaka *et al*, 1978).

To isolate rice starch, alkaline solvents, surfactants or protein hydrolysing enzymes are used to remove rice protein from rice flour. Alkaline solvents such as NaOH and surfactants such as dodecylbenzene sulfonate (DoBS) and sodium lauryl sulphate (SLS) are commonly used in the protein extraction for starch isolation. These solvents destroy the oligomeric protein structures and transform them to the soluble form. In the case of surfactants, complete removal of the surfactant from the starch is, often not easy. Pronase treatment does not damage starch granules due to enzyme specificity, but the enzyme is expensive and the purity of the isolated starch is relatively low.

Juliano and Boulter (1976) reported that protein extraction reached 94 – 94 % with 0.1 N NaOH and 0.5 % sodium dodecyl sulphate (SDS) solution containing β-mercaptoethanol (0.6 %). But the alkali and protein denaturing agents may alter the granular structure of starch, affecting the physical properties of starch. Lee *et*

al, 1999 reported successful protein extraction solution using 1.2 % DoBs, 0.2 % NaOH and 1.2 % sodium sulphite.

2.6.5. LIPID AND RICE TEXTURE

Lipids in rice can be divided into (i) non-starch bound lipids (unbound lipid) and (ii) starch lipids (bound lipids). The percentage of lipids in rice is only about 0.5 - 1.0%. Starch lipids are present in relatively low concentrations and primarily complexed with amylose. Lipids in rice are suggested to contribute to the texture of rice. Eliasson and Krog (1985) and Biliaderis and Tonogai (1991) reported that complexing of lipids (free fatty acids) with amylose (referred as LAM complex) contributed to the rigidity of rice and resulted in increasing the firmness of cooked rice texture. Parboiled rice contains a higher concentration of amylose-lipid complex II (Biliaderis *et al*, 1993) which explains the hard texture of cooked rice (Juliano, 2005).

Lipids are added to cooked rice products, such as coconut milk to waxy rice cake, ghee or oil to cooked rice, to coat milled rice surface and reduce the stickiness of cooked rice (Juliano, 1983). From these studies, it can be hypothesised that there is negative correlation between rice lipid content and cooked rice adhesiveness. This means that decreased amount of non-starch lipid content in raw rice grains result in a more adhesive rice texture.

Total rice lipids is usually determined by hydrolysis, non-starch lipids are determined by extraction by 2:1 chloroform methanol and starch lipids determined by extraction by cold water saturated butanol. Marshall *et al*, 1990 conducted lipid

removal from the surface of rice kernels using lipid extraction solvents, hexane and 2:1 chloroform:methanol.

2.7. FOURIER TRANSFORM INFRARED SPECTROSCOPY

2.7.1. INFRARED SPECTROSCOPY

Infrared spectroscopy is a physicochemical method that measures the vibration of bonds within functional groups. An infrared spectrum is obtained by passing infrared radiation through a sample and determining what fraction of the incident radiation is absorbed at a particular energy. The energy at which any peak in an absorption spectrum appears corresponds to the frequency of vibration of the particular functional group in the sample molecule (Griffiths and Haseth, 2007).

2.7.2. ATTENUATED TOTAL REFLECTANCE-FOURIER TRANSFORM INFRARED SPECTROSCOPY (ATR-FTIR)

The technique used in this project is Attenuated Total Reflectance-Fourier Transform Infrared (ATR-FTIR) which is the combination of a fourier transform infrared spectrometer with attenuated total reflectance cell.

2.7.3. PRINCIPLE OF FOURIER TRANSFORM INFRARED SPECTROSCOPY

The principle of the FTIR spectroscopy is based on the Michelson interferometer (Smith, 1996). The structure of the interferometer consists of four arms; infrared light source, fixed mirror, moving mirror and detector and the intersection is a beam-splitter (**Figure 8**). The way it works is that a beam of infrared light source is

split it into two beams (**Figure 8A**). One (or half) of the beams is transmitted (**Figure 8B**), while another is reflected (**Figure 8C**). The transmitted beam strikes the fixed mirror while the reflected beam strikes the moving mirror. Both beams are then reflected off their respective mirrors and recombine at the beam-splitter. Finally, the light beam then interacts with the sample and strike the detector.

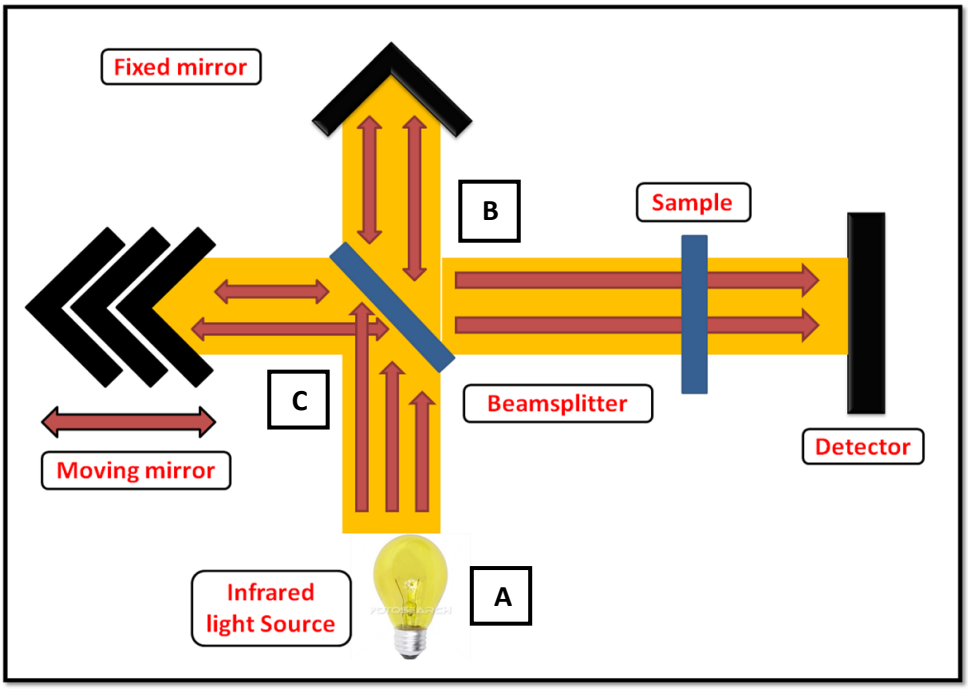

Figure 10. Basic principle of a Michelson interferometer; (A) light source, (B) transmitted beam, (C) reflected beam (Adapted from Smith, 1996).

2.7.4. ATTENUATED TOTAL REFELECTANCE

Attenuated Total Reflectance (ATR), or Internal Reflectance Spectrometry (IRS) is a technique whereby the sample is placed in contact with a sensing element, and a spectrum is recorded as a result of the contact (Griffiths and Haseth, 2007). When an infrared beam passes through a crystal it is expected that the radiation passes through the crystal and leaves its top surface.

However, according to Harrick, 1967, when sin $\theta_i > n_2/n_1$, where θ_i = angle of incidence on the crystal, n_1 = the index of refraction of the crystal and n_2 = the index of refraction of sample, the beam is internally reflected at the top of the crystal (**Figure 9**). When an infrared is inside the crystal, a standing wave of radiation is created, called an evanescent wave. A unique property of the wave is that the wave is slightly larger in amplitude than the crystal, so it penetrates a small distance beyond the crystal surface. When this occurs, the beam penetrates a fraction of wavelength beyond the crystal surface and hence, penetrates the sample. When a sample material that selectively absorbs radiation is in close contact with the crystal surface, the beam loses energy at the wavelength where the material absorbs.

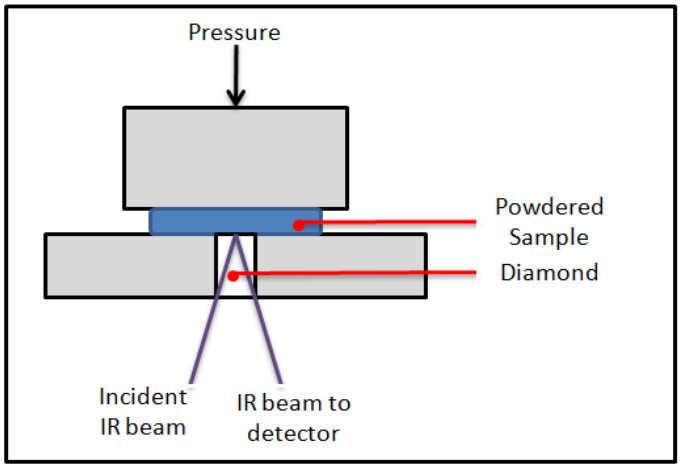

Figure 11. Attenuated total reflectance, where infrared incident beam penetrate diamond and reflected infrared beam goes to detector (Adapted from Sevenou *et al*, 2002).

The crystal used in ATR cells that are made from materials that have low solubility and are of a very high refractive index, which includes zinc selenide, germanium

and diamond. In this study, diamond was used. The intensity of the absorption depends on good contact between the sample and the diamond and the depth of the penetration of the evanescent wave (Stuart, 2004). Hence, ATR is considered a surface method due to the ability to control the depth of the penetration of the wave. The depth of penetration can be expressed as **Equation (1)**, where λ is the wavelength of the incident wave, θ_i is the incident angle, n_1 and n_2 the refractive indices of the ATR crystals and the sample. Considering $\theta_i = 45^0$, $n_1 = 2.4$ for diamond, and $n_2 = 1.5$, the relation can be simplified by **Equation (2)**.

Thus, the penetration depth is directly related to the wavelength. In this study, since polysaccharides, such as starch absorb in the region 1200 - 800 cm^{-1} which correspond to a wavelength between 8 – 12 µm, hence, penetration depth used is 2 µm.

$$d_p = \frac{\lambda}{2\pi n_1 \sqrt{\sin^2\theta_i - \left(\frac{n_2}{n_1}\right)^2}} \quad \text{.....Equation (1)}$$

$$d_p \sim 0.2\lambda \quad \text{.....Equation (2)}$$

2.7.5. SPECTRAL MANIPULATIONS

The interpretation of the spectra can be simplified by the fact that the bands of a spectrum can be assigned to particular parts of a molecule, producing 'group frequencies' (Stuart, 2004). Group frequencies can be divided into the far-infrared region (between 400 and 100 cm^{-1}), mid-infrared region (4000 – 400 cm^{-1}) and the

near-infrared region (13000 - 4000 cm^{-1}). The mid-infrared regions can further be divided into; X-H stretching region (4000 - 2000 cm^{-1}), the double-bond region (2000 - 1500 cm^{-1}) and the fingerprint region (1500 - 600 cm^{-1}). Each band in an infrared spectrum can be assigned to a particular functional group of the molecule; however, there are some vibrations that are not 'well-behaved' (Stuart, 2004). This applies to most bending and skeletal vibrations which absorb in the 1500 - 650 cm^{-1} region, called the fingerprint region (Sevenou *et al*, 2002). This study concerns starch, which is a carbohydrate, which absorbs in the region of 1200 - 800 cm^{-1}.

When an interferogram is Fourier transformed, a single beam spectrum is obtained, which is a plot of raw detector response versus wavenumber. However, signal assignment is generally limited due to overlapping and poor resolution of the detected bands. Enhanced resolution of overlapped bands can be achieved by deconvolution. There are several spectral manipulations that can be performed on raw data, which includes spectral subtraction, baseline correction, smoothing, curve-fitting, deconvolution and normalisation (Sevenou *et al*, 2002). In this report, only baseline correction, deconvolution and normalisation are used.

A. BASELINE CORRECTION

Baseline correction is process of quantifying the absorbance spectrum (Griffiths and Haseth, 2007). This is performed by producing a baseline joining the lowest absorbance points and a line joining the peak of the absorbance points. The difference between the baseline and the top line is used for quantitative analysis.

B. NORMALISATION

The intensity of the IR spectrum obtained by the ATR depends on the quantity of sample which covers the diamond during the measurement (Griffiths and Haseth, 2007). In-order to compare spectra of different intensities, a normalisation of spectra is applied. This is performed to remove differences in peak heights between spectra required under different conditions, for example, different particle size. This is done by dividing all the absorbances in a spectrum by the largest absorbance in a spectrum.

C. DECONVOLUTION

Deconvolution is the process of mathematically enhancing the resolution of the spectrum, which results in a maximised spectrum and more resolved overlapping bands (Griffiths and Haseth, 2007). Original peaks are retained but peak shapes and peak areas are altered. The deconvolution technique involves several steps; (i) initially the spectrum produces an inverse Fourier-transform, called cepstrum, followed by (ii) a multiplication by a smoothing function consisting of a Gaussian-Lorentzian bandshape, $e^{\alpha x}$, where x is the optical retardation and α is the amount of resolution enhancement, and finally (iii) the altered cepstrum is fourier transformed to obtain the resolution enhanced spectrum. It must be ensured that the lineshape is adjusted so that excessive distortion does not occur. The factors to be considered are proportion of Gaussian and Lorentzian lineshapes, and half-width. If it is too small, it will not be significantly different from the original, and if

it is too large, the spectrum may produce false peaks as noise starts to be deconvolved.

D. ABSORBANCE RATIOS

A study conducted by van Soest *et al* (1995) found that the ATR-FTIR spectrum band at 1045 cm^{-1} is sensitive to the amount of crystalline starch while the band at 1022 cm^{-1} is sensitive to amorphous starch. The ratio of absorbance value of the ATR-FTIR bands at 1047 cm^{-1} and 1022 cm^{-1} have been found to be proportional to the ratio of native/amorphous starch in mixtures of native and amorphous starch (van Soest e*t al*, 1995) and can be used to measure a degree of order in starch samples. ATR-FTIR spectroscopy has been used to investigate the external regions of starch granules which used the ratio of absorbance 1047/1022 (Sevenou *et al*, 2002).

2.8. X-RAY DIFFRACTION

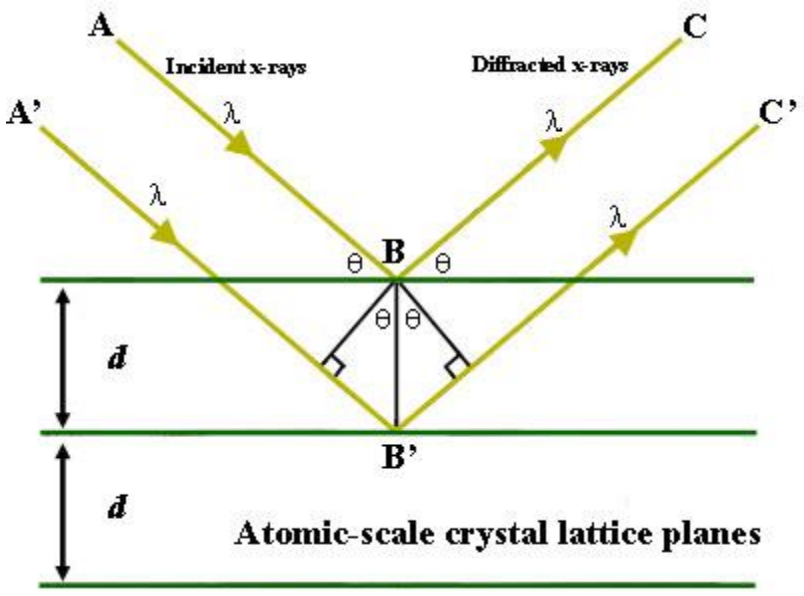

Figure 12. Principle of Bragg's Law, $n\lambda=2d \sin\theta$ (Suryanarayana & Grant Norton, 2013).

X-Ray Diffraction measure the average spacing between layers or row of atoms to determine the crystal structure of an unknown material (Suryanarayana & Grant Norton, 2013). An X-ray which reflects from the surface of a substance has travelled less distance than an X-ray which reflects from a place of atoms inside the crystal. The penetrating X-ray travels down to the internal layer, reflects and travels back over the same distance before being back at the surface. The distance travelled depends on the separation of the layers and the angle at which the X-ray entered the material. Bragg expressed this in an equation now known as Bragg's Law: Bragg's Law n = 2 d sinϴ, where is the wavelength of the rays, ϴ is the angle between the incident rays and the surface of the crystal, d is the spacing between layers of atoms and constructive interference occurs when n is an integer.

X-ray diffraction is based on constructive interference of monochromatic X-rays and a crystalline sample. These X-rays are generated by a cathode ray tube, filtered to produce a monochromatic radiation, collimated to concentrate and directed towards the sample. The interaction of the incident rays with the sample produces constructive interference (and a diffracted ray) when conditions satisfy Bragg's Law ($n\lambda=2d \sin\theta$). This law relates the wavelength of electromagnetic radiation to the diffraction angle and the lattice spacing in a crystalline sample. These diffracted X-rays are then detected, processed and counted.

By scanning the sample through a range of 2θangles, all possible diffraction directions of the lattice should be attained due to the random orientation of the powdered material. Conversion of the diffraction peaks to d-spacings allows identification of the mineral because each mineral has a set of unique d-spacings.

Typically, this is achieved by comparison of d-spacings with standard reference patterns. A detector records and processes this X-ray signal and converts the signal to a count rate which is then output to a device such as a printer or computer monitor.

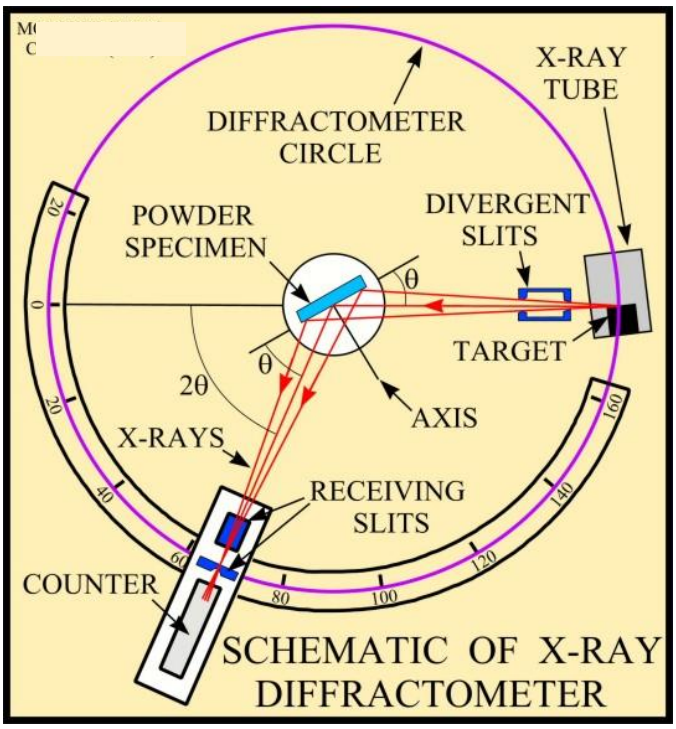

Figure 13. Schematic of X-ray diffractometer (Cullity, 1956).

2.9. NUCLEAR MANGNETIC RESONANCE (NMR)

Nuclear Magnetic Resonance (NMR) spectroscopy is an analytical chemistry technique used in quality control and research for determining the content and purity of a sample as well as its molecular structure. The principle behind NMR is that many nuclei have spin and all nuclei are electrically charged (Callaghan, 1993). If an external magnetic field is applied, an energy transfer is possible between the base energy to a higher level energy (generally a single energy gap). The energy transfer takes place at a wavelength that corresponds to radio frequencies and the

spin returns to its base level, energy is emitted at the same frequency. The signal that matches this transfer is measured in many ways and processed in order to yield an NMR spectrum for the nucleus concerned.

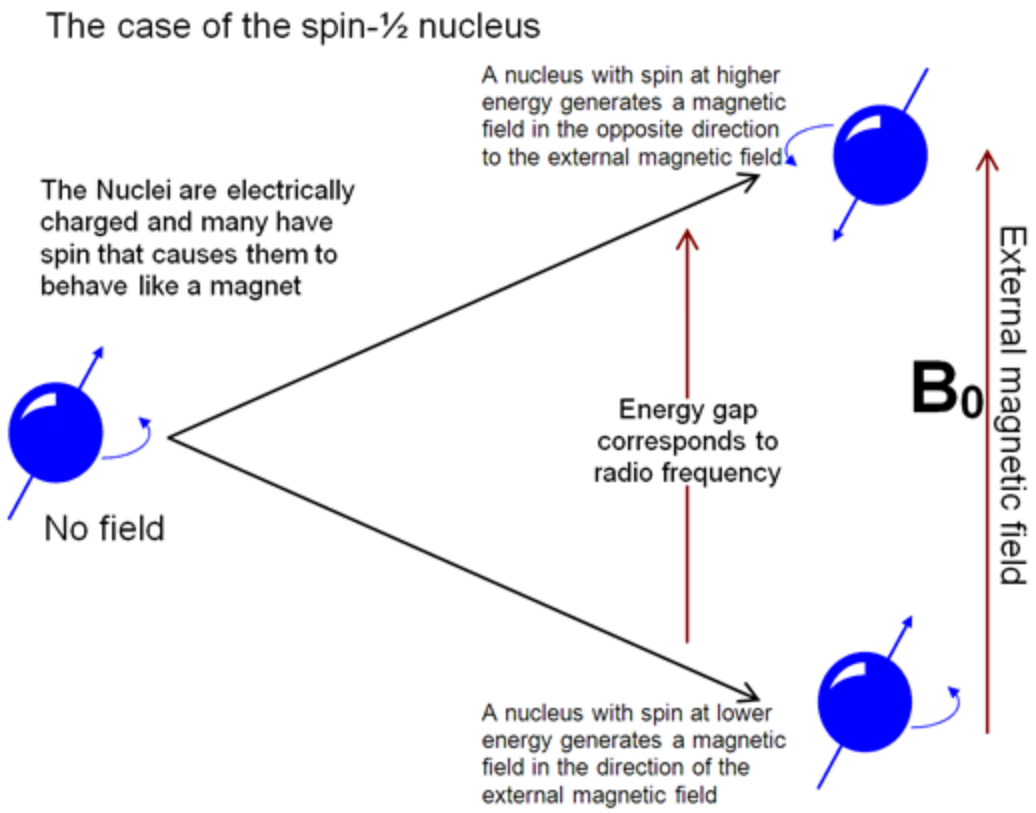

Figure 14. Principle of Nuclear Magnetic Resonance.

The NMR phenomenon is based on the fact that the nuclei of atoms have magnetic properties that can be utilized to yield chemical information. Quantum mechanically subatomic particles (protons, neutrons and electrons) have spin. In some atoms, (^{12}C, ^{16}O, ^{32}S) these spins are paired and cancel each other out so that the nucleus of the atom has no overall spin. Many atoms (^{1}H, ^{13}C, ^{31}P, ^{15}N, ^{19}F) the nucleus possess and overall spin.

.

3. MATERIALS AND METHODS

This chapter covers the materials and methods used in this study. The methods section will include an elaboration of the methods used to prepare milled rice powder and rice grains for further analysis, together with the analytical techniques used in this study and compositional and statistical analyses employed.

3.1. MATERIALS

3.1.1. NATIVE STARCH

Native rice (non-waxy) starch and waxy rice starch samples used were sourced from Witwood Food Products, Banbury, Oxfordshire.

3.1.2. RICE GRAINS

Rice grain samples used were commercially sourced. The rice varieties were; (A) Tilda brand: long grain, basmati, thai jasmine. (B) Sainsbury's brand: long grain, basmati, thai jasmine, arborio, paella. (C) Tesco brand: long grain, basmati, thai jasmine. Brunei laila rice was brought over from Brunei with permission from the Brunei Agrifood, Ministry of Industry and Primary Resources.

3.2. PREPARATION OF RICE POWDER

3.2.1. MILLING

Milling of samples was performed following the procedure of Sevenou *et al*, 2002 using a Laboratory Mill 3600, Perten, USA, using the setting number which yields

the finest powder which is 0. This was performed twice to ensure proper milling of samples.

3.2.2. SIEVING

Sieving of native starch and rice grain samples was performed using Cyclotec mill, USA, for 2 minutes with 15 second intervals. To ensure an equal distribution of particle size of milled sample, the fraction size collected was between 125 and 250 µm.

3.2.3. DRYING

Drying of sample was performed by vacuum drying of samples until constant weight was reached. This was done at 60 ^{O}C for 48 hours.

3.2.4. GELATINISATION AND RETROGRADATION

Rice samples (14 % by weight) were cooked using a Rapid Visco Analyser, Super4, Perten Instruments, Perkin Elmer, USA, using Standard Profile 1. Each sample was heated from 50 ^{o}C to 90 ^{o}C to 50 ^{o}C for 15 minutes and stirred at a speed of 960 rpm for 10 seconds and at constant rate of 160 rpm for the rest of the cooking time. For gelatinisation studies, each sample was immediately crash cooled in ice after cooking while for retrogradation studies, the sample was allowed to retrograde at room temperature for 7 days and then crash cooled in ice.

3.2.5. PREPARATION OF AMORPHOUS SAMPLES FOR XRD

Amorphous, fully gelatinised rice samples used for X-Ray Diffraction in this project were first prepared by RVA (**3.2.4. Gelatinisation**), frozen in liquid nitrogen and then freeze-dried. The freeze-dried samples were then milled, sieved, stored in phosphorus pentoxide and stored in zip loc bags before analysis (**Figure 15**).

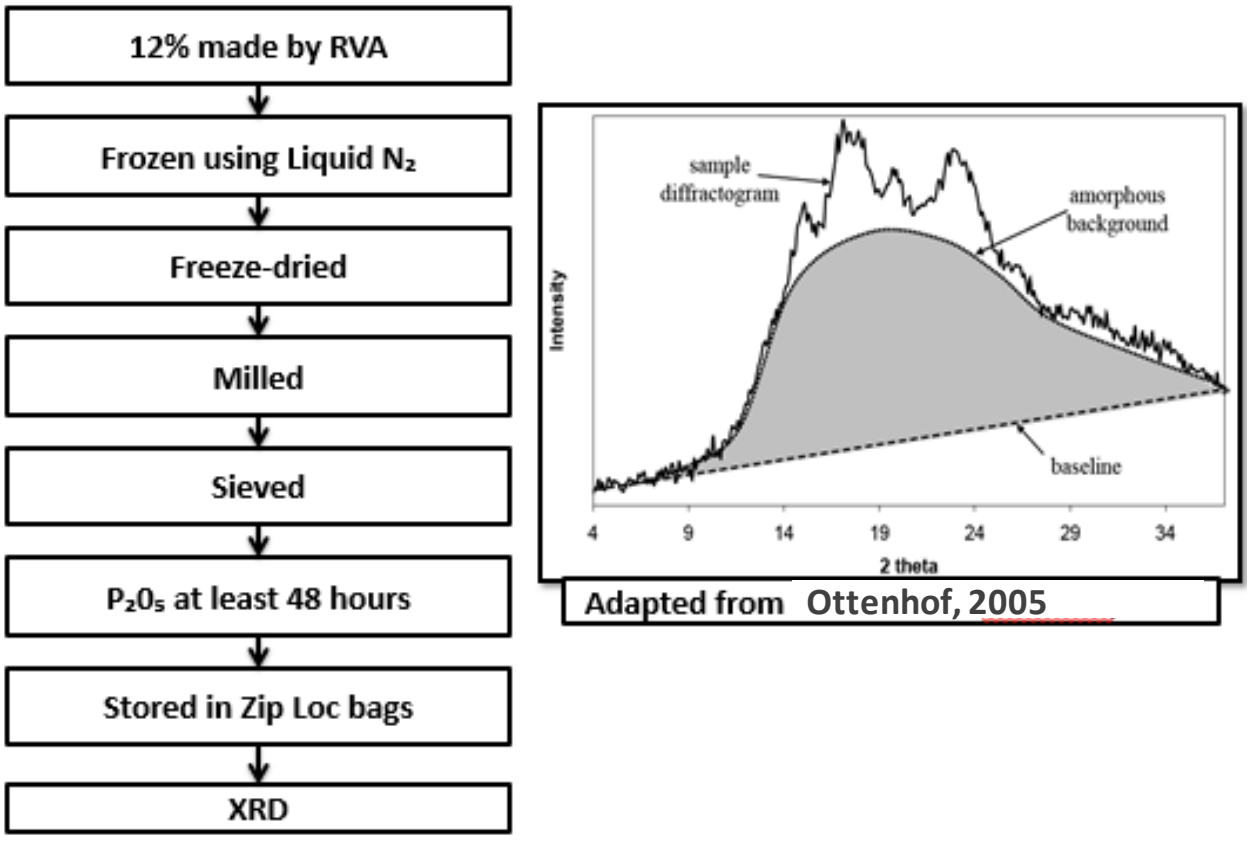

Figure 15. Preparation of amorphous samples for x-ray diffraction, showing how the amorphous samples can be used to produce a baseline to determine crystalline peaks.

3.3. METHOD: PREPARATION OF RICE GRAINS

3.3.1. CUTTING OF RICE GRAINS

Raw rice grains were cut with a standard blade and the dimensions of the external and internal regions of raw rice grains defined in this study are shown in **Figure 16**. The samples were then ground using Perten laboratory mill 3600, sieved using Cyclotec mill for 2 minutes, where the fraction size collected was between 125 and 250 µm, and dried using a vacuum oven at 60 °C for 48 hours until constant weight was reached and then stored in P_2O_5 for 7 days.

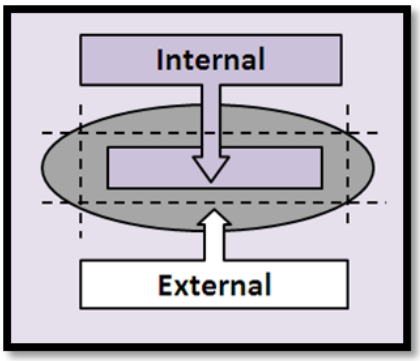

Figure 16. External and internal regions of rice grains as defined in this study.

3.3.2. CRYO-MICROTOME

The cryo-microtome used in this experiment was a Cryotome CM1900, Leica, Germany. Raw rice grains were first softened in methyl cellulose in vacuum for 1 hour. Each rice grain was embedded in a square block of 3 cm diameter and 1.5 cm thickness, filled with Optimal Cutting Temperature (OCT) medium at -30 °C for 10 minutes until it solidified (**Figure 17**). The block of solid was pasted on the chuck holder for cutting. Samples used were of 5 µm thickness as it is considered an optimum thickness to obtain good quality FTIR absorbance without the risk of tearing the sample.

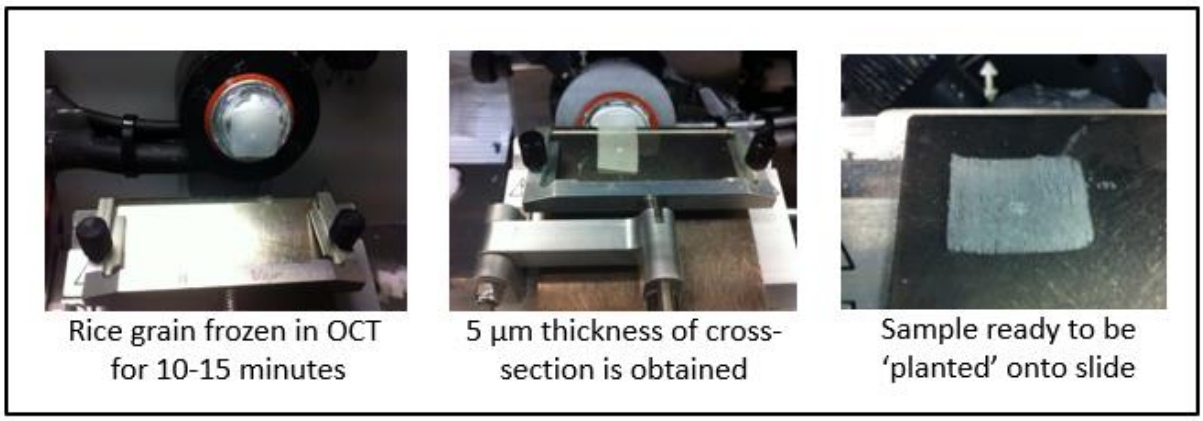

Figure 17. Cross-section of rice grains cut using cryo-microtome.

3.3.3. COOKING OF RICE

The rice used in the texture analysis was cooked in a glass beaker with 2:1 water to rice ratio. The glass beaker was covered with aluminum foil and forked for ventilation. The rice was brought to boil on a digital heating pad for about 5 minutes and simmered for another 25 minutes. The rice was then gently stirred with a glass rod every 5 minutes to ensure a more homogenous cooking.

3.4. METHODS: WASHING OF RICE FLOUR AND RICE GRAINS

3.4.1. WATER SOAKING

Each sample (5 g) was immersed in 10 g water in a centrifuge tube for time intervals of 10, 20, 30, 40, 50 and 60 minutes. Rice powder was vortex mixed for 1 minute and centrifuged for 30 minutes at 1800 g while rice grains were shaken in a circular motion by hand. All supernatant and filtrate were collected, oven-dried at 40 °C overnight and used for further analysis.

3.4.2. REMOVAL OF PROTEINS

The extraction of proteins was performed using sodium hydroxide, sodium chloride, ethanol and water (Lim *et al*, 1999). To remove glutelin, samples were mixed with 0.2 % NaOH on a roller mixer for 4 hours, neutralised with HCl and then centrifuged at 8000 rpm. To remove globulins, samples were mixed with NaCl on a roller-mixer for 1 hour. Prolamin was removed using 80 % ethanol. Filtrates as a result from washing with sodium hydroxide, sodium chloride were then washed three times with distilled water. Distilled water was used to remove albumin, shaken for 1 hour. All supernatants and filtrates were collected, oven-dried at 40 °C overnight and used for further analysis (**Figure 18**).

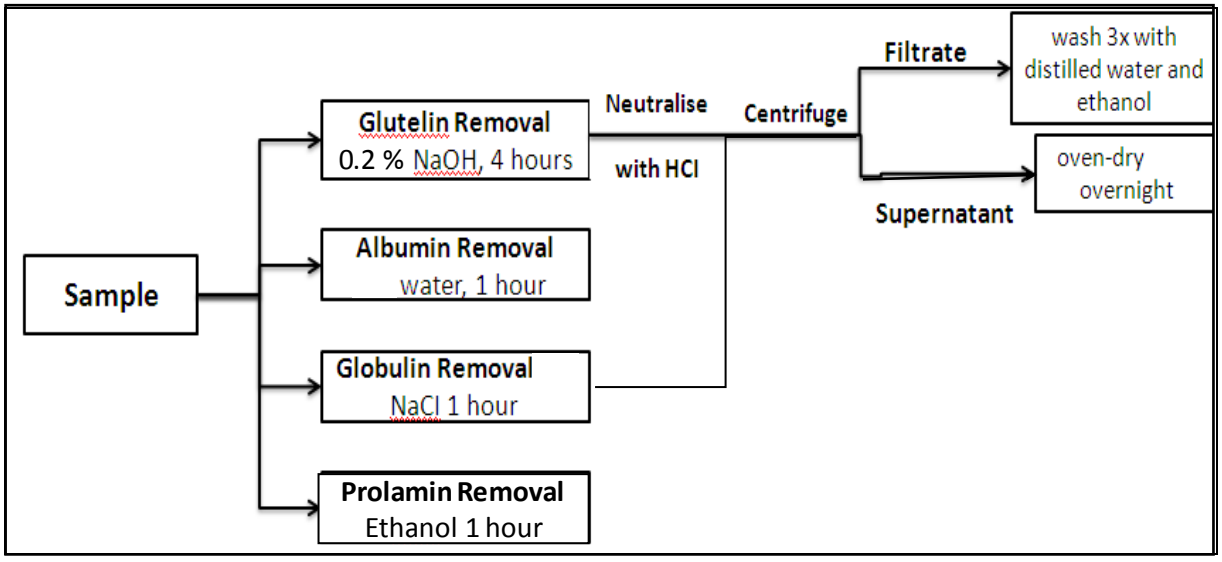

Figure 18. Protein removal from rice flour using 0.2 % NaOH, water and NaCl to remove glutelin, albumin and globulin respectively.

3.4.3. REMOVAL OF LIPIDS

Removal of lipids was performed using chloroform, hexane, methanol and 2:1 ratio of chloroform:methanol. In the case of milled rice powder, samples were centrifuged for 30 minutes at 1800 g and supernatant and filtrate collected for further analysis. In the case of rice grains, the filtrate was collected for further analysis.

3.5. ANALYTICAL TECHNIQUES

3.5.1. TEXTURE ANALYSER

Texture measurements of rice were measured by the texture analyser. In this project, texture analysis of rice samples was performed using TA.XT.Plus stable micro system. The software used for analysis was Texture Exponent 32. The weight and height of probe was calibrated before analysis. Parameters used are according to TPA profile; double compression of 5.0 g force, 10 mm depth, speed of 1 mms^{-1} before touch, 2 mms^{-1} during touch and 2 mms^{-1} after touch, and a 2 seconds gap in between the two cycles. Rice is cooked according to **4.2.4: Cooking of rice** and then pressed onto an aluminium bowl (**Figure 19**). Cooked rice was analysed 5 minutes after cooking and it was ensured that the rice samples have as consistent a height as possible. For each rice type, seven duplicates were used to ensure more reliable texture measurements, which are analysed randomly. The probe was cleaned with deionised/distilled water before and after use, and in between samples.

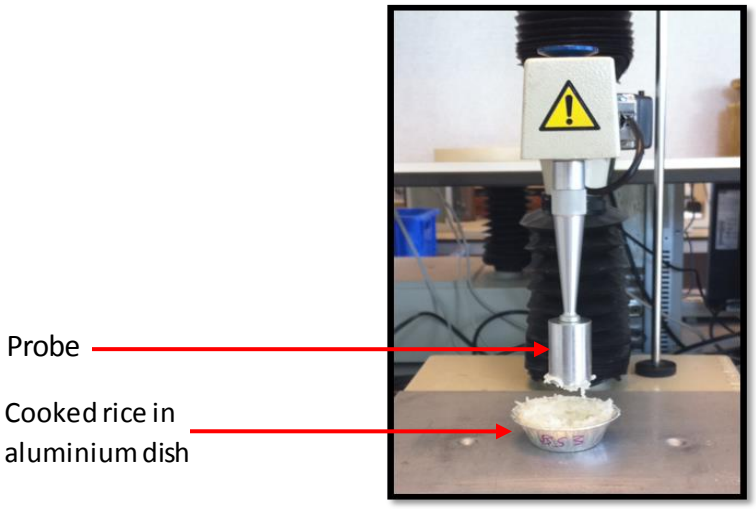

Figure 19. Texture analysis of cooked rice

2.5.2. ATTENUATED TOTAL REFLECTANCE – FOURIER TRANSFORM INFRARED SPECTROSCOPY

The ATR-FTIR spectrophotometer used in this study was a Bruker Optic Tensor 27 spectrometer, USA and the software used for analysis was the OPUS 6.5 package. Initially, a background spectrum was obtained, where a single spectrum was collected in the absence of sample. Approximately 20 g of powdered solid sample was loaded onto the circular plate. The pivot was then pressed onto the sample and screwed with a torque of 80 N.cm (**Figure 20**). The particular parameters used in this study were; resolution: 4 cm^{-1} and scan: 64 scans. Spectral manipulations used were; (i) baseline correction, (ii) deconvolution; where bandshape was Lorentzian with a bandwidth of 36.7 cm and noise reduction of 0.19, and (iii) vector normalisation in the region 800 – 1200 cm^{-1}. Spectra were baseline corrected, deconvoluted before absorbance ratios are calculated, and then normalised for

peak comparison. The surface of diamond was cleaned with ethanol before and after use and between each sample load.

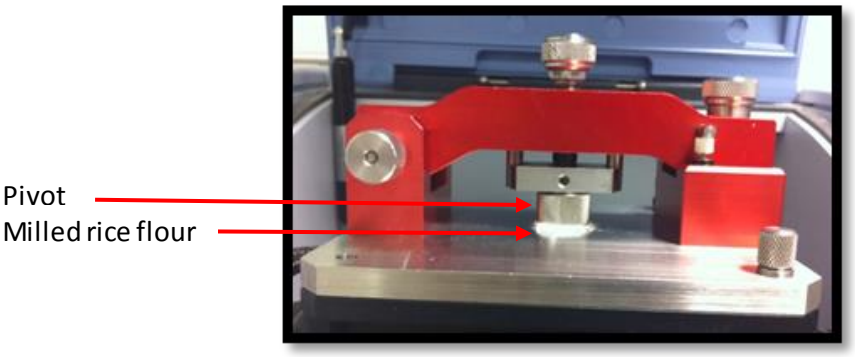

Figure 20. ATR-FTIR sampling cell.

3.5.3. FOURIER TRANSFORM INFRARED MICROSCOPY

The FTIR microscope used in this study was the Bruker Optic Hyperion 2000, USA, which was attached to a Tensor 27 spectrometer ATR-FTIR and software used for analysis is OPUS 6.5. In this study, the transmission mode was used where infrared light passes through the sample and is collected by a second IR objective that re-collimates the beam and sends it to the IR detector (**Figure 21**). Transmission mode was used because transmission produces significantly better spectra than those made in reflection mode due to decreased incident influx (40 – 50 % less) of reflectance mode.

Initially, a background spectrum was obtained, where a single spectrum was collected when IR transmits through an empty CaF window, in the absence of sample. Approximately 100 spectra of the outer and inner region were obtained and the average was taken. For a spectrum collected in the transmission mode,

samples must be thin enough to ensure sufficient infrared to be transmitted through the sample and collected/read by the detector below the sample. Hence, sample preparation was done by a cryo-microtome.

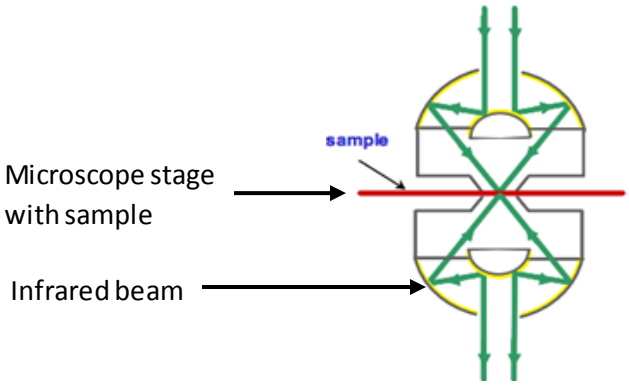

Figure 21. Pathway of transmission mode of FTIR microscope to the detector.

3.5.4. X-RAY DIFFRACTION (XRD)

Diffractograms were acquired using a Siemens D5005 wide-angle X-ray diffractometer equipped with a copper source operating at 40kV and 40mA producing a CuK_{α} radiation over the 2θ range 5 – 35 °. Relative crystallinity was calculated as the ratio of the area of the crystalline to the total region of the X-ray diffractograms. All measurements were performed in duplicate and were reported as an average. Approximately 2.0 - 3.0 g was placed in a circular sample load with circular ridges with a circumference of about 5 cm.

3.5.5. RAPID VISCO ANALYSER, RVA

The RVA used in this study is Super4, Perten Instruments, Perkin Elmer, USA. Using standard profile 1, samples was heated from 50 °C to 90 °C to 50°C for 15 minutes

and stirred at a speed of 960 rpm for 10 seconds and at constant rate of 160 rpm for the rest of the cooking time.

3.5.6. CROSS POLARIZATION – MAGIC ANGLE SPINNING (CP-MAS) ^{13}C NUCLEAR MAGNETIC RESONANCE

The Cross Polarization – Magic Angle Spinning (CP-MAS) ^{13}C NMR spectra were recorded on a Bruker MSL 300 equipped with CP-MAS (cross-polarization magic-angle-spinning) accessories. Dipolar decoupling was systematically used during the acquisition sequence. The samples were spun at a rate of 7.5 kHz at room temperature in a 4 mm ZrO_2 rotor, the accumulation of 3072 and 2048 scans were used for native starches, to obtain a satisfactory signal to noise ratio. For all hydrations, a repetition time of 2 s appeared to be sufficient and the optimal contact time was in the order of 1.25 ms after probing the range 0.75 – 2.25 ms. Spectra were referenced using a high field resonance adamantine (29.5 ppm).

3.6. COMPOSITIONAL ANALYSIS

3.6.1. MEGAZYME TOTAL STARCH ASSAY

This assay procedure was according to: Megazyme total starch assay procedure (Megazyme, 2016), Megazyme International, Ireland (amyloglucosidase/α-amylase method) and the procedure lasts for approximately 4 hours on average. Firstly, 100 mg of powdered sample of physical size 100 mg was vortexed with 0.2 ml of 80 % aqueous ethanol. Secondly, 3 ml of thermostable α-amylase was added and incubated in boiling water bath of 6 minutes, while stirring vigorously after 2, 4, 6

minutes. The tube is placed in a bath at 50 ^{o}C and add 4 ml sodium acetate buffer, followed by 0.1 ml amyloglucosidase and vortex. The samples were washed by transferring the entire content to a 100 ml volumetric flask and a funnel to assist transfer. Then centrifuged at 3000 rpm for 10 minutes. 3.0 ml of GOPOD reagent were added and tubes incubated at 50 ^{o}C for 20 minutes. The absorbance of each sample was read and a D-glucose control employed using Jenway spectrophotometer at 510 nm against the reagent blank.

The principle behind Megazyme total starch assay procedure, (amyloglucosidase/α-amylase method) is: Thermostable α-amylase hydrolyses starch into soluble branches and unbranched maltodextrins (Equation 1). Amyloglucosidase (AMG) quantitatively hydrolyses maltodextrins to D-glucose (Equation 2). D-glucose is oxidised to D-gluconate with the release of one mole of hydrogen peroxide (H_2O_2) which is quantitatively measured in a colourimetric reaction employing peroxidase and the production of a quinoneimine dye (Equation 3).

Starch + H_20 → maltodextrins ……Equation (1)

Maltodextrins → D-glucose……Equation (2)

D-Glucose + O_2 + H_2O → D-gluconate + H_2O_2 ……Equation (3)

2 H_2O_2 + ρ-hydroxybenzoic acid + 4-aminoantipyrine → quinoneimine dye + 4 H_2O

3.6.2. MEGAZYME AMYLOSE/AMYLOPECTIN RATIO ASSAY

This assay procedure was according to the booklet: Megazyme amylose/amylopectin assay procedure (Megazyme, 2016), Megazyme International, Ireland and the procedure took 7 hours on average. Firstly, the sample was pre-

treated with dimethyl sulphoxide, DMSO and ethanol to remove lipids (**Figure 22A**). Starch samples are completely dispersed by heating in DMSO and lipids are removed by precipitating the starch in ethanol and recovering the precipitated starch. The sample was then centrifuged; the supernatant (lipid) is removed and the pellet (starch) is used for subsequent amylose/amylopectin ratio and total starch assay (**Figure 22B**).

For the amylose/amylopectin ratio assay, initially the sample was reacted with lectin concanavalin A, Con A and then centrifuged; the pellet (amylopectin) is removed and the supernatant (amylose) was used for further amylose content assay (**Figure 22C**). Basically, after dissolution of the precipitate sample in an acetate/salt solution, amylopectin is specifically precipitated by the addition of Con A and removed by centrifugation.

In this case, amyloglucosidase/α-amylase enzyme and glucose oxidase/peroxidise reagent, GOPOD was added and absorbance is read using a spectrophotometer at 510 nm (**Figure 22D**). The amylose, is an aliquot of the supernatant, is enzymically hydrolysed to D-glucose, which is analysed using glucose oxidase/peroxidase reagent. At the same time, for the total starch assay was also treated with amyloglucosidase/α-amylase enzyme and GOPOD (**Figure 22E**). The total starch, in a separate aliquot of the acetate/salt solution, is similarly hydrolysed to D-glucose and measure colourimetrically by glucose oxidase/peroxidase.

The ratio of the absorbance of amylose determination and total starch assay gives the amylose content (% amylose). The concentration of amylose in the starch

sample is estimated as the ratio of GOPOD absorbance at 510 nm of the supernatant of the Con A precipitated sample to that of total starch sample. Calculation of amylose content (%) is:

$$\frac{\text{Absorbance (Con A Supernantant)}}{\text{Absorbance (Total Starch Aliquot)}} \times \frac{6.15}{9.2} \times \frac{100}{1}$$

where 6.15 and 9.2 are dilution factors for the Con A and total starch extracts respectively.

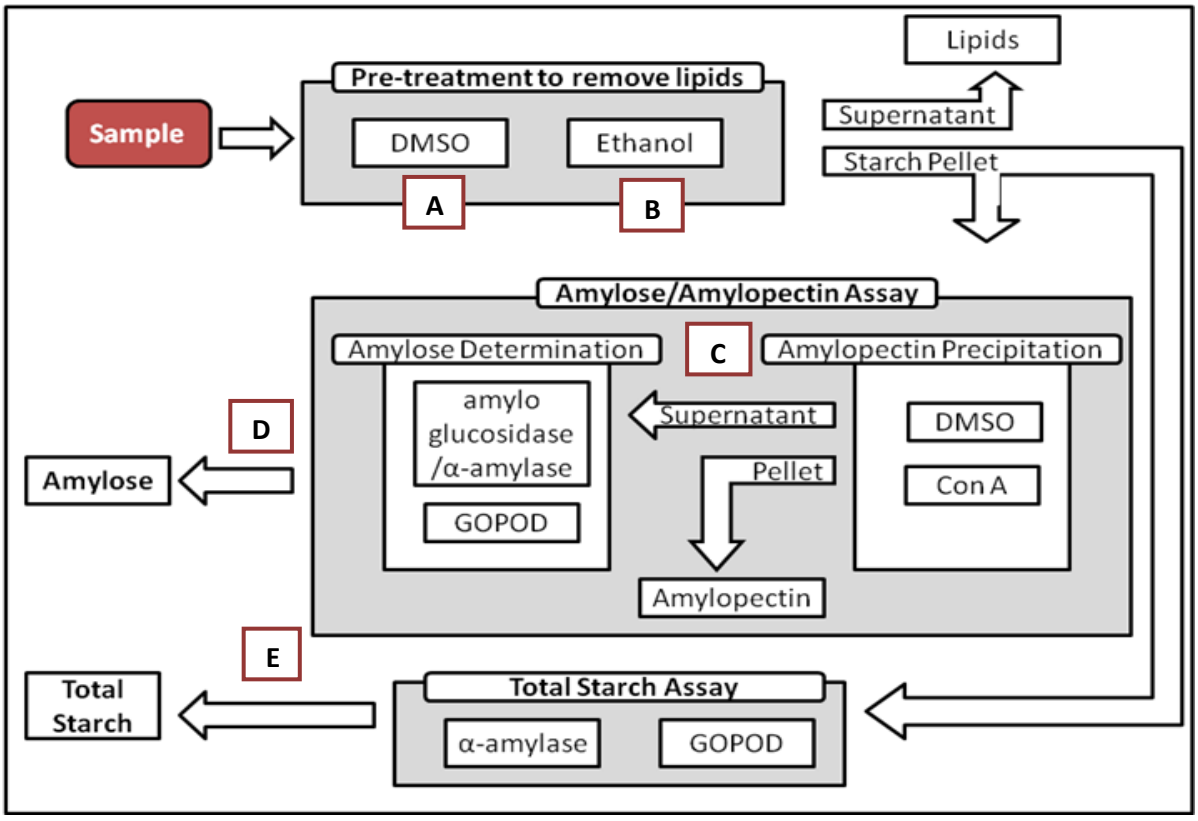

Figure 22. Summary of Megazyme amylose/amylopectin ratio assay (Adapted from Megazyme, 2016).

3.6.3. SOLUBLE STARCH ASSAY

In this study, a modified version of the amylose leaching is used namely the soluble starch assay. The soluble starch assay was initially used for determining the amount of starch leached during cooking, as measured by the amount of starch which dissolves in 60 ^{o}C water, hence the term 'soluble starch'. There are two main differences between the two methods; amylose leaching uses amylose and amylopectin standards at wavelengths 630 nm and 590 nm respectively, and the calibration curve used is amylose concentration against iodine affinity (absorbance). Meanwhile, soluble starch assay uses only iodine reagent as standard at 630 nm and the calibration curve used is soluble starch against iodine affinity (absorbance).

Soluble starch assay was performed by initially cooking the starch samples, then diluting to an acceptable concentration and finally treating it with iodine reagent before absorbance reading. Starch was cooked in the RVA according to **4.2.4: Gelatinised starch** (**Figure 23A**) is then stirred with a Silverson mixer at low speed for 5 minutes to homogenise the paste. The sample underwent 10^{-3} dilution; initially 1ml of the sample was diluted to 100 ml with water at 60 ^{o}C (**Figure 23B**), followed by centrifugation and further dilution where 1 ml of the supernatant was diluted with 10 ml water (**Figure 23C**). Iodine reagent (0.2 ml) was then added before absorbance measurements at 630 nm (**Figure 23D**). A calibration curve was made where different concentrations of starch were dissolved in 60 ^{o}C water and their absorbance measurements are taken.

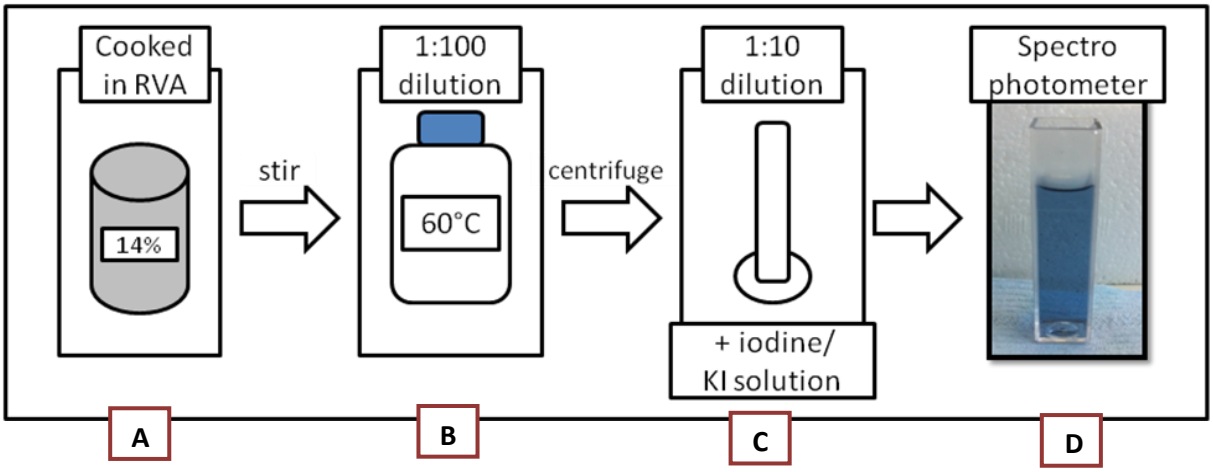

Figure 23. Steps in involved in soluble starch assay.

3.6.4. BOVINE SERUM ALBUMIN PROTEIN KIT

The protein content of the defatted sample was measured using the Pierce Bicinchoninic Acid, BCA protein assay kit (Thermo Fisher, 2016): Test-tube procedure, Thermo Fisher Scientific. Each standard and samples (0.1 ml) was vortexed with 2 ml of working reagent (**Figure 24B**). Room Temperature, RT protocol was used: RT for 2 hours as the working range of protein concentration is 20 – 2000 µg/mL. Absorbance at 562 nm was read on Jenway spectrophotometer (**Figure 24D**). It must All samples were 'read' within 10 minutes. A standard curve was prepared by plotting the average blank corrected 562 nm for each standard against protein concentration in µg/mL and use the standard curve was used to determine the protein concentration of samples.

Thermo Scientific Pierce BCA protein assay is a detergent compatible formulation based on Bicinchoninic Acid (BCA) for the colorimetric detection and quantification of total protein. This method combines the well-known reduction of Cu^{2+} to Cu^{1+} by protein in an alkaline medium (the biuret reaction) with the highly sensitive and

selective colorimetric detection of the cuprous cation (Cu^{1+}) using a unique reagent containing Bicinchoninic Acid. The purple coloured reaction product of this assay is formed by the chelation of two molecules of BCA with one cuprous ion.

The principle of BCA protein assay relies on the formation of a Cu^{2+} protein complex under alkaline conditions, followed by the reduction of the Cu^{2+} to Cu^{1+}. The amount of reduction is proportional to the amount of protein present. BCA forms a purple-blue complex with Cu^{1+} in alkali environments, thus providing a basis to monitor the reduction of alkaline Cu^{2+} by proteins.

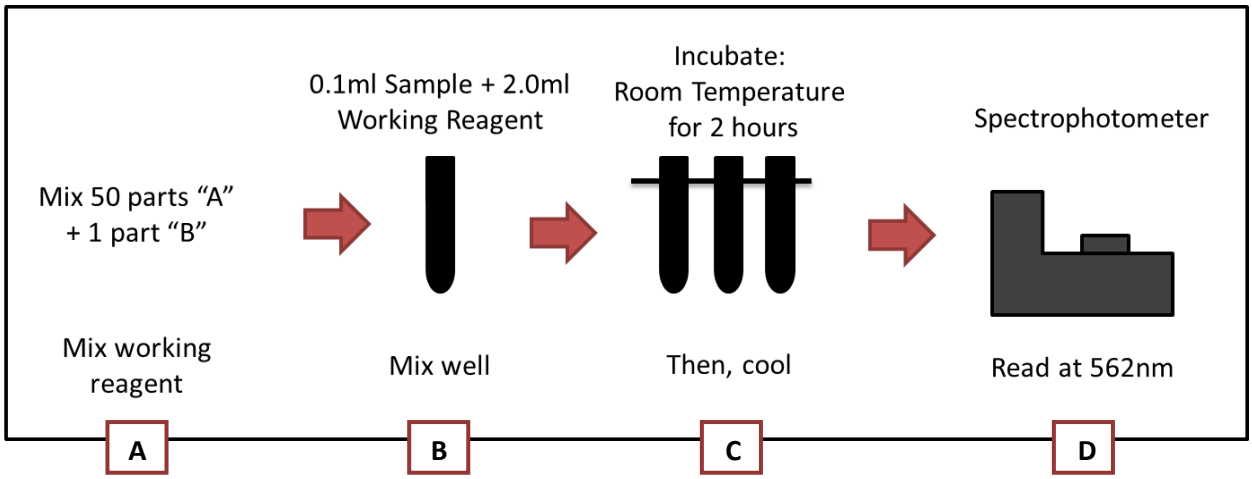

Figure 24. Steps involved in Pierce BCA protein assay kit (Adapted from Thermo Fisher, 2016).

3.6.5. LIPID EXTRACTION AND WEIGHING

As a result of the extraction with 2:1 chloroform methanol, lipid from the rice flour was then evaporated with nitrogen gas. Rice flour is mixed with 2:1 chloroform methanol, where chloroform and methanol dissolves the lipid. The mixture is then filtered. Then lipid-chloroform methanol mixture is subjected to nitrogen gas until

all solvents are evaporated. The final obtained sample was then weighed. Control used was lipid extracted from sunflower oil.

3.6.6. MOISTURE CONTENT DETERMINATION

All the moisture content of samples in this study was determined using dried in vacuum oven at 60 °C until the weight stop fluctuating. The dried weight sample over the weight of the original sample times a hundred is the moisture content, dry weight basis.

3.7. STATISTICAL ANALYSIS

For characterization of the samples, at least three replicate measurements were performed, unless otherwise specified. All data were reported as the mean ± standard deviation (mean ± SD). Results with a corresponding probability value of $p < 0.05$ were considered to be statistically significant.

4. EVALUATION OF COOKED RICE TEXTURE

As stated on Page 3, the main objective of this PhD project was to investigate how the components of raw rice grains have an effect on texture of cooked rice. To provide a reliable comparison between the different textural properties of cooked rice, it is crucial to establish concrete methods for texture evaluation. This chapter aims to establish an effective and repeatable method for the texture evaluation of cooked rice. The chapter starts by providing a comparison of several methods that can be used to quantify cooked rice texture, followed by a demonstration on how the texture analysis is developed and finally, a selection of rice varieties with desired textural traits to be studied throughout this project.

4.1. DETERMINATION OF TEXTURE EVALUATION

4.1.1. SELECTION OF TEXTURE EVALUTION METHOD

There are several different methods that have been used to quantify the texture of cooked rice. These cover (i) instrumental methods, such as texture analyser, (ii) sensory methods, which include visual observation, oral consumption and physical touch by trained panellists, and (iii) chemical methods; such as starch composition of raw rice grains. **Table 2** shows the different quantification methods and a consideration of their advantages and limitations for this project.

Chemical textural evaluation was not considered in this study as the chemical composition of rice is not a solid representation of its texture. Instrumental

methods are relatively easy and fast to perform and to replicate experiments. In addition, texture analyser machines are readily available in most food laboratories, making it the most common method to study texture. However, the limitation of this method is the textural evaluation is not based on real human oral consumption.

On the other hand, sensory textural evaluation provides a more realistic study where people consume cooked rice and give feedback. However, according to Dr Alina Surmacka Szczesniak, founding editor of the Journal of Texture Studies, this method is extremely time-consuming and expensive to conduct (Stable micro systems, 2015). A textural sensory experiment requires intensive planning, training of panellists to understand the desired textural trait to be quantified and money compensation for the training and consequent analyses.

Lyon *et al*, 2000 studied the relationship between sensory, physical and chemical studies of rice texture and concluded that sensory analysis has the highest variation while instrumental texture evaluation has the least variation in texture differences between cooked rice grains. Although sensory analysis has the benefit of analysing consumer preference, this factor is not beneficial for this study. It might also affect results if trained panellists do not favour the texture, aroma or taste of the rice samples tested. Due to time constraints, this project only focuses on instrumental methods to quantify cooked rice texture. As mentioned in **3.5.1. Texture analyser**, the equipment used is TA.XT.Plus Stable micro system.

Table 2. Different methods of cooked rice texture evaluation considered.

Method	Example	Advantages	Limitations	Verdict
Instrumental	▪ Texture analyser ▪ Rapid Visco Analyser	▪ Easy and fast to perform and replicate ▪ Machine readily available in most food laboratories	Machine-based; not based on real oral consumption and mouth-feel	Selected
Sensory	Trained panellists, can be based on ▪ Aroma ▪ oral consumption; mouth feel texture ▪ Visual observation ▪ Physical touch	Uses real subjects – real oral consumption with real surface properties and mouth feel	▪ Require proper planning ▪ Time-consuming ▪ Slow to perform replicates ▪ Expensive ▪ Sensory laboratory conditions not comparable to home conditions	Considered but not selected
Chemical	▪ Starch composition ▪ Amylose/ Amylopectin Composition	▪ Kits readily available ▪ Can be straight-forward and reproducible	▪ Not actually based on texture	Not considered

4.1.2. INSTRUMENTAL TEXTURE EVALUATION

There are several types of machines available that can be used to measure cooked rice texture. This includes texture analyser, instron tester, general food texturometer and Rapid Visco Analyser (RVA). Both texture analyser and instron tester require the use of whole kernel rice samples. This provides a better representation of texture as rice is consumed as whole kernels. However, Rapid Visco Analyser (RVA) uses ground up rice samples and uses viscosity profile. Compared to the instron tester, texture analyser has more user friendly software and is more adapted to food applications. In addition, it is readily available in the University of Nottingham food science laboratory. Therefore, in this study, the

texture analyser is used for analysing cooked rice texture, which method development will be explained in greater detail in this chapter.

Table 3. Different types of instruments that can be used for instrumental texture evaluation in this study.

	Texture analyser	**Rapid visco analyser**	**Instron tester**
Sample	Uses whole rice samples - real	Uses ground up rice	Uses whole rice samples - real
Results obtained	▪ Shows hardness, adhesiveness, represents movement of mouth chewing ▪ User friendly software ▪ More application for food available	Shows in viscosity profile, breaking of starch granules, shearing	Less user friendly
Used in this study	Yes	Yes/No	No

4.2. TEXTURE ANALYER

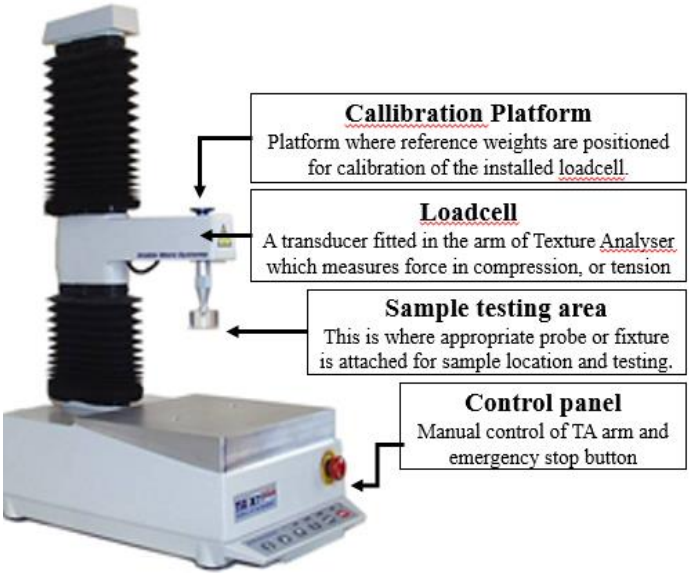

Force Capacity: 50 kg.f (500N)

Force Resolution: 0.1 g

Loadcells: 0.5, 5, 30, 50 kg.f

Speed Range: 0.01 – 40 mm/s

Maximum Aperture: 370 mm

Data Channels: Filtered force at 20 bit, distance at 24 bit

External Instrument Channels: Four channels of RS485

Power supply: Universal mains input voltage

Net weight: 16.2 kg

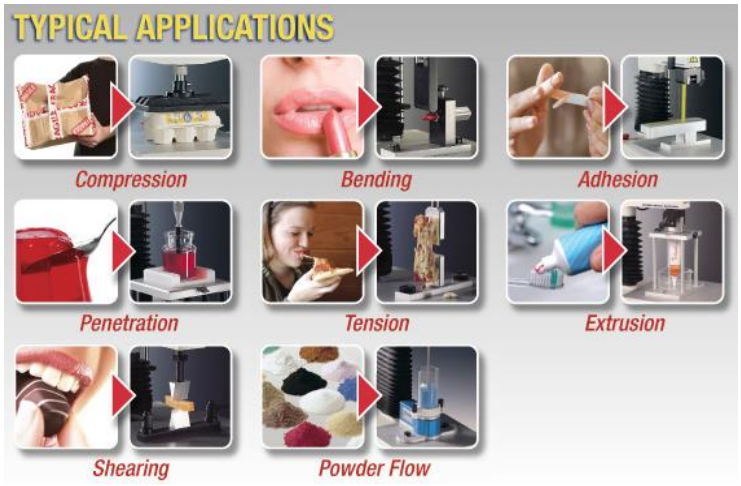

Figure 25. Brief description of TA.XT Stable micro systems texture analyser, its technical specifications and typical applications.

TA.XT plus texture analyser is a Stable micro systems' texture analysis instrument, capable of measuring any physical product characteristic, such as hardness, fracturability, adhesiveness, gel strength and extensibility of foods. The instrument is commonly employed to measure and quantify fundamental, empirical and imitative tests in compression and tension, texture analysis as well as the effect of rheology of solid and semi-solid. The analyser covers compression, bending, adhesion, penetration, tension, extrusion, shearing and powder flow. Results that can be obtained from this equipment include hardness and cohesiveness, making it useful for this project (**Figure 25**).

Each probe or fixture is designed for specific group of applications, and can be attached to the texture analysers base and/or arm. Samples are placed on the base or between two fixtures. The arm of the texture analyser, contaning a loadcell, moves down to penetrate or compress the profuct, and then returns to its initial posiiton. This is considered a standard test within an industry.

4.2.1. TEXTURE PROFILE ANALYSIS

Texture Profile Analysis (TPA) is a double compression test for determining textural properties of foods. Samples were compressed twice to provide insight into how samples behave when chewed. It is often called a "two bite test" because texture analyser mimics the mouths biting action. Texture of food is multi-faceted. The advantage of TPA is that it can quantify multiple textural parameters in one experiment. Many researchers rely on TPAs labelled characteristics without considering whether the test method provides metrics that are relevant to the

experimental objective. Hence, it is important to establish which of the parameter is considered in this study. TPA shows factors such as hardness, cohesiveness, springiness, stickiness, chewiness. **Table 4** shows a typical result from a TPA test, conducted in this study.

Compression Type	Result of Texture Profile Analysis
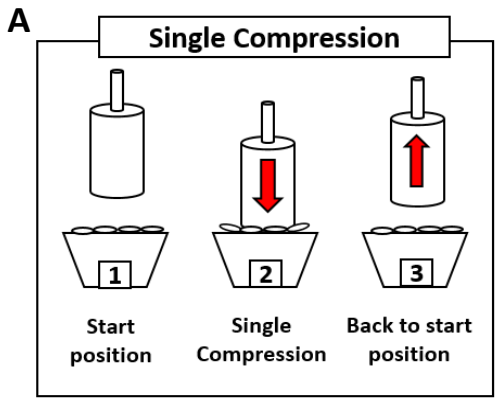	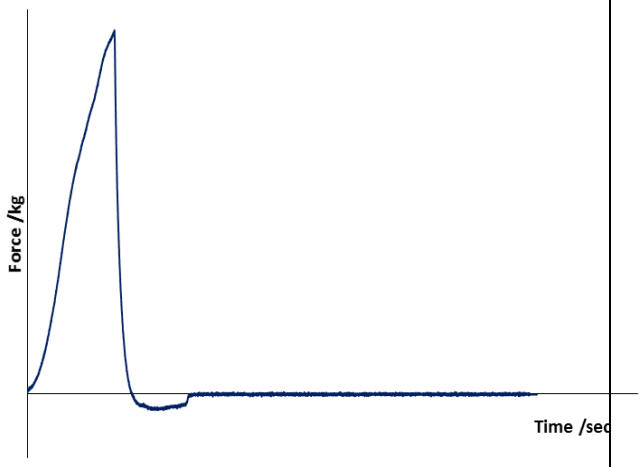
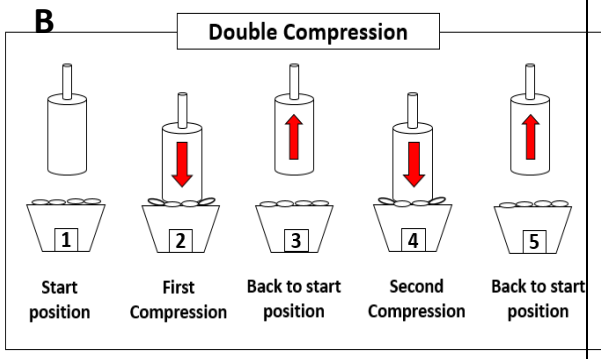	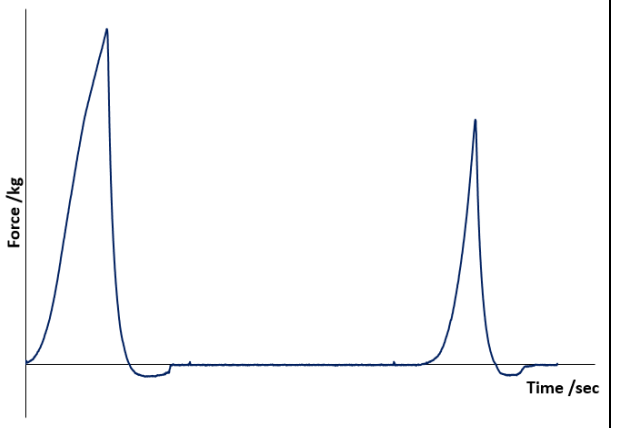

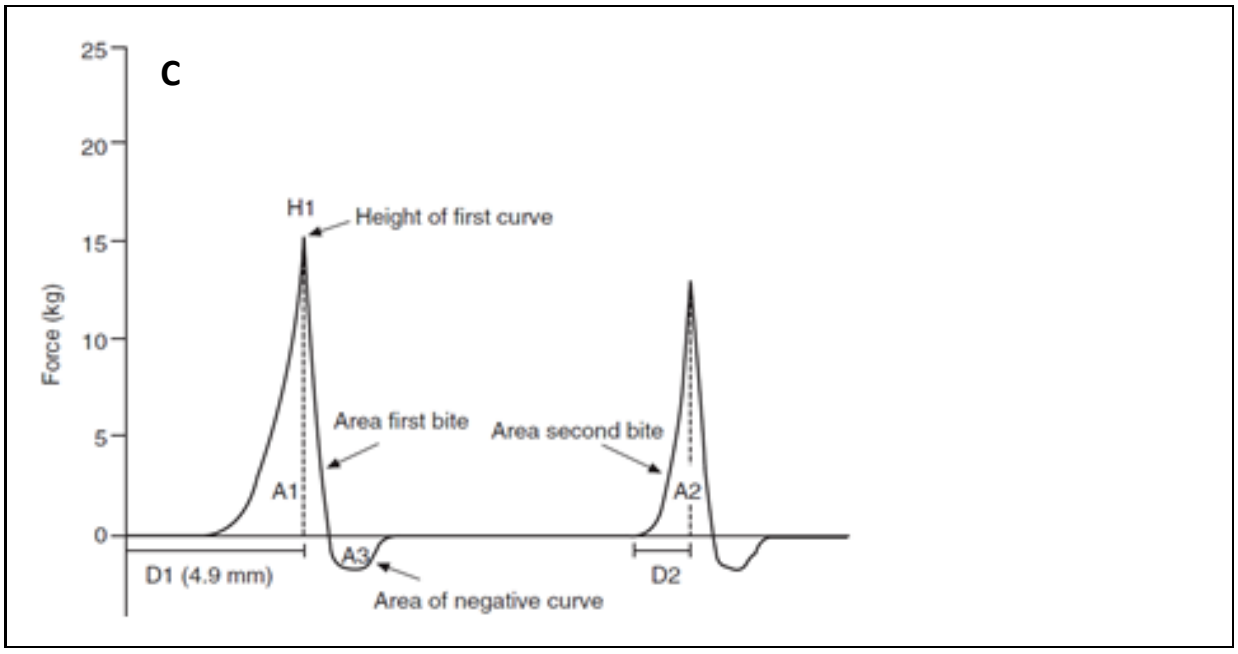

Figure 26. TPA test: (A) single compression, (B) double compression. (C) explanation of double compression test.

Lyon *et al*, 2000 reported that the two-cycle compression for texture profile parameters accounted for the least variation in the data on texture differences. Therefore, in this study, the double compression test is used (**Figure 26B**). With reference to **Figure 26C**, adhesiveness is measured as **A3**, which is the area of negative curve, in this case, representative of the first 'pull' or the first, in other words, work necessary to pull compressing probe away from sample. Meanwhile hardness is represented by **H1**, which is the peak force of the first compression cycle, which in sensorial definition is force required to compress a food between molars, also defined as force necessary to attain given deformation.

Table 4. Table of results computed from a Texture Profile Analysis, TPA test.

Test ID	Hardness g	Adhesiveness g.sec	Springiness	Cohesiveness	Gumminess	Chewiness	Resilience
Sample T1	521	-117	0.750	0.316	165	124	0.106
Sample T4	578	-137	0.642	0.298	172	111	0.095
Sample T7	650	-177	0.576	0.325	211	122	0.118
Sample T6	561	-165	0.591	0.288	161	95.3	0.098
Sample T5	572	-166	0.605	0.381	218	132	0.144
Sample T2	443	-145	0.622	0.364	161	100	0.123
Sample T3	657	-157	0.645	0.309	203	131	0.113
End of Test Data							
Average:	569	-152	0.633	0.326	185	116	0.114
S.D.	73.5	20.4	0.0570	0.034	25.1	14.5	0.0170
Coef. of Variation	12.9	-13.4	9.08	10.5	13.6	12.5	14.7

4.2.2. TEXTURE PARAMETERS FOR COOKED RICE ANALYSIS

TPA parameters are automatically calculated which encourages researchers to use results without considering whether the parameters are appropriate for the objective of the project. Hardness and adhesiveness are the most frequently tested parameters for cooked rice texture. Hardness parameter is used because it is measures the force required to compress cooked rice grains between the molars and acts as the force necessary to attain a given deformation. Adhesiveness parameter was used because it represents the work necessary to overcome the attractive forces between the surface of rice grains and the surface of teeth.

Springiness is defined as the height that the food recovers during the time that elapses between the end of the first bite and the start of the second bite. Springiness is not useful as we do not need to analyse how shape/size rice grains 'springs' back after being compress between teeth. Also, the factor of samples having different lengths is not important as part of this study, as rice cluster samples are of the same volume and height. Cohesiveness was not used as it is a

measure how the product can withstand compression, which is the strength of internal bonds making up the body of product. This study is interested more in the surface properties of the rice grains and sticky behaviour sticking to the surface of molars when chewing, not relevant to the internal body of rice grains.

Table 5. Sensory and instrumental definition of texture parameters in TPA.

PARAMETERS[1]	SENSORY DEFINITION	INSTRUMENTAL DEFINITION
Hardness	Force required to compress a food between the molars. Defined as force necessary to attain a given deformation.	Peak force of the first compression cycle.
Springiness Index Preferred for comparing samples of different lengths	Ratio of the height the sample springs back after the first compression compared to the maximum deformation.	Springiness divided by total deformation.
Corrected Cohesiveness (PELEG, 1976)	Net work invested in the non-recoverable deformations of the first and second chews.	The ratio of the net work of the second cycle $B_1 - B_2$ divided by that of the first cycle $A_1 - A_2$.
Corrected Chewiness	The net energy required to chew a SOLID food to the point required for swallowing it.	The product of hardness, corrected cohesiveness and springiness index
Resilience (PELEG, 1976)	Measurement of how a sample recovers from deformation in relation to speed and forces derived.	Resilience is the ratio of work returned by the sample as compressive strain is removed (known as recoverable work done A_2), to the work required for compression (known as hardness work done A_1).
Adhesiveness	The work necessary to overcome the attractive forces between the surface of the food and the surface of other materials with which the food comes into contact (e.g. tongue, teeth, palate). Work required to pull food away from a surface.	The negative area for the first bite, representing the work necessary to pull the compressing plunger away from the sample. (No adhesiveness is seen in graphs above.)
Adhesive Force (Fiszman and Damaio, 2000)	The maximum force required to separate teeth after biting sample.	Maximum negative force generated during probe return.
Gumminess Applies to semi-solid products only if they have no springiness & undergo permanent deformation	Energy required to disintegrate a SEMI-SOLID food product to a state ready for swallowing. Related to foods with low hardness levels.	The product of hardness and cohesiveness.
Cohesiveness A measurement of how well the structure of a product withstands compression	The strength of internal bonds making up the body of the product (greater the value the greater the cohesiveness)	The ratio of the work during compression (downward stroke only) of the second cycle B_1 divided by that of the first cycle A_1.
Chewiness Solid foods only	The energy required to chew a SOLID food to the point required for swallowing it.	The product of hardness, cohesiveness and springiness.

4.3. EXPERIMENTAL CONSIDERATIONS

Several factors need to be considered when using the texture analyser, which can all affect results (Stable micro systems, 2015). This includes (i) TPA settings, (ii) selection of the probe, (iii) number of replicates needed for a reliable data (iv) sample preparation, which is the cooking of rice for analysis (v) sample presentation, or sample size and shape; the amount of rice grains and (vi) sample temperature. In addition, Dr Bourne, editor of Journal of Texture Studies emphasized on close observation of samples during testing instead of just watching the graphs being plotted.

4.3.1. TEXTURE PROFILE ANALYSIS (TPA) SETTINGS

T.A. Settings:- TPA

Sequence Menu (Click to see options)

Caption	Value	Units
Pre-Test Speed	1.00	mm/sec
Test Speed	1.70	mm/sec
Post-Test Speed	1.70	mm/sec
Target Mode	Strain	
Strain	75.0	%
Time	1.00	sec
Trigger Type	Auto (Force)	
Trigger Force	5.0	g
Break Mode	Off	
Tare Mode	Auto	
Advanced Options	On	
Control Oven	Disabled	
Frame Deflection Correction	Off (XT2 compatability)	

Alterations that were made for this study:

Settings:

Pre-Test Speed: 1 mm/sec

Test Speed: 2 mm/sec

Post-Test Speed: 2 mm/sec

Distance: 10 mm

Trigger force: 5.0 g

Time: 2 sec

Figure 27. Settings used for Texture Profile Analysis (TPA) in Texture Exponent 32 software.

Szczesniak (2015) advised to not deviate greatly from TPA methods and to use the Simplified TPA versions of the TPA project that is preloaded in the latest version of the Texture Exponent 32 software. It uses an advanced macro to analyze TPA curves and does not require a separate TPA results file. Therefore, this project used a preloaded rice adhesiveness study, with several adjustments. In order to properly calculate many TPA parameters, tests were conducted with the same speed for compression and withdrawal, or in other terms, same test and post-test speeds. Therefore, in this study, 2 mm/s was selected for test and post-test speed, which is recommended in the sample rice project in the exponent software.

The settings works by the probe searches for the top of the sample. The instrument begins recording data as soon as the automatic trigger is achieved at the specified trigger force (5.0 g). The probe then compresses the sample at the test speed (2 mm/s) and travels the target distance or percent strain. Once it has achieved the target distance or strain the probe ascends to the original trigger position at the test speed. The instrument then waits for the target time before the second compression occurs at the test speed. The probe finally ascends all the way to the starting position at the post-test speed (2 mm/s). Time between cycles is set to 2 sec to represent gap between rice chewing. This can influence whether the samples have enough time to recover between cycles and it needs to be adjusted to how consumers usually consume their rice.

4.3.2. SELECTION OF PROBE AND FIXTURES

Szczesniak (2015) advised only to use test products which are larger than the probe if resilience, springiness and cohesiveness values are be looked at skeptically. This does not apply to this study as those parameters were not be used. Penetration, bending, cracking, tensile strength probes were not considered as they do not represent rice eating biting action, which is not useful for cooked rice perception. Suitable probes are such that it compresses the sample and measures the sample break and pull from the sample. Hence, the probe shown in **3.5.1. Texture analyser** was used. It was important to observe adhesion tests to prevent bias in results. In many instances cooked rice grains sticks to the probe and lifts partially (**Figure 28**). This is considered failed TPA adhesive which result in probe reaching the same highest point as the original product height even when highest point is lowered as a result of lifted rice.

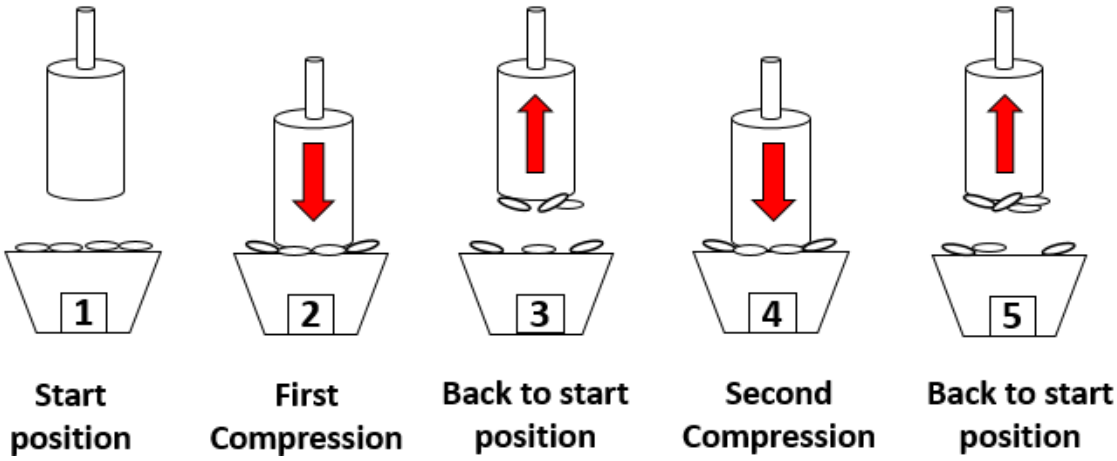

Figure 28. Failed adhesiveness Texture Profile Analysis (TPA) test for this project.

4.3.3. NUMBER OF REPLICATES

Since the texture analyser and its adhesive parameter is considered temperamental and is known for its high standard deviation and standard error, it was essential to establish number of replicates needed for this study. **Figure 29** shows how the number of replicates affect adhesiveness of cooked rice. The first three replicates obtained in a randomized texture analysis experiment were taken and averaged to obtain an adhesiveness of 24.7 g.sec. This is calculated up to 15 replicates.

It was observed that with increasing number of replicates, the error bars were wider and there is also a slight decrease in adhesiveness. The decrease in adhesiveness can be explained by prolonged exposure to room temperature, causing rice to slightly retrograde and become harder. As different rice varieties were selected randomly for analysis, there was a time gap between the first few replicates and the last few. Therefore, there is need to ensure balance of sufficient number of replicates to result in a good adhesiveness data but not too many replicates to introduce high standard error and lower adhesive value. In this study, the number of replicates used for cooked rice texture analysis was between 7 and 10. Most studies were carried out with 8 replicates.

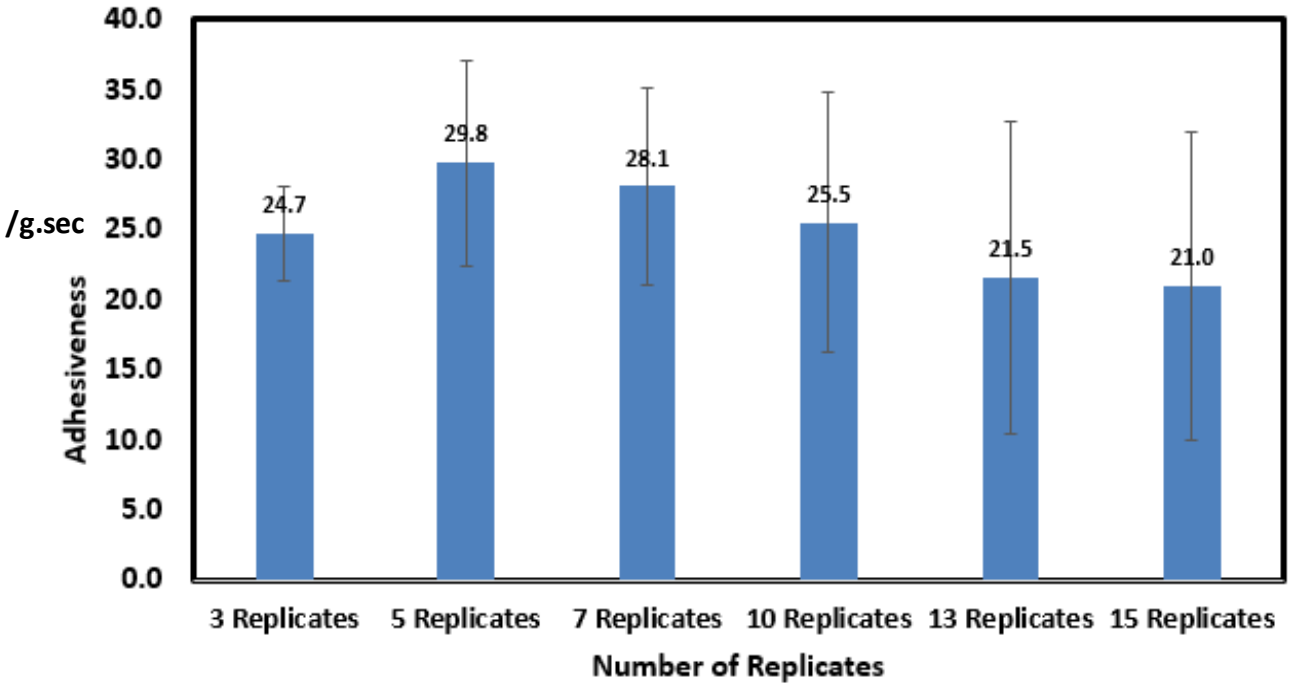

Figure 29. How number of replicates affect cooked rice textural result of a rice variety.

4.4. SAMPLE PREPARATION

4.4.1. DEVELOPMENT OF COOKING METHODS

Before developing texture analyser methods, it is essential to develop a repetitive, reliable cooking method for rice. Different rice cooking methods include excess water (open pan) method, limited water (covered pan) method, using a rice cooker, using microwave and oven baking (**Table 6)**. The first three methods were studied as they are the top three methods used by researchers as well as traditionally cooked at home. Microwave cooking is too unconventional while oven-baking takes too long.

Oven and microwave methods were the first two to be rejected as it is not the conventional method to cook rice traditionally at home and the final rice texture is also different and hence, cannot be compared. Although it takes a longer time than open and covered pan method, the rice cooker method is the easiest method as it requires little to no attention. However, as there are too many different sample types used, the number of rice cookers needed is not feasible. To accommodate large sample varieties, volumes and replicates, a closed pan method was used to cook rice used in this project.

Table 6. Selection of cooking of cooked rice for this project.

	Excess water (Open Pan)	**2:1 Water:Rice (Closed Pan)**	**Rice cooker**	**Microwave**	**Oven**
Rice	50g	50g	50g	50g	50g
Water	500g	100g	100g	100g	100g
Covered?	No	Yes	Yes	Yes	No
Duration	10-12minutes	10-12minutes	20minutes	10minutes	40minutes
Attention	No	Yes	No	Yes	No
Heat source	Heating pad	Heating pad	Rice cooker	microwave	oven
Require Temperature control	Yes	Yes	No	No	No
Large sample varieties, volume plus replicates	Feasible	Feasible	Not feasible	Not feasible	Not feasible
Selected	X	√	X	X	X

Key: Desirable factor; Undesirable factor; Neutral

4.4.2. COOKING MILLED RICE POWDER

One method of ensuring that rice samples are cooked uniformly is by cooking the ground rice powder. This eliminates external factors which can affect rice cooking procedure, which includes different sizes of rice grains, uniform rice cooking, accurate temperature and time. Rapid Visco Analyser (RVA) cooks rice powder the same way each time, as long as the parameters are set. **Figure 30** shows the same trend in hardness and adhesivess in all samples, which indicates, if using RVA rice powder, that when rice is hard, it is sticky too, which does not make sense. Champagne, 1999 also reported that results of TPA were not modelled by RVA with high accuracy (i.e., high r^2). Hence, this method was not followed.

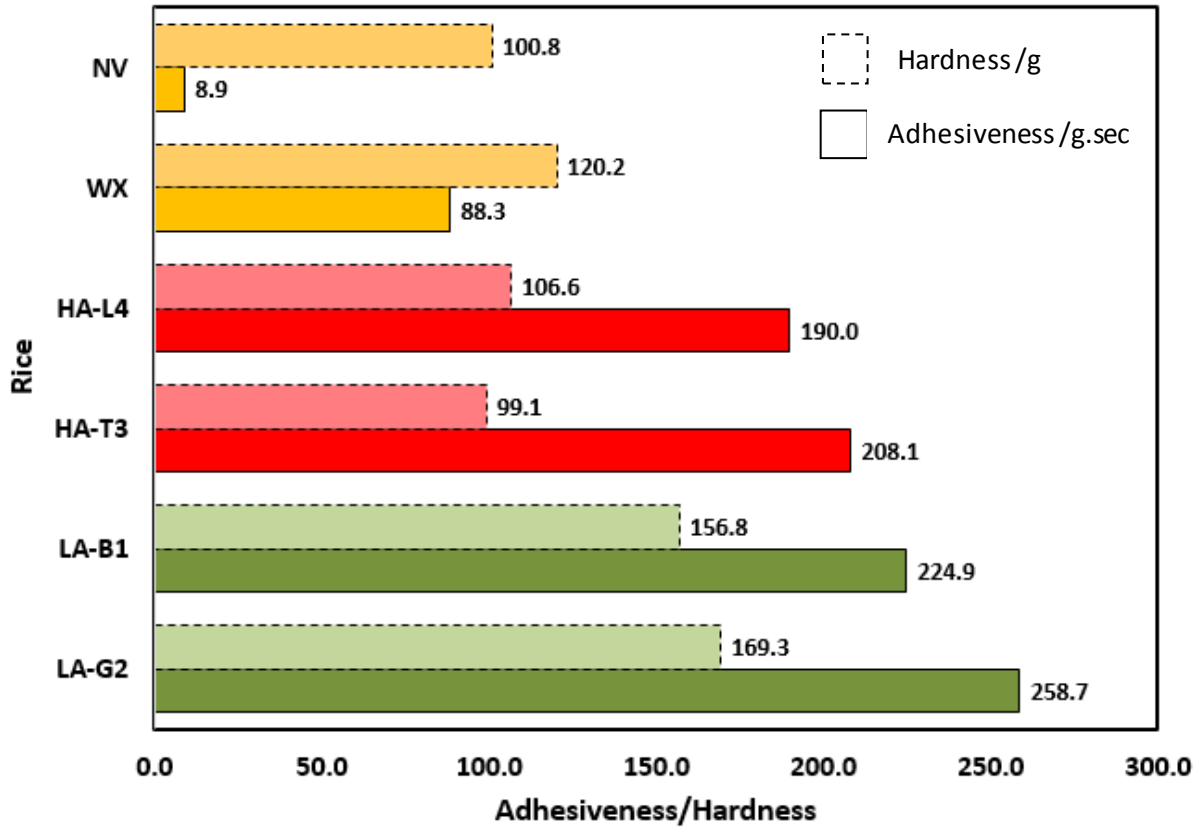

Figure 30. Rapid Visco Analyser (RVA) of rice flour and starches.

4.4.3. RICE SAMPLE SIZE

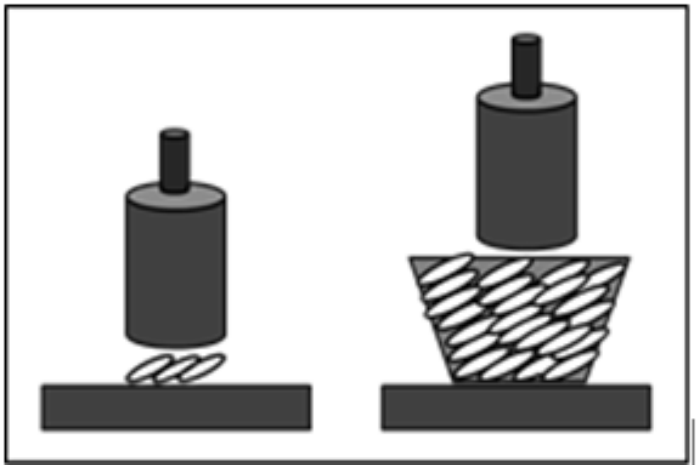

Figure 31. Individual rice and set weight/volume rice grains compression.

This is to note that this was performed but results were unsatisfactory for analysis (results not shown in this thesis).

4.5. HARDNESS AND ADHESIVENESS

As discussed earlier, hardness /g and adhesiveness /g.sec are the two selected parameters for cooked rice analysis in this project. **Figure 32** shows results of texture analysis conducted on 12 different rice varieties randomly selected for this selection process. These consist of rice varieties which are both commercially available in UK supermarkets and grown in Brunei Darussalam; TL - **BS**, TL - **LG**, TL - **TJ**, TS - **BS**, TS – **LG**, TS - **TJ**, SS - **BS**, SS - **LG**, SS - **TJ**, SS - **AR** and **LL**. The second code for rice varieties, denotes BS for Basmati rice, LG for Long Grain and TJ codes for Thai Jasmine varieties.

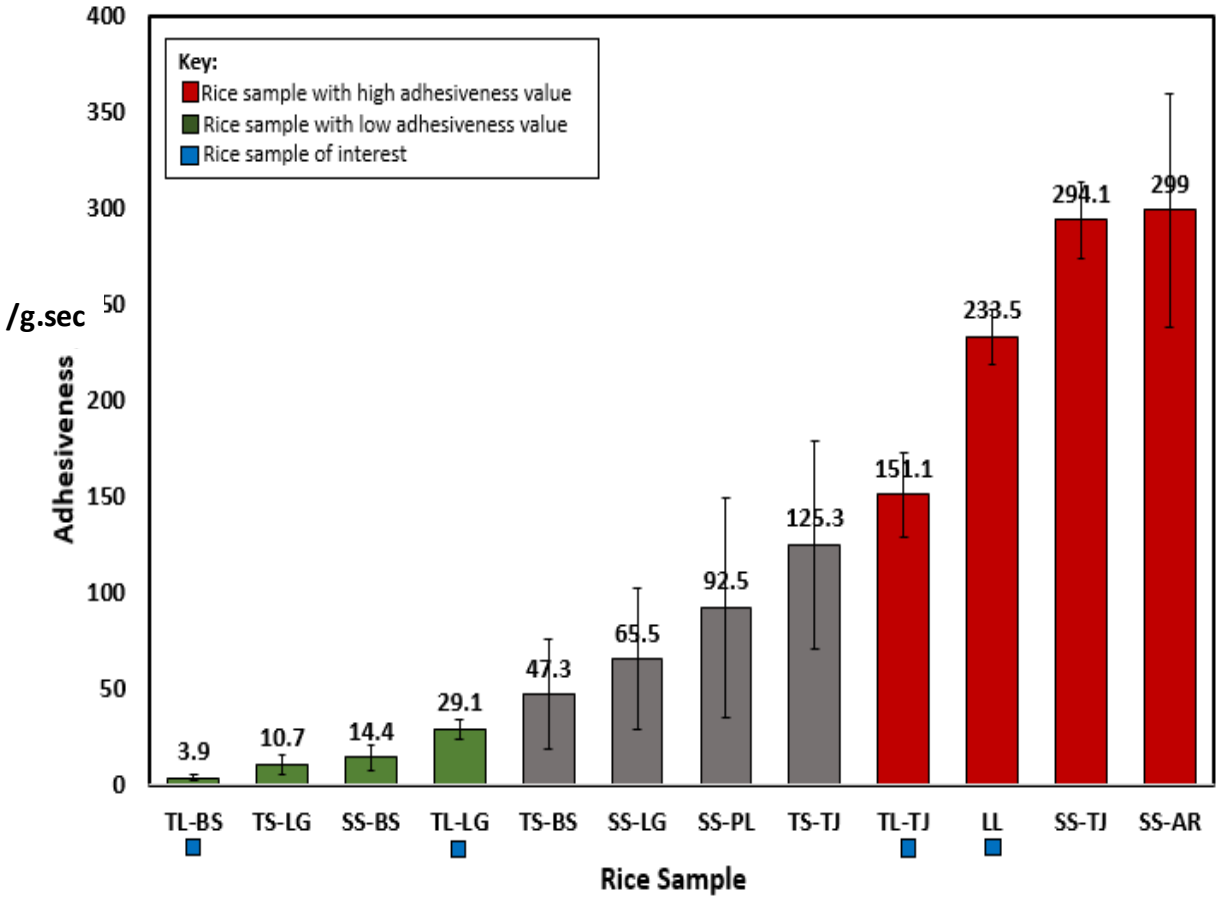

Figure 32. Graph showing adhesiveness /g.sec of the 12 commercial rice varieties considered for this study.

Adhesiveness values of the 12 rice samples range from 3.9 to 299.0 g.sec. TL-BS had the lowest adhesiveness (3.9 g.sec) while SS-AR has the highest adhesiveness (299.0 g.sec). All basmati and long grain varieties are in the low adhesive group while Thai Jasmine varieties are in the high adhesive groups. This shows that same rice variety but of different brands have different adhesiveness but the trend is the same amongst the same brand.

Hardness values for the 12 different rice types range between 382.6 g to 747.8 g. Amongst the 12 rice types, TS-LG has the highest hardness (747.8 g) and TS-BS has

the lowest (382.6 g). However, there is no observable difference between rice varieties or brands. In addition, the standard error is very high and there is no significant difference between most samples. Therefore, hardness parameter is not used further in this study which only focuses on adhesiveness. This corresponds with objective of this project whereby it concentrates on the stickiness of cooked rice.

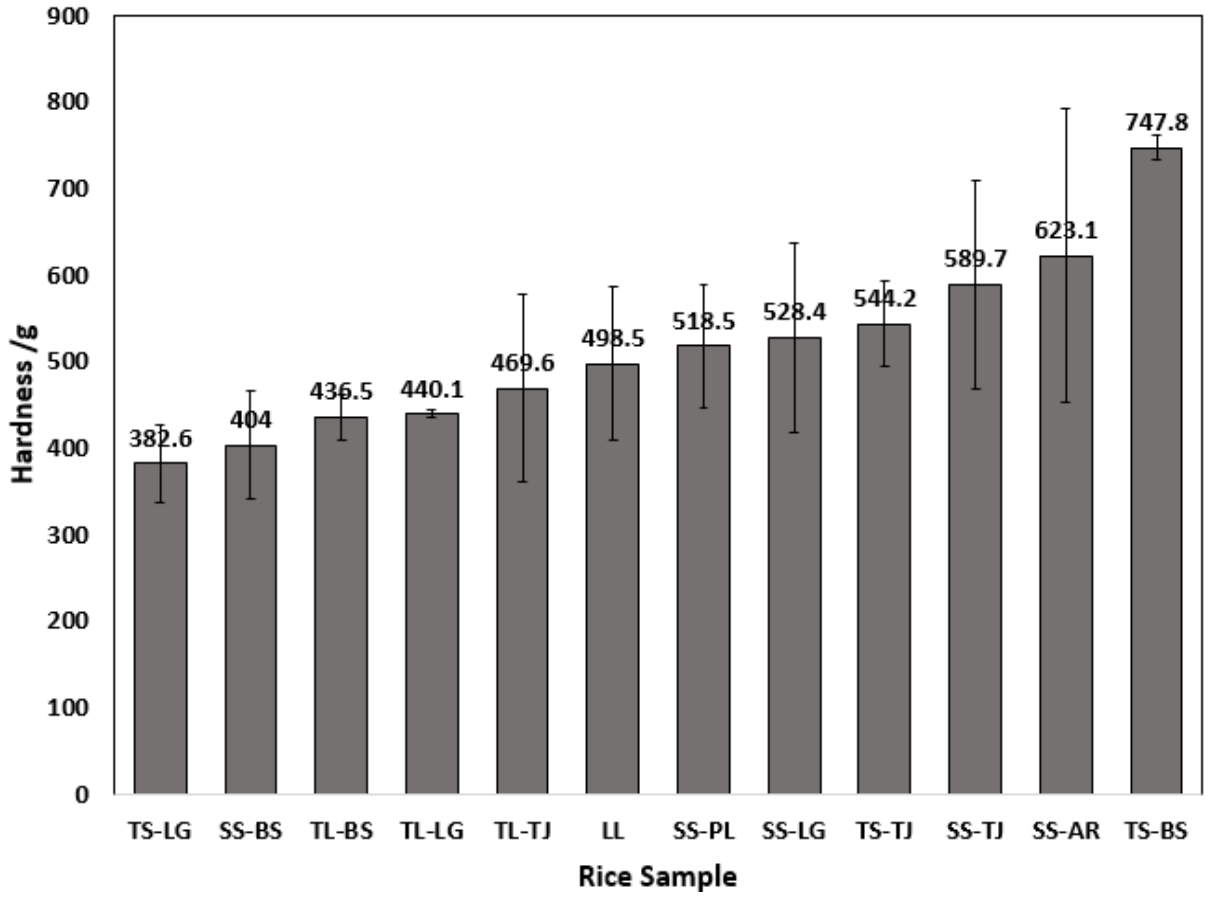

Figure 33. Hardness /g the 12 commercial rice varieties considered for this study.

4.6. SELECTION OF RICE SAMPLES FOR PROJECT

It has been shown that TL-BS, TS-LG, SS-BS, TL-LG have lowest adhesiveness while TL-TJ, LL, SS-TJ and SS-AR has highest adhesiveness. In-order to understand and study the factors that contribute to the adhesive texture of cooked rice, a selection of rice types was considered essential further study. For low adhesive studies, Low adhesive TL-BS (3.9 g.sec) and TL-LG (29.1 g.sec) were selected because both were in the low adhesive group and they were significantly different from one another. TS-LG and SS-BS were not considered as the samples were not significantly different. It is good to have different levels of adhesive samples to observe whether they are different.

For the high adhesive rice studies, TL-TJ (151.1 g.sec) and LL (233.5 g.sec) were selected because both were in high adhesive group and they were significantly different from one another. SS-AR was not used as the sample was too unstable, the standard deviation was high despite repetitive sample preparation. Despite SS-TJ having a very high adhesiveness value, TL-LG was selected for this study as it is the same brand as the low adhesive samples, making it a good comparison. LL is Laila rice which is grown in Brunei was good to include in this project in-order to have a better understanding of its textural properties. For the rest of this study, low adhesive group is referenced as: **LA-B1** (low adhesiveness TL-BS) and **LA-G2 (**low adhesiveness TL-LG) and high adhesive group sample is referenced as: **HA-T3** (high adhesiveness TL-TJ) and **HA-L4** (high adhesiveness LL).

4.7. SUMMARY AND CONCLUSION OF CHAPTER

From this chapter, it is established that throughout this project:

- To quantify the texture of cooked rice, instrumental texture evaluation was used, specifically the TA.XT texture analyser. Texture Exponent 32 software was used to perform Texture Profile Analysis (TPA).
- The TPA parameter selected was adhesiveness (g.sec) for determining the sticky texture of cooked rice.

From the results of texture analysis, it can be concluded that:

- Due to their favourable textural properties of low and high adhesiveness, low adhesive LA-B1 and LA-G2, and high adhesives HA-T3 and HA-L4 rice samples were selected for further study in this project.

5. BASIC RICE COMPOSITION

The previous chapter reports four rice varieties selected for this project: low adhesives LA-B1, LA-G2 and high adhesives HA-T3, HA-L4. In-order to have a better understanding of factors that contribute to differences in their texture, the profiles of these rice grains were obtained. This chapter aims to provide an analysis of the composition of the rice varieties used in this study. As previously mentioned in **2.1.1. Rice grain**, an individual rice grain is composed of 90 % starch, 7 % protein and 1 % lipids. This chapter starts with an analysis of starch composition and structure, followed by protein and lipid analysis and ends with a conclusion of how their composition correlates with their texture.

5.1. STARCH COMPOSITION

5.1.1. TOTAL STARCH ASSAY

Figure 34 shows results of Megazyme total starch analysis (**3.6.1. Megazyme total starch assay kit**) of chosen rice samples, ground to a powder form (**3.2.1. Preparation of rice powder: milling**). Pure starches waxy and native rice are used as controls as this provides a good comparison between extracted rice starch and milled rice grains or 'rice flour'.

Results showed that the starch content of the samples ranged between 87.0 – 92.0 % for pure starches and between 80.4 – 85.4 % for milled rice grains. It is interesting to note that even for pure starches, starch values were not near 100 %. Rice starch isolation studies conducted by Lumdubwong and Seib (2000) and Wang and Wang (2001) yield between 73 – 95 % starch. This can explained by difficulties

in starch extraction, where minor constituents including protein, lipids and phosphorus are commonly found in isolated rice starch (Champagne, 1996). Morrison *et al*, 1984 also reported the presence of starch complexes, such as amylose-lipid complexes. Compared to the pure rice starches, the rice flours exhibit lower total starch content. This is expected as milled rice grains still contains native rice protein and native rice lipid (Bao and Bergman, 2004), hence, lowering the percentage of rice starch present.

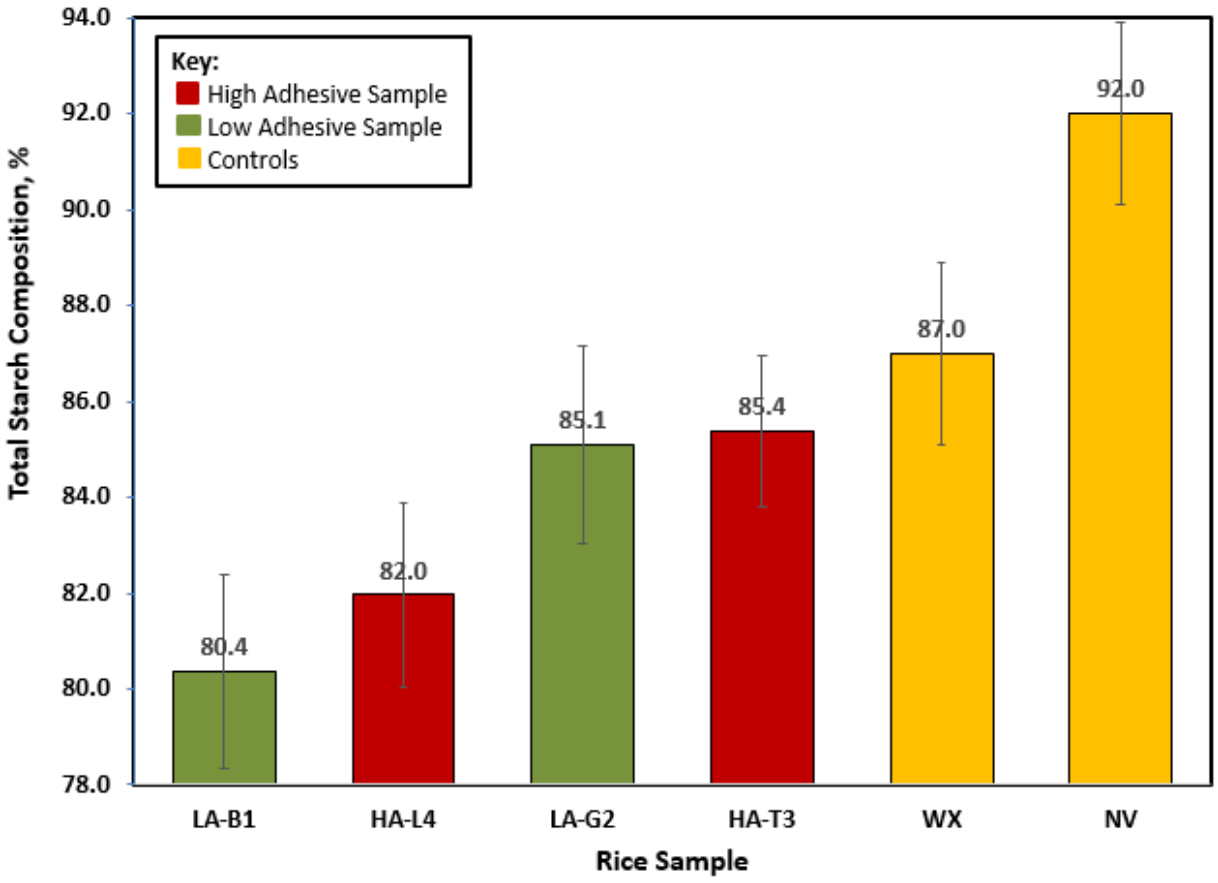

Figure 34. Total starch content (%) of the rice flours chosen in this study; low and high adhesiveness LA-B1, LA-G2, HA-T3, HA-L4, and waxy and native rice starches.

High adhesive HA-T3 and low adhesive LA-G2 had the highest starch content amongst the chosen rice samples at 85.4 % and 85.1 % respectively, followed by

high adhesive HA-L4 (82.0 %) and low adhesive LA-B1 (80.4 %). There was no significant difference in starch content between low adhesive and high adhesive rice samples. Therefore, it can be concluded that in this study and for the four samples used, there was no correlation between total starch content and cooked rice texture, and that the total starch content of rice has no contribution to cooked rice texture.

5.1.2. AMYLOSE AND AMYLOPECTIN ASSAY

Since starch content did not have any correlation with cooked rice texture, the breakdown of the starch components was analysed further. **Figure 35** shows results of amylose/amylopectin assay (**3.6.2. Megazyme amylose/amylopectin assay**). Results showed that pure starches native and waxy contain 27.1 % and 2.0 % amylose respectively. Meanwhile, for the milled rice grains, the percentage of amylose ranged from 19.3 % to 27.1 %.

Apart from potential inefficient removal of protein and lipid components during the assay, differences in amylose contents between rice starch and rice flour should not be affected by the presence of native and protein content. Several studies have reported similar results whereby isolated rice starch contains nearly 30 % amylose (Bao and Bergman, 2004), short, medium and long rice grains contains between 18–26 % amylose while waxy rice starch contains approximately 0 - 2.3 % amylose (Shelton and Lee, 2000).

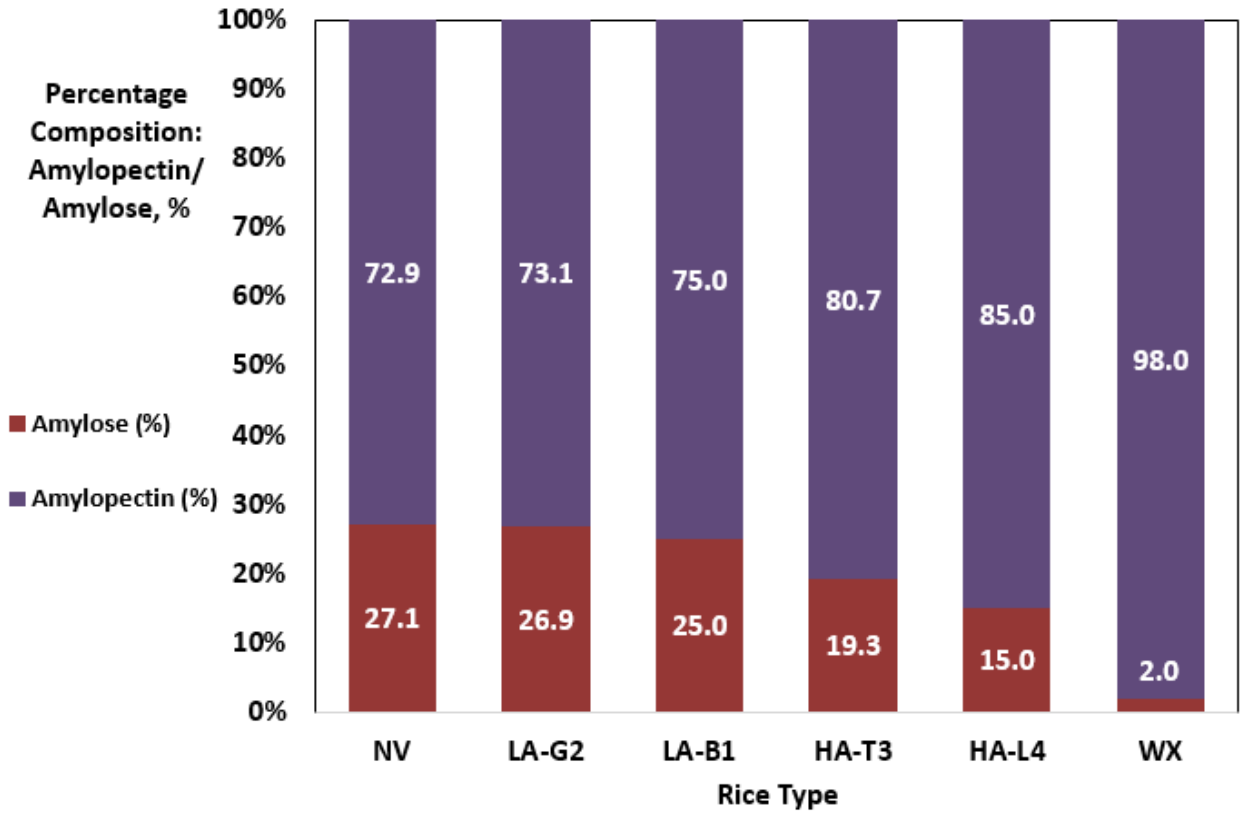

Figure 35. Percentage of amylose and amylopectin (%) in the starch granule of rice rice flours and rice starches used in this study; low and high adhesiveness LA-B1, LA-G2, HA-T3, HA-L4, and waxy and native rice starches.

There is a significant difference between the low adhesives (25.0 % - 26.9 %) and high adhesives (15.0 % - 19.3 %) rice samples (**Figure 35**). High adhesives have significantly higher percentage of amylopectin content (or lower percentage of amylose content) compared to the low adhesive rice group. This suggests that there is correlation between ratio of amylose and amylopectin in the starch granule of rice samples and cooked rice texture. This matches studies by Reddy *et al* (1993) and Cameron and Wang (2005) whereby either amylose or amylopectin contributes to the sticky behaviour of cooked rice.

(A)

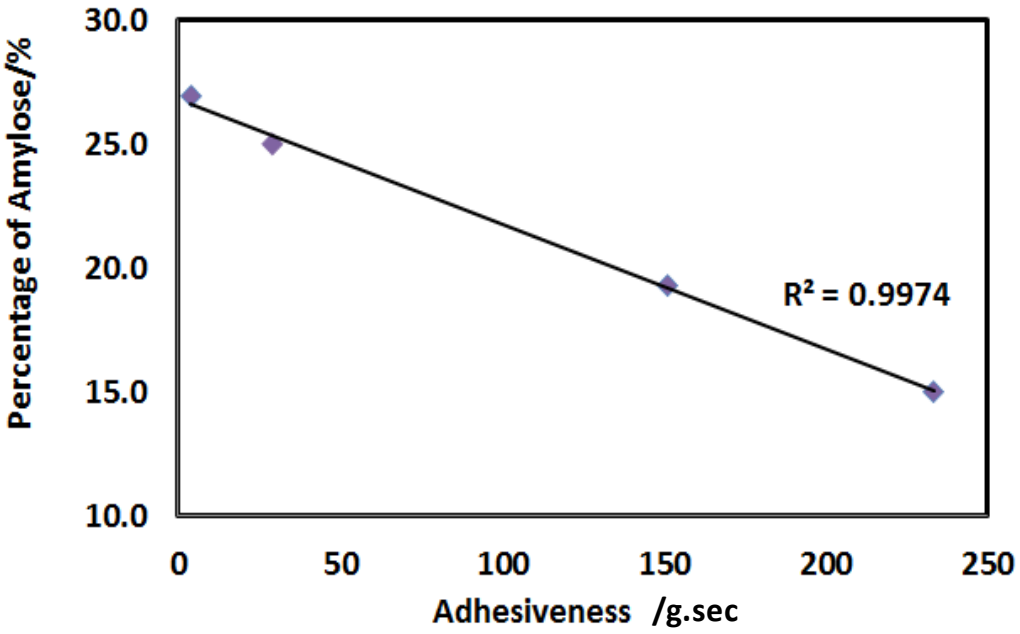

(B)

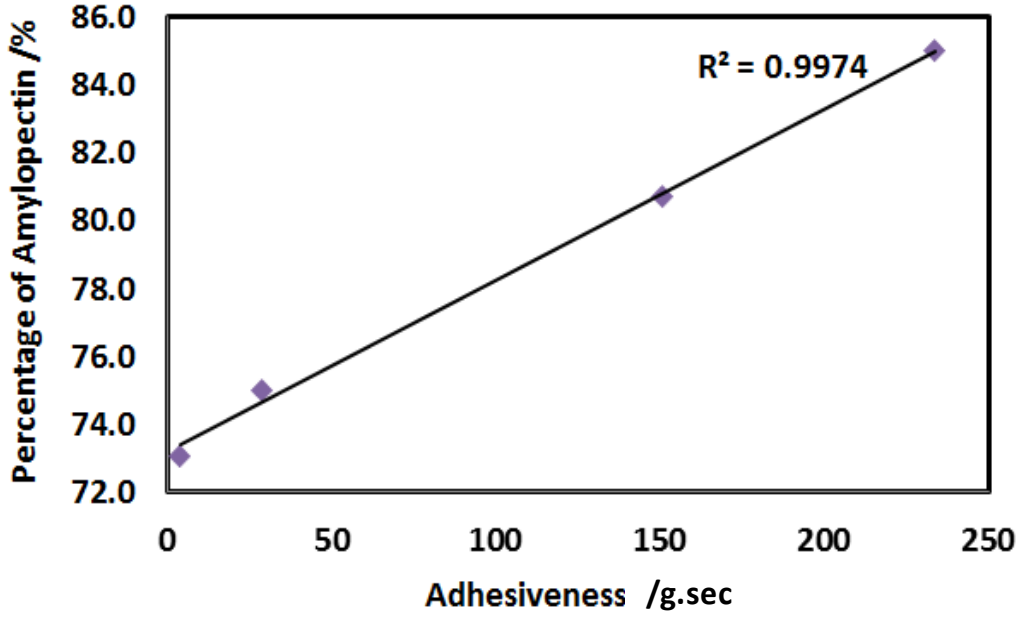

Figure 36. Correlation between adhesiveness of rice (g.sec) and (A) amylose content (amylose %) and (B) amylopectin content (% amylopectin).

There is a negative correlation between amylose content and sticky texture of rice as quantified by adhesiveness /g.sec (**Figure 36A**) while a positive correlation between amylopectin content and rice texture (**Figure 36B**). This indicates that the

lower amylose and higher amylopectin content of the rice sample, contributes to the stickiness of the rice texture. This trend correlates with earlier literature by Juliano (1985) where amylose content was believed to contribute to rice texture. More recent literature by Reddy *et al* (1993), Cameron and Wang (2005) and Ayabe *et al* (2009) concluded that not amylose, but amylopectin contributes to the sticky texture of rice. Hence, it is better concluded that the higher the amylopectin content of the rice, the stickier the rice texture.

5.1.3. SOLUBLE STARCH ASSAY

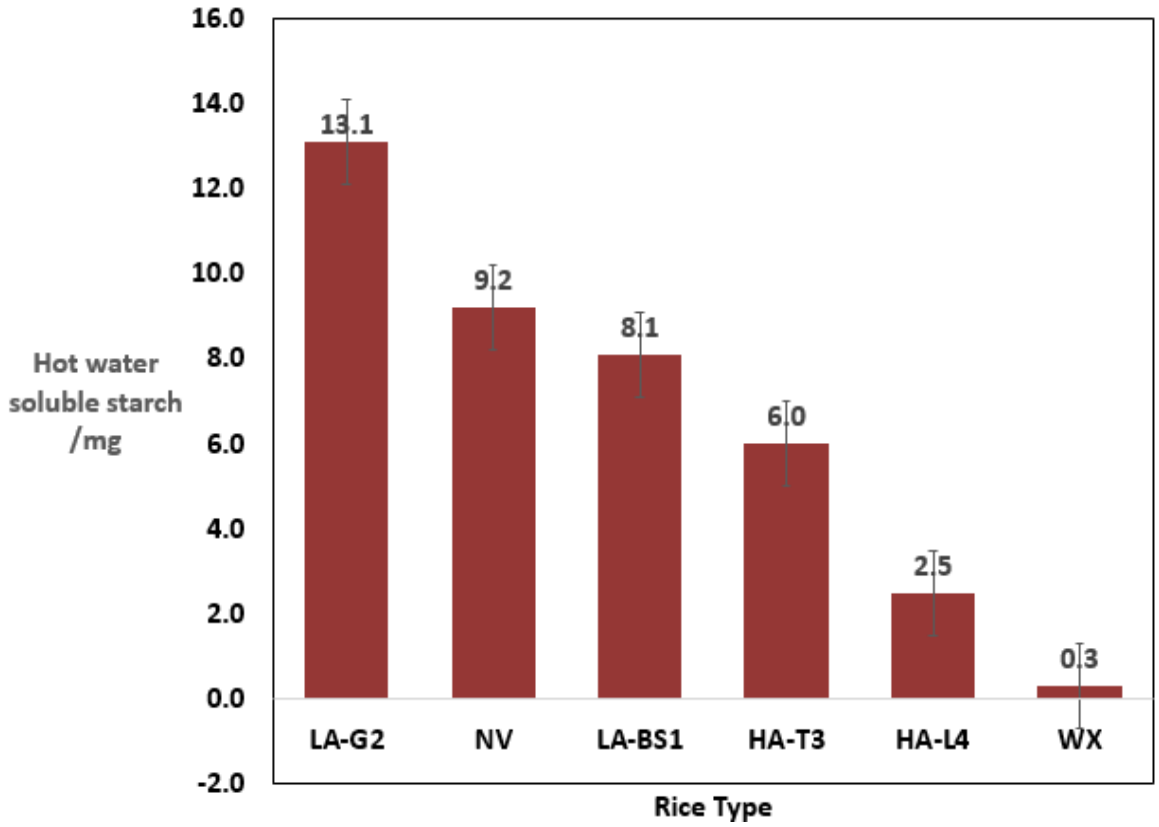

Figure 37. Results of soluble starch assay of rice starches and rice flours used in this study; low and high adhesiveness LA-B1, LA-G2, HA-T3, HA-L4, and waxy and native rice starches.

When iodine reagent is added to starch, amylose and amylopectin in starch reacts with iodine and forms amylose-iodine and amylopectin-iodine complexes. Since amylose has a higher iodine affinity than amylopectin, it is assumed that the absorbance measurement mostly represents amylose-iodine complex. In addition, spectrophotometer measurements were taken at 630 nm, which minimises the presence of amylopectin-iodine complex (Fitzgerald *et al*, 2009). Therefore, leached starch results can represent the relative amylose content of the rice samples. It is termed as 'relative amylose content' and not actual % amylose because actual starch content was not calculated simultaneously in the experiment.

When rice flour is cooked, high adhesive rice releases less hot water soluble starch (2.5 - 6.0 mg) compared to low adhesive rice (8.1 - 13.1 mg). This indicates that the relative amylose content of high adhesive rice varieties is lower than rice varieties with low levels of adhesiveness. This trend is also observed in the results of Megazyme amylose/amylopectin assay where amylose content is negatively correlated with rice adhesiveness texture, which justifies the validity of the results in the assay. Rice flour with highest amylose content (LAG2 – 26.9 %) leach the most hot water soluble starch fractions (13.1 mg) while lowest amylose content waxy starch (2.0 %) leach the least hot water soluble starch (0.3 mg). This shows that the soluble starch assay can be used as a faster and cheaper alternative method for comparison of amylose content in rice starches. However, for actual percentage of amylose/amylopectin, Megazyme amylose/amylopectin assay was used.

5.2. STARCH CRYSTALLINITY

5.2.1. X-RAY DIFFRACTION PATTERN

X-Ray Diffraction, XRD pattern of native and waxy rice starch is presented in **Figure 38**. XRD pattern displays a typical A-type diffraction pattern with an unresolved peak at 17° and 18° and with individual peaks at 15°, 20° and 23°. Lopez-Rubio *et al*, 2008 have predicted that 15°, 17°, 18° and 23° peaks represent relative starch crystallinity while 20° represents V-amylose crystallinity. Upon first glance of raw data, it can be roughly observed that apart from the V-amylose, waxy rice starch exhibited higher 15°, 17°, 18° and 23° peaks compared to native rice.

2.3.2. Semi-crystalline growth rings explain that the starch can be organised into crystalline regions, which can be used to explain the arrangement of amylose and amylopectin in a starch granule. Since waxy rice starch contains more amylopectin (98.0 %) than native rice starch (72.9 %), this can explain why waxy rice has higher crystalline peaks compared to native rice. This will be proven further with calculations of relative starch crystallinity measurements later in this sub-chapter. However, it is interesting to note that for the V-amylose crystalline peak at 20°, the peak is higher in native rice than in non-waxy, which will be elaborated further in the lipid section of this chapter.

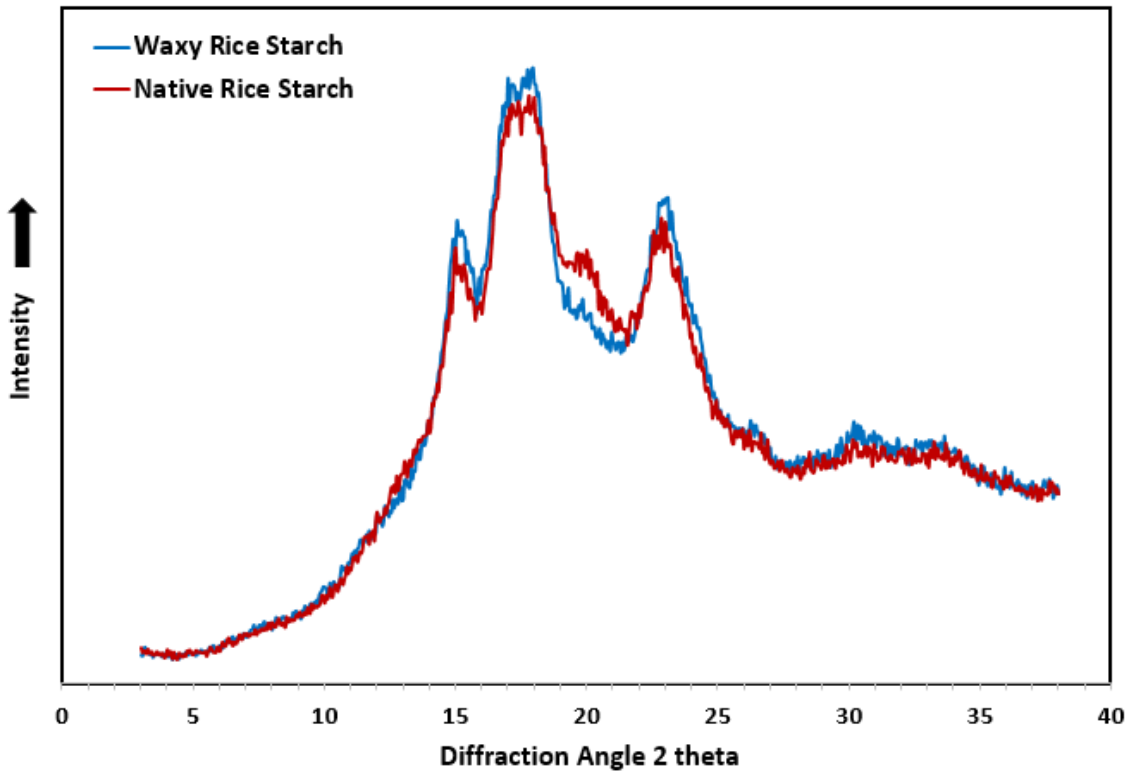

Figure 38. X-ray diffraction pattern of native and waxy rice starch**.**

5.2.2. DETERMINING CRYSTALLINITY MEASUREMENT

As explained in **2.3.3. Starch crystallinity**, the degree of crystallinity is defined as the percentage of crystalline regions with respect to the total material. To be able to quantify the crystalline peaks in X-Ray Diffraction pattern, the method of calculating percentage of crystalline region in a starch granule needs to be established. The 3 known methods are (i) two Phase, (ii) gaussian method using excel solver and (iii) gaussian method using excel solver and incorporating actual amorphous (**Fig 39**). All of the methods have a similar concepts that starch has amorphous and crystalline regions. Non-peak regions represent amorphous

regions, while the peaks represent crystalline region. If the amorphous area is set, the rest of the area is crystalline.

Methods 1 (two-phase) and 2 (gaussian method) generates an estimation of the amorphous area. **Fig 39.1A** shows raw rice starch and rice flour XRD patterns which has been smoothed and the background baseline was subtracted using Diffrac software. **Fig 39.1B** shows XRD data after estimated amorphous area has been subtracted, leaving crystalline region. The area under the curve of **Fig 39.1B** was then calculated to obtain relative starch crystallinity. **Fig 39.2** shows the excel solver drawn up by Dr Bill McNaughtan with gaussian fitting function adapted from Lopez-Rubio *et al* (2008). The native rice starch XRD pattern (blue) was subtracted using the background baseline (red) and estimated amorphous regions (purple) to obtain starch crystalline peaks (green) and V-amylose crystalline peak (black). This method is more reliable as provides optimisation of each individual crystalline peak, minimizes errors by selecting function that provides lowest standard deviations and does not include V-amylose crystalline peak.

Method 3 shown in **Fig 39.3** takes into consideration real amorphous samples, where each sample has its own respective amorphous area, and uses **Method 2** to optimise raw data and real amorphous samples together. However, it is necessary ensure that the amorphous samples are fully amorphous, or properly broken down. This is used by Lopez-Rubio *et al* (2008) and Ottenhof *et al* (2005). This is not commonly used in other samples types, such as cellulose as there is difficulty in obtaining fully amorphous sample.

	Method	Comments	Example results
1	**Two phase Method**	-Diffrac Software -Estimated best fit amorphous area -Does not differentiate starch and V-amylose crystallinity	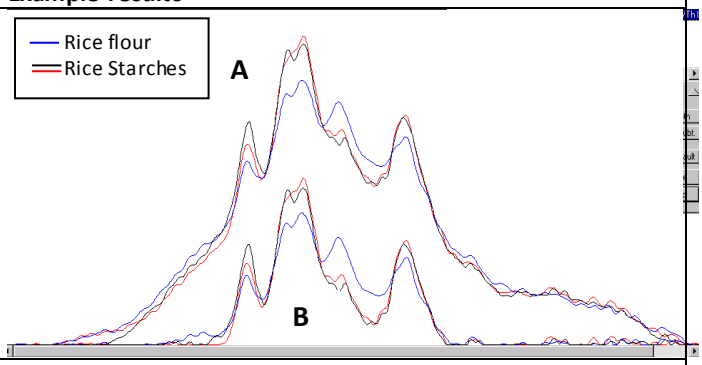
2	**Gaussian Method using Excel Solver**	-Excel Solver -Gaussian Fitting Function -Estimated best fit amorphous region -Calculates starch crystallinity and V-amylose crystallinity separately	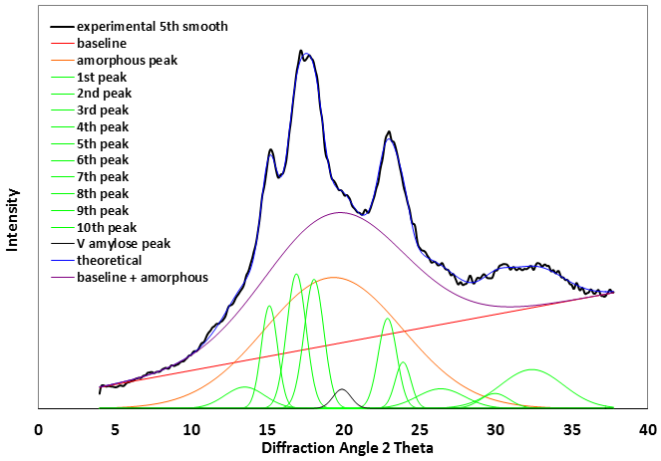
			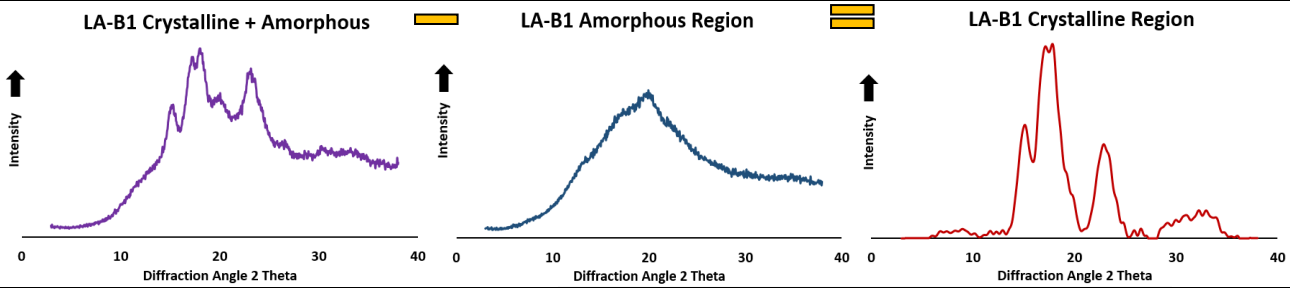
3	**Gaussian Method using Excel Solver and incorporating actual amorphous sample**	-Excel Solver -Gaussian Fitting Function -Actual starch amorphous region -Calculates starch crystallinity and V-amylose crystallinity separately	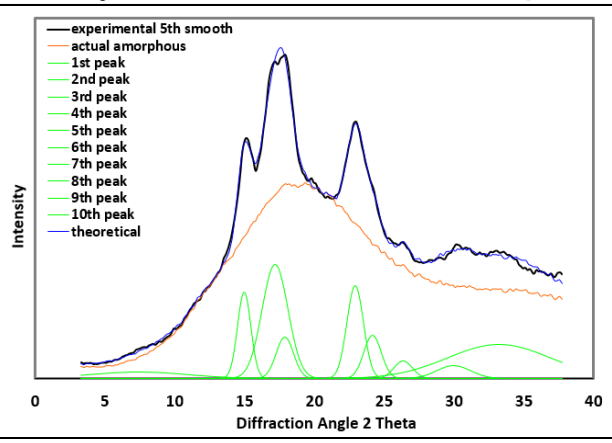

Figure 39. Comparison of methods; (1) two-phase, (2) gaussian Method using excel solver, (3) gaussian Method using excel solver and incorporating actual amorphous sample to calculate relative starch crystallinity using XRD.

Table 7. Results of XRD crystallinity measurements using (1) two-phase method, (2) gaussian method using excel solver, (3) gaussian method using excel solver and incorporating actual amorphous.

	Percentage Crystallinity, %		
	Two phase method	**Gaussian method using excel solver**	**Gaussian method using excel solver and actual amorphous**
Native Rice Starch	31.4 ± 0.6	33.3 ± 0.5	37.0 ± 0.3
Waxy Rice Starch	39.4 ± 0.9	40.0 ± 0.3	40.0 ± 0.3

Table 7 shows that percentage crystallinity obtained for the rice starch samples ranged between 31.4 % and 40.0 %. This corresponds with Lopez-Rubio *et al*, 2008 where pure rice starch crystallinity for two-phase was 31.9 % and Ong and Blanshard, 1995 where relative crystallinity ranged from 29.2 % to 39.9 % for various rice starches. For all 3 methods, waxy rice starch exhibited a higher percentage crystallinity compared to native rice starch. This can be explained by waxy starch (98.0 %) having higher percentage of amylopectin than native starch (72.9 %).

Despite not including V-amylose peak onto crystallinity calculations, gaussian methods (33.3 % - 40.0 %) yielded higher crystallinity values compared to using Diffrac software method (31.4 % - 39.4 %). This can be explained by **Figure 39.2** where gaussian method using excel solver uncovered more peaks compared to the two phase method. Two phase takes into account 5 crystalline peaks and the rest is considered amorphous, while excel solver takes into account 9 crystalline peaks.

Meanwhile, incorporating actual amorphous samples yield equal or higher % crystallinity values (37.0 % - 40.0 %) compared to using best fit amorphous (31.4 % - 40.0 %). The gaussian method using excel Solver and actual amorphous area was further used in this study as the method accounts for actual amorphous regions in the starch and the gaussian method provides a better fit to X-ray Diffraction peaks as opposed to simply an estimation.

5.2.3. UNDERSTANDING STARCH CRYSTALLINITY: LOSS AND GAIN

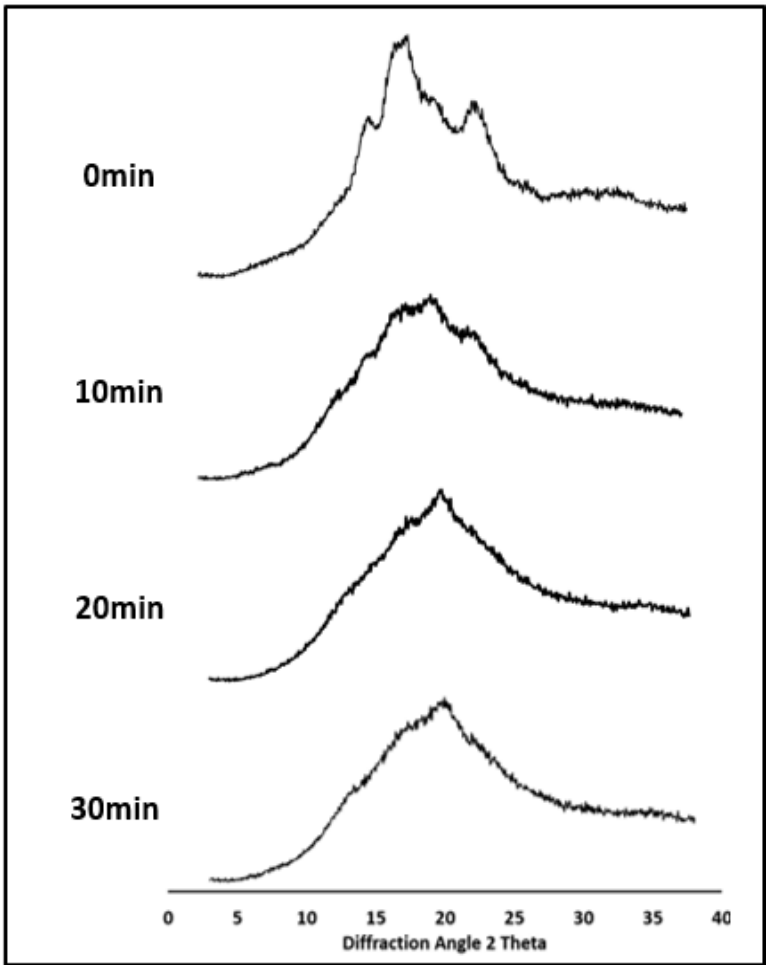

Figure 40. X-Ray Diffraction (XRD) pattern of raw milled LA-B1 rice flour during gelatinisation, at 0, 10, 20 and 30 minutes.

Figure 40 demonstrates changes in crystalline peaks when rice flour is gelatinised. From 0 to 30 minutes gelatinisation, there is gradual disappearance of crystalline peaks 15^{o}, 17^{o}, 18^{o} and 23^{o}. On the other hand, there is still presence of peak at 20^{o}, which is the V-amylose crystalline peak, which remains almost unaffected by the process**.** **Table 8** shows that at 10 minutes of gelatinisation, there is substantial loss of crystallinity from 37.0 % to 8.4 %, followed by further loss of crystallinity at 20 minutes to 3.6 %. Up to 30 and 40 minutes gelatinisation, there is not much change in crystallinity, from 1.8 to 1.5 %. This suggests an almost fully amorphous sample has been attained. Leftover 1.5 % crystalline peaks at 40 minutes gelatinisation can be explained by the fact that the rice sample not fully gelatinised or there are traces of other components which contribute to the crystalline structure. This clearly demonstrates how starch crystallinity is lost when rice flour is gelatinised.

Table 8. Starch crystallinity /% of LA-B1 during gelatinisation at 0, 10, 20, 30 and 40 minutes gelatinisation.

Minutes Gelatinisation	**0**	**10**	**20**	**30**	**40**
Percentage crystallinity /%	37.0 ± 0.5	8.4 ± 0.3	3.6 ± 0.3	1.8 ± 0.2	1.5 ± 0.3

5.2.4. CORRELATION BETWEEN STARCH CRYSTALLINITY AND RICE ADHESIVENESS

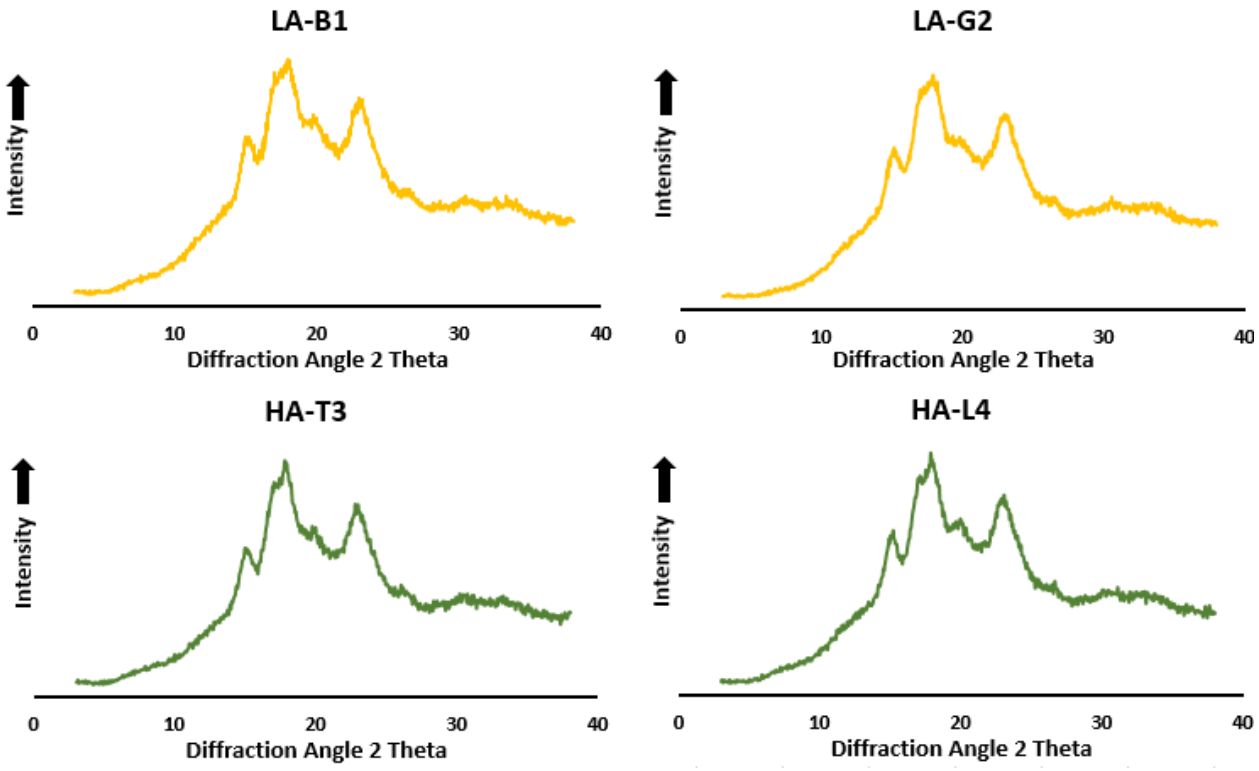

Figure 41. X-Ray Diffraction pattern of rice varieties: LA-B1, LA-G2, HA-T3, HA-L4.

XRD pattern of rice flours exhibit same pattern as isolated rice starches, which are peaks at 15°, 17°, 18°, 20° and 23° (**Figure 41**). Compared to low adhesive rice LA-B1 and LA-G2 (35.1 % and 34.5 % respectively), high adhesive rice HA-T3 and HA-L4 (38.3 and 39.2 % respectively) had higher percentage of starch crystallinity (**Table 9**). **Figure 42** shows positive correlation (R^2 = 0.9747) between starch relative crystallinity and adhesiveness of cooked rice. This shows that the stickier the rice texture, the higher relative crystallinity.

Table 9. Results of starch crystallinity, % of rice varieties: LA-B1, LA-G2, HA-T3, HA-L4 as calculated from X-Ray Diffraction.

	LA-B1	LA-G2	HA-T3	HA-L4
Starch crystallinity, %	35.1 % ±0.1	34.5 % ±0.1	38.3 % ±0.3	39.2 % ±0.3

Assuming that crystalline structure of starch is mainly contributed by amylopectin content, this suggests that high adhesive rice has more amylopectin than low adhesive rice. This is confirmed as results of amylopectin assay shows amylopectin percentage higher in high adhesive rice compared to low adhesive samples. Chung *et al*, 2011 also reported that lower amylose % (consequently higher amylopectin %) of rice exhibit higher relative crystallinity.

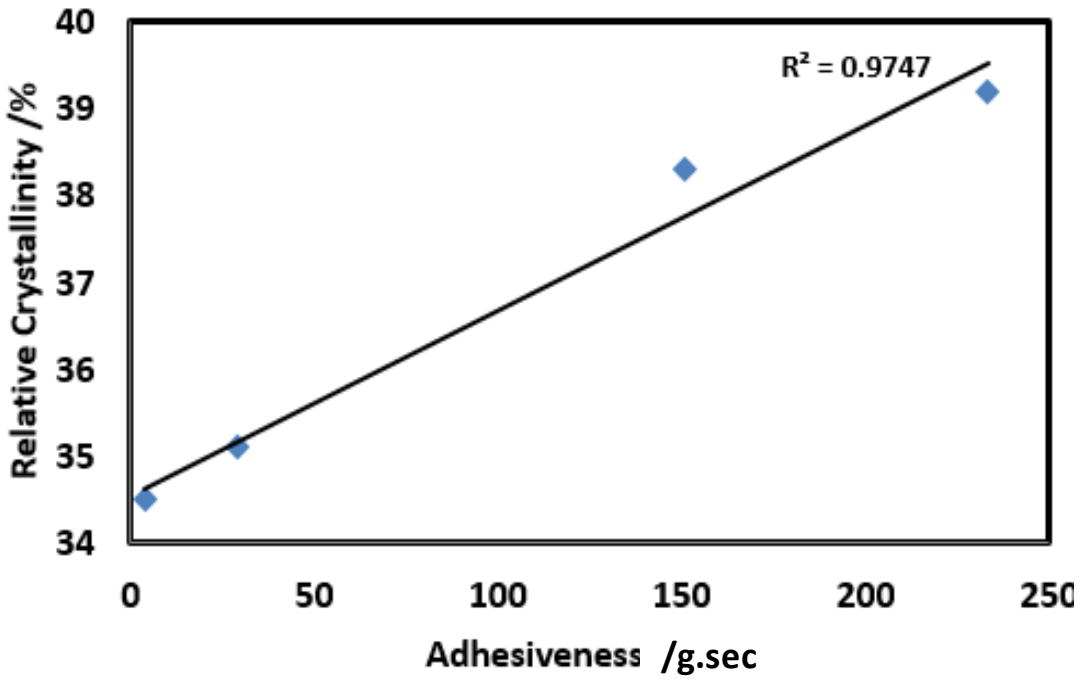

Figure 42. Correlation between starch crystallinity /% and rice adhesiveness /g.sec.

5.3. ORDER OF STARCH

5.3.1. ATTENUATED TOTAL REFLECTANCE-FOURIER TRANSFORM INFRARED (ATR-FTIR).

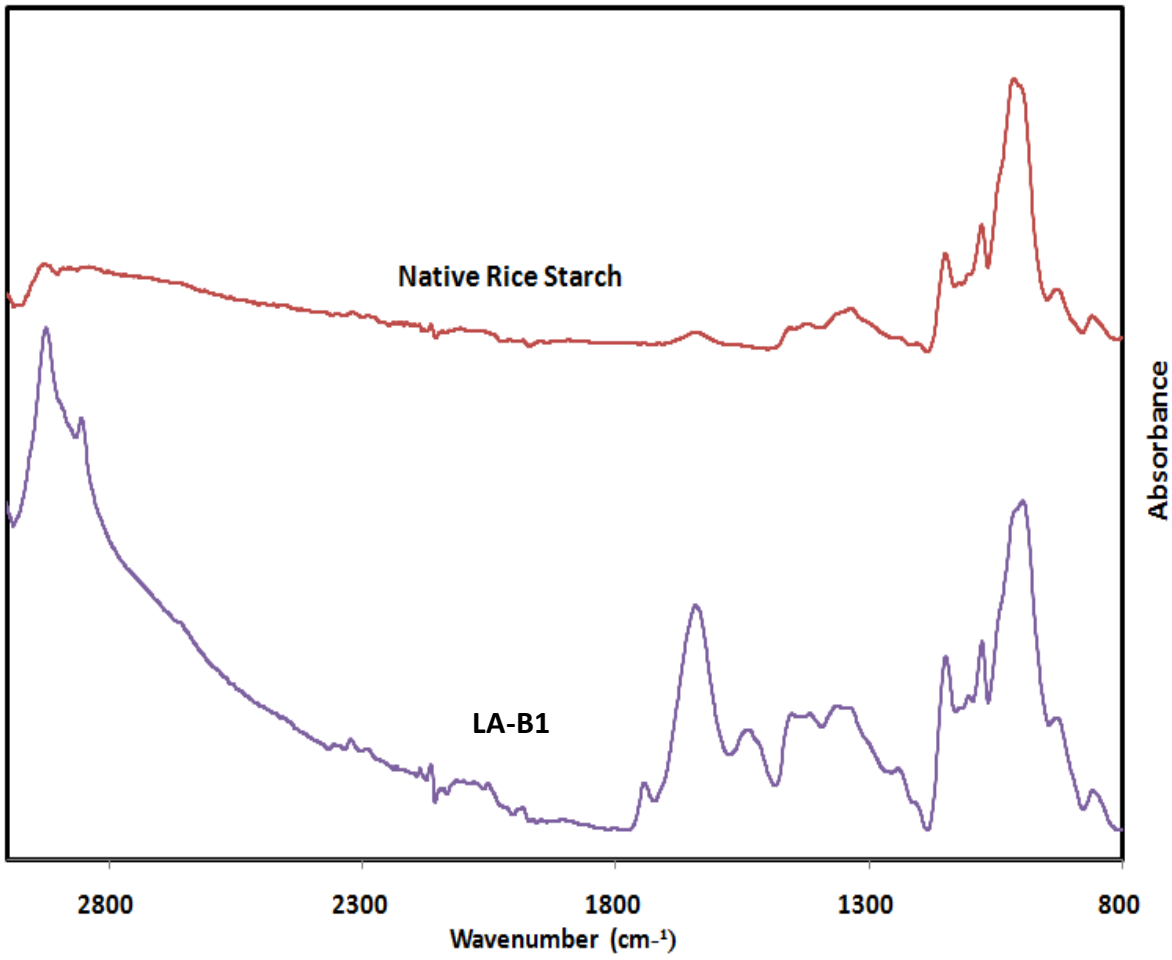

Figure 43. ATR-FTIR spectra of native rice starch and LA-B1 rice flour.

Figure 43 shows typical ATR-FTIR spectra of native rice starch and LA-B1 milled rice at 0 % moisture content. The most distinctive spectral features of LA-B1 rice are the following peaks; 2950 cm^{-1}, 2850 cm^{-1}, 1738 cm^{-1}, 1650 cm^{-1}, 1550 cm^{-1} and the region between 1200 and 800 cm^{-1}. The band between 2950 cm^{-1} and 2850 cm^{-1} is contributed by lipids due to the CH_2 and CH_3 while the 1738 cm^{-1} peak is due to lipid ester as a result of the C=O bond.

The amide I band arises at 1650 cm^{-1}, between 1690 and 1630 cm^{-1} mainly due to C=O bond stretching while the amide II band arises around 1550 cm^{-1}, between 1570 and 1540 cm^{-1} due to a combination of C-N bond stretching and N-H bond bending (Kong & Yu, 2007). The amide bands are affected by hydrogen bonding and thus will be sensitive to any change in the secondary structure of the protein. The overlapping peaks in the region 1200-800 cm^{-1} is the so-called polysaccharide band is characteristic of saccharides. These bands arise from C-O and C-C stretching mode of COH and COC group of carbohydrate.

As discussed in **5.1. Starch composition**, isolated native rice starch contains traces of native rice protein and rice lipid, hence, ATR-FTIR spectra shows presence of small lipid (2950 cm^{-1}) and amide I (1650 cm^{-1}) peaks. This clearly shows a difference between the composition of pure rice starch and rice flour.

5.3.2. DETERMINING ORDER OF STARCH MEASUREMENT: RAW AND DECONVOLUTED DATA

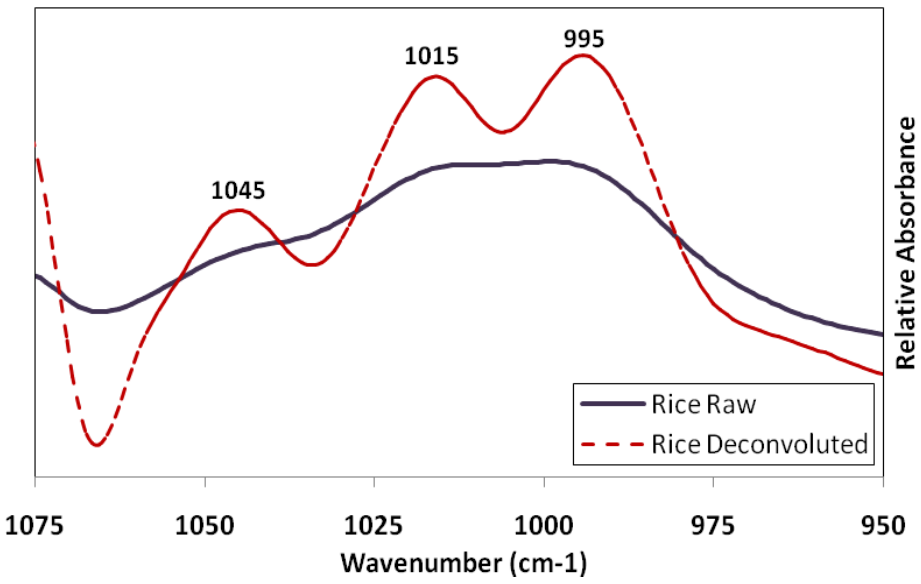

Figure 44. Comparison of raw and deconvoluted ATR-FTIR spectra of native rice starch in the region 1075 – 950 cm^{-1}.

A study conducted by van Soest *et al*, 1995 found that the ATR-FTIR spectrum band at 1045 cm^{-1} is sensitive to the amount of crystalline starch while the band at 1022 cm^{-1} is sensitive to amorphous starch. The ratio of absorbance value of the ATR-FTIR bands at 1047 cm^{-1} and 1022 cm^{-1} have been found to be proportional to the ratio of native/amorphous starch in mixtures of native and amorphous starch (van Soest e*t al*, 1995) and can be used to measure a degree of order in starch.

Figure 44 shows the results of the deconvolution spectral manipulation of desired saccharide, 1200-800 cm^{-1} region which is used to predict order of starch. As observed in a study by Sevenou *et al*, 2002, more overlapped peaks are uncovered and present peaks are maximised. It can be observed that the deconvoluted spectra shows 3 peaks, which are at wavenumbers 1045, 1015 and 995 cm^{-1}. This confirms absorbance ratios where 1047 and 1022 cm^{-1} are peaks of concern, which represents crystallinity and amorphous starch regions respectively. In this study, the 1047 peaks vary from 1045 - 1043 cm^{-1} while 1022 peaks from 1015 – 1018 cm^{-1}.

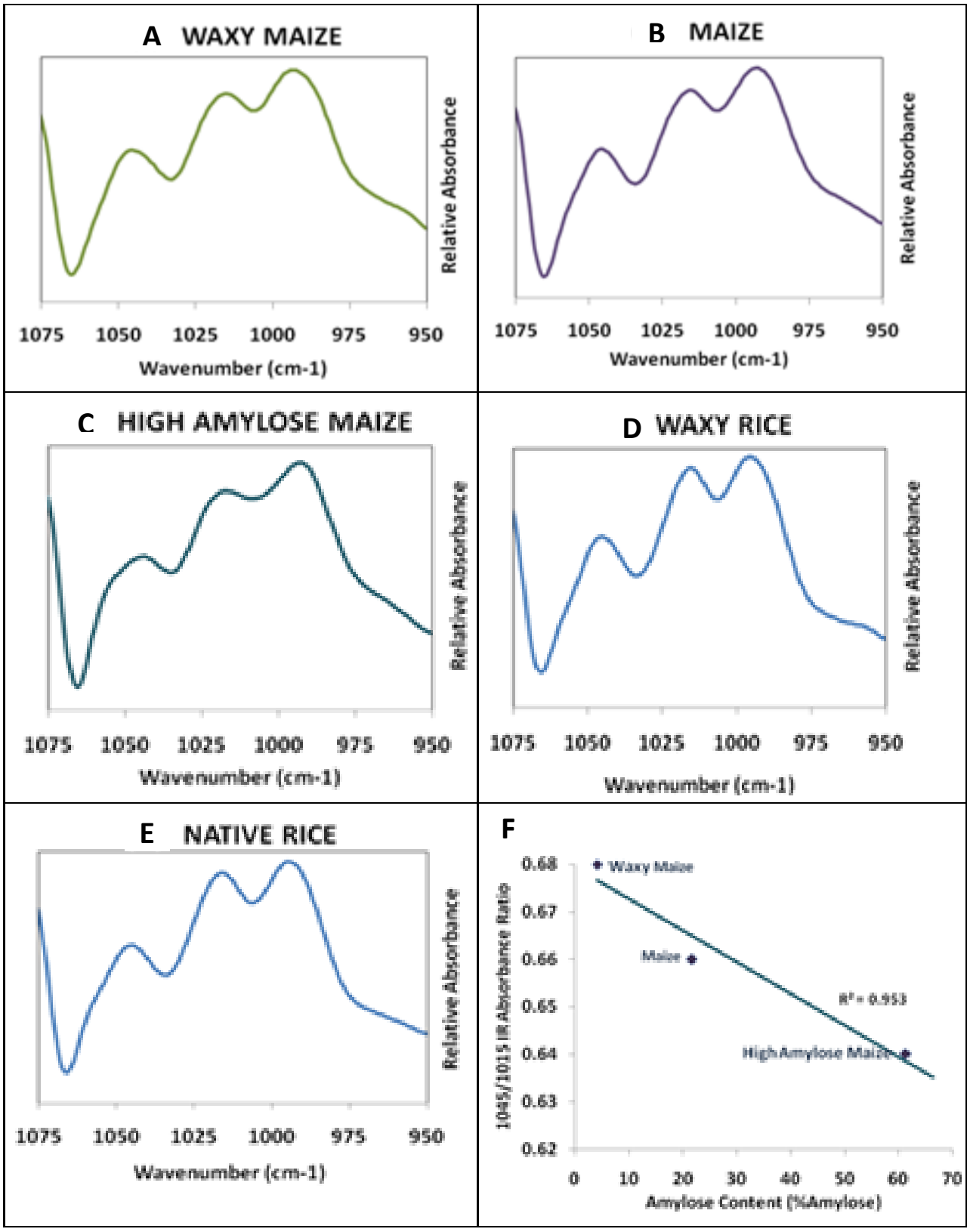

Figure 45. Individual ATR-FTIR spectrum for maize starches: (A) waxy, (B) native, (C) high amylose, and rice starches (D) waxy, (E) native. (F) correlation between ATR-FTIR 1045/1015 absorbance ratio and amylose content of isolated starches.

Figure 45.A - 45.F shows an individual spectrum for waxy, native and high amylose maize starches and waxy and native rice starches and their 1045/1015 absorbance ratio is calculated in **Table 10**. For both maize and rice, waxy versions have a higher 1045/1015 ratio than non-waxy. The difference in ratio values for different starch type may be explained by the different properties of each starch. There is negative correlation when the amylose content of the same starch type is plotted against 1045/1015 ratio, as demonstrated in maize (**Fig 45.F, R^2=0.95**). It is interesting to note that the correlation is only observed with the same starch type. It can be suggested that other different properties of different starches can affect the degree of order in starch varieties, which may include long amylopectin chain content and amylose/amylopectin binding. It can be concluded that with the same starch type, the lower amylose content of the starch, the more ordered is the external region.

Table 10. 1045/1015 absorbance ratios of maize and rice starch.

Starch Type	1045/1015 Absorbance Ratio
Maize	0.66
High Amylose Maize	0.64
Waxy Maize	0.68
Rice	0.61
Waxy Rice	0.64

5.3.3. UNDERSTANDING ORDER OF STARCH: LOSS AND GAIN

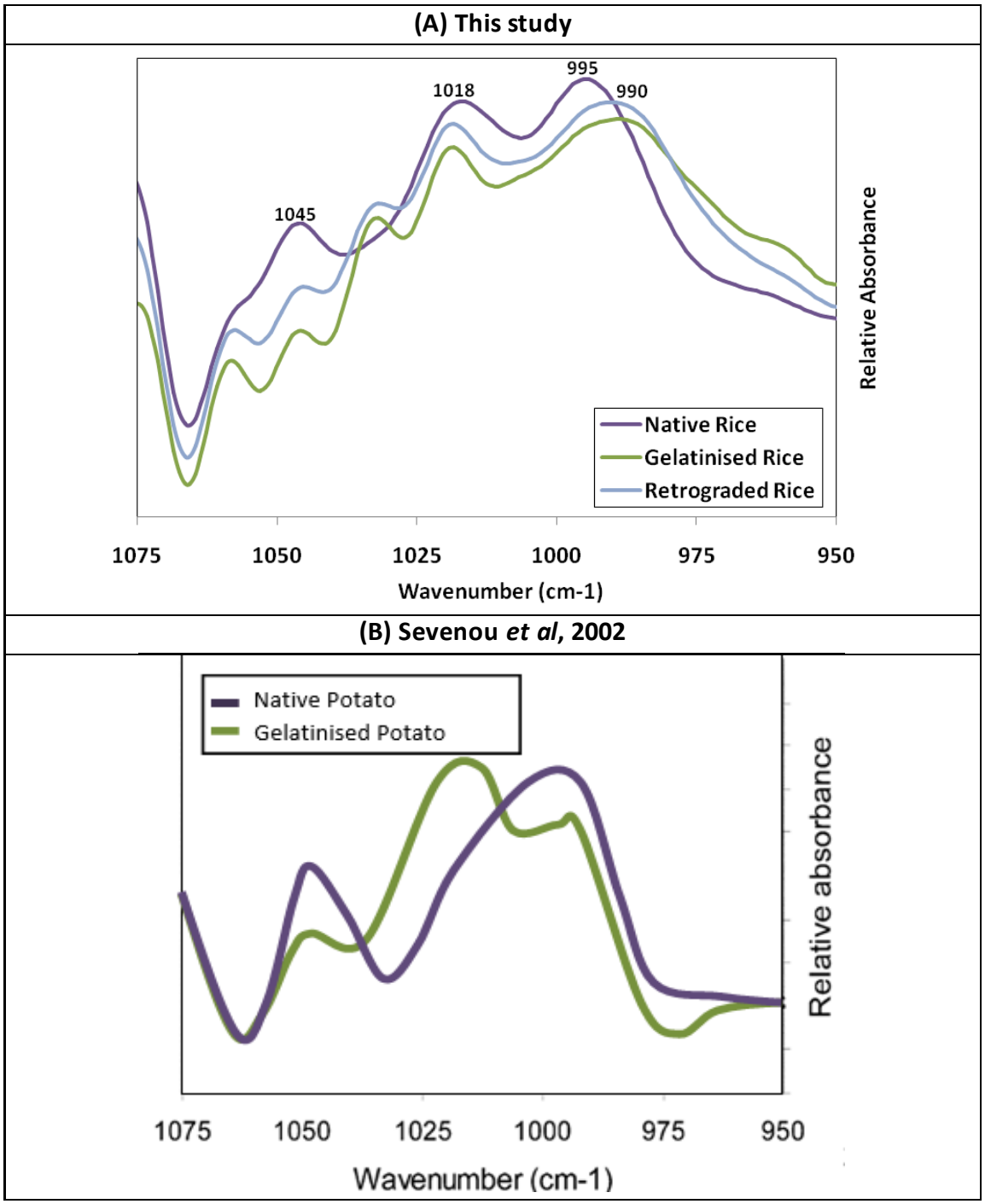

Figure 46. ATR-FTIR baseline corrected, deconvoluted and normalised spectra of (A) native, gelatinised and retrograded rice starch in this study and (B) native and gelatinised potato starch performed by Sevenou *et al*, 2002.

Fig 46A shows spectra of native, gelatinised and retrograded rice starch done in this study while **Fig 46B** shows native and gelatinised potato starch by Sevenou *et al*, 2002. There are big differences observed, where **Fig 46A** shows presence of extra peaks between 1030 and 1060 cm^{-1} in gelatinised starch while **Fig 46B** shows a higher 1022 peak than 995 cm^{-1}. This may be due to Sevenou *et al*, 2002 using different starch type (potato) and different sample preparation (water dispersion).

Calculation of 1045/1018 ratios in **Table 11** shows that gelatinised rice starch has the lowest 1045/1018 ratio, followed by retrograded and native. This indicates that gelatinised rice has the lowest order in its external region, followed by retrograded and native. This can be explained where native rice still has its crystalline region intact, hence having the highest crystallinity. When starch is gelatinised, crystalline region is disrupted and crystallinity is lost, hence having the lowest crystallinity. When starch is retrograded, amylose and amylopectin re-associate to form gel, regain crystalline region and hence, crystallinity. This demonstrates clearly where the 1045/1015 ratio represents crystallinity/amorphous ratio.

Table 11. Absorbance ratios of native, gelatinised and retrograded rice starch.

Starch Type	Process	Absorbance ratio 1045/1018
Rice	**Native**	0.61
	Gelatinised	0.16
	Retrograded	0.37

5.3.4. CORRELATION BETWEEN ORDER OF STARCH AND RICE ADHESIVENESS

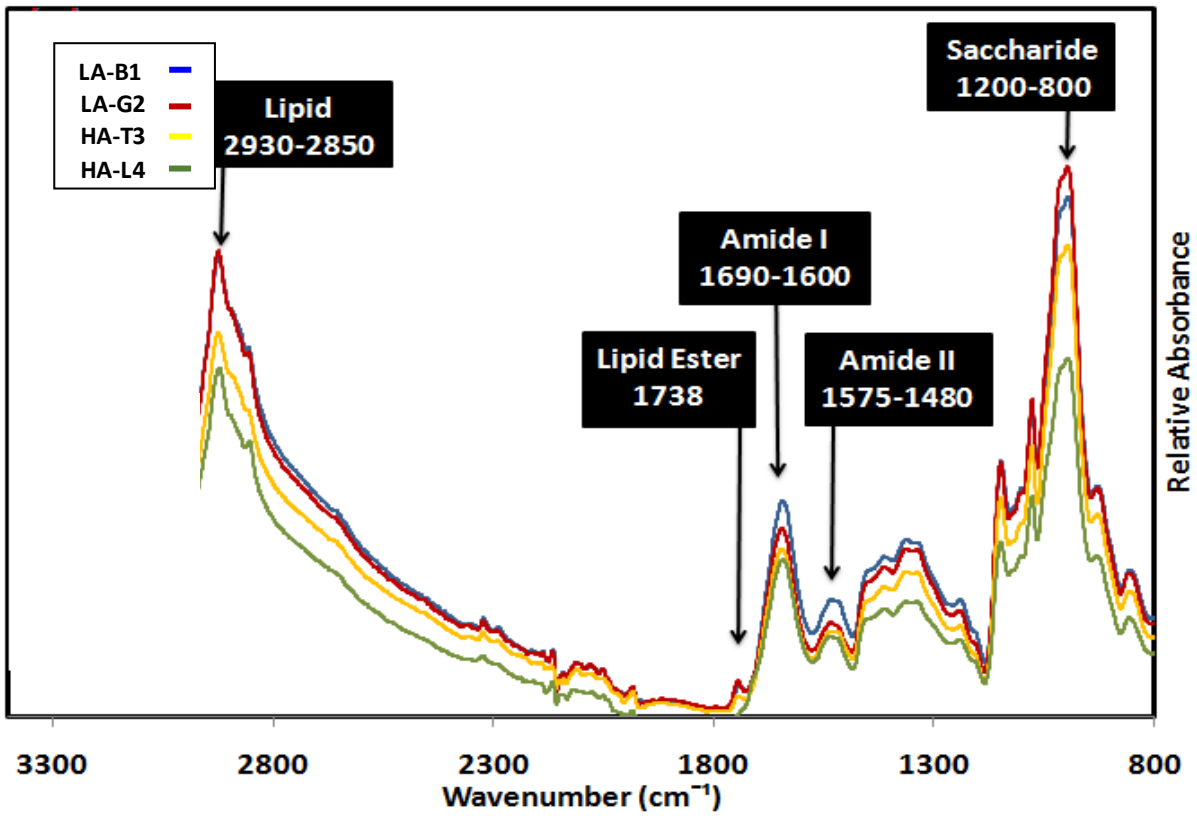

Figure 47. ATR-FTIR raw data of rice varieties: LA-B1, LA-G2, HA-T3, HA-L4.

Figure 47 shows ATR-FTIR results of samples chosen. Upon first glance of raw data, it can roughly observed that low adhesive LA-B1 and LA-G2 rice samples have higher lipid, amide and saccharide peaks compared to high adhesive HA-T3 and HA-L4 samples. It can also be noted that high adhesive HA-L4 has low to negligible lipid ester peak.

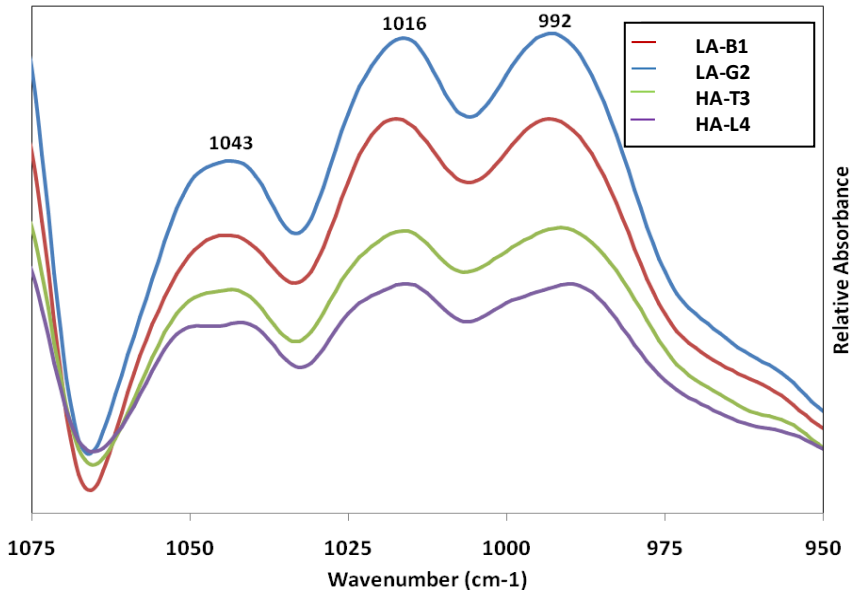

Figure 48. ATR-FTIR baseline corrected, deconvoluted spectra of LA-B1, LA-G2, HA-T3, HA-L4.

Figure 48 shows the cumulative ATR-FTIR spectra of LA-B1, LA-G2, HA-T3, HA-L4. The ratio of the peaks (1045/1022) was then calculated to obtain degree of order in starch. **Table 12** shows results of ratio of peaks of the samples chosen. High adhesive rice varieties (HA-T3: 0.67 and HA-L4:0.70 respectively) exhibited a higher order of starch compared to the low adhesive varieties (LA-B1:0.65 and LA-G2:0.65 respectively).

Table 12. Results of ratio of peaks 1045/1022 of rice varieties: LA-B1, LA-G2, HA-T3, HA-L4 as calculated from ATR-FTIR.

	LA-B1	**LA-G2**	**HA-T3**	**HA-L4**
Order of Starch	0.65 ±0.01	0.65 ±0.01	0.67 ±0.01	0.70 ±0.01

Figure 49 shows a positive correlation between 1045/1015 ratios and the sticky texture of rice as measured by adhesiveness (g.sec). This indicates that the stickier the cooked rice texture is, the more ordered external region it has. Long amylopectin chain contributes to a more crystalline, and hence, a more ordered starch structure. With the assumption that the absorbance ratio represents the bulk of the starch body, the higher the amylopectin content of the starch, the more highly ordered and the more crystalline the sample was. This result correlated with those of Bielinski *et al*, 2003, where it was concluded that the higher amylopectin content in starch, resulted in increased crystallinity. This also confirms literature findings that the crystalline region of starch is mostly due to amylopectin. This is also observed in relative crystallinity.

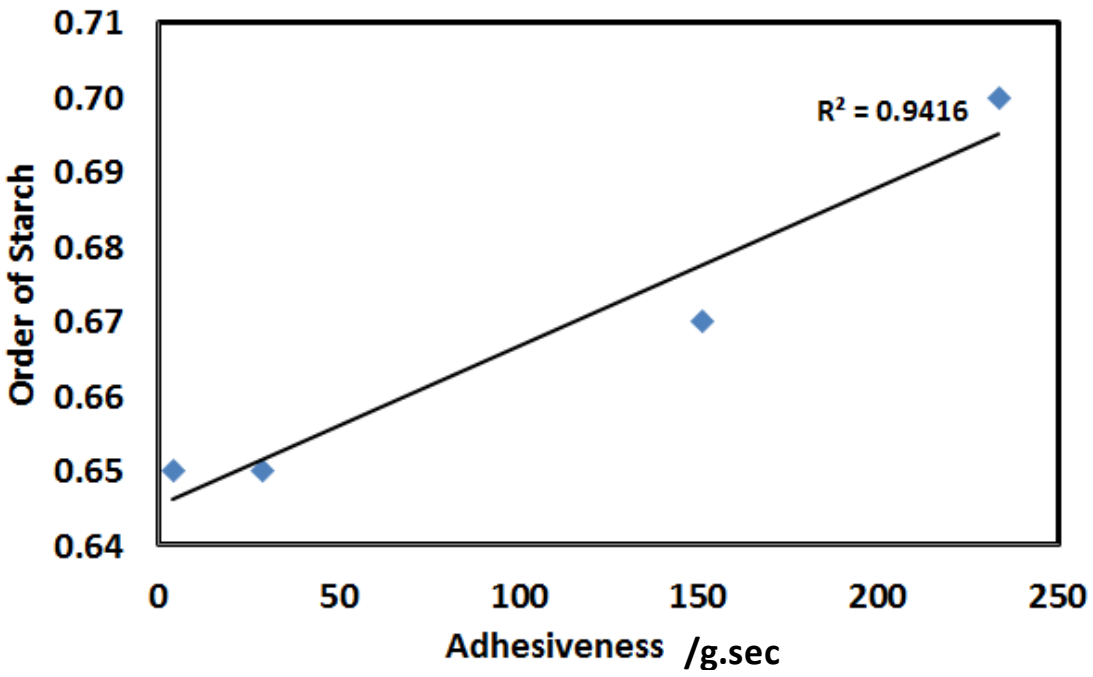

Figure 49. Correlation between 1045/1015 absorbance ratio and adhesiveness (g.sec).

5.3.5. CORRELATION BETWEEN STARCH CRYSTALLINITY AND ORDER OF STARCH

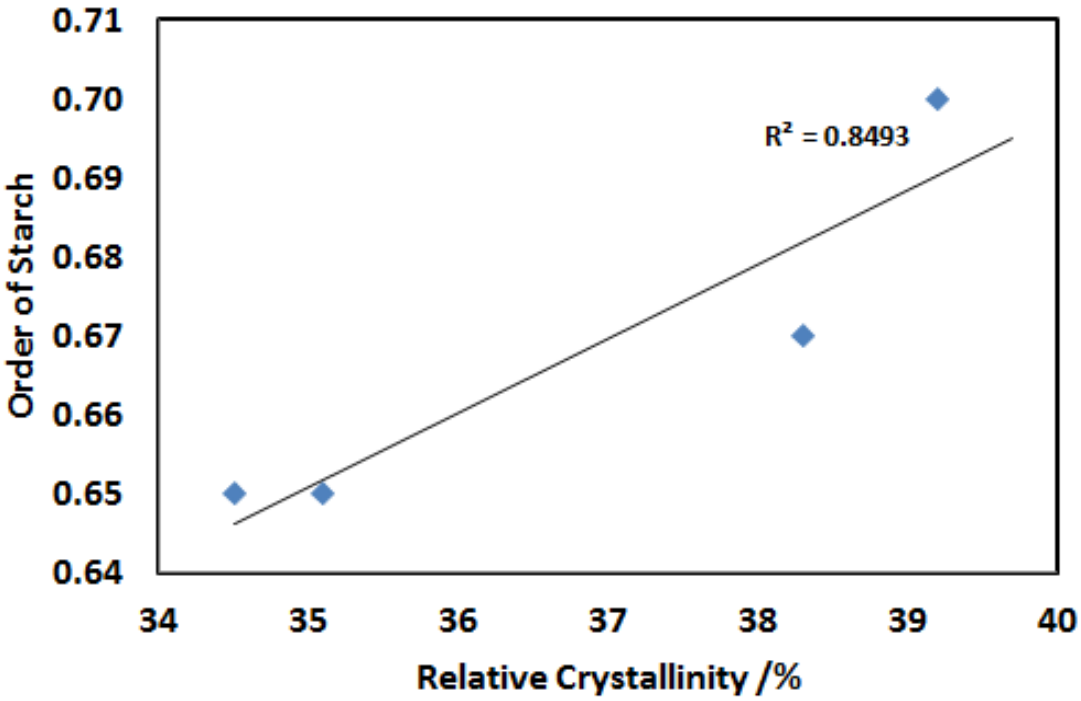

Figure 50. Correlation between order of starch, calculated from ATR-FTIR and relative crystallinity /% calculated from XRD.

Results show high adhesive rice has a higher percentage of starch crystalline structure and order of starch compared to low adhesive rice. Order of starch is also believed to correlate with relative crystallinity. Therefore, it is interesting to observe any correlation between the two. Both relies on the same principle of predicting the arrangement of crystalline and amorphous structures; with XRD crystallinity in this study takes into account the percentage of crystalline region relative to the overall crystalline and actual amorphous region while order of starch takes into account the ratio of crystalline to amorphous.

Figure 50 shows a positive correlation between the two measurements of starch crystalline structures (R^2=0.8493). It can be said that both order of starch and starch crystallinity are good predictors of starch arrangements, with relative crystallinity having a better trend with regression value of 0.9747 compared to order of starch (0.9416). This shows the potential of ATR-FTIR to be used as a faster and more rapid method which requires little sample preparation to calculate starch crystallinity.

5.4. STARCH BEHAVIOUR

5.4.1. STARCH PASTING PROPERTIES

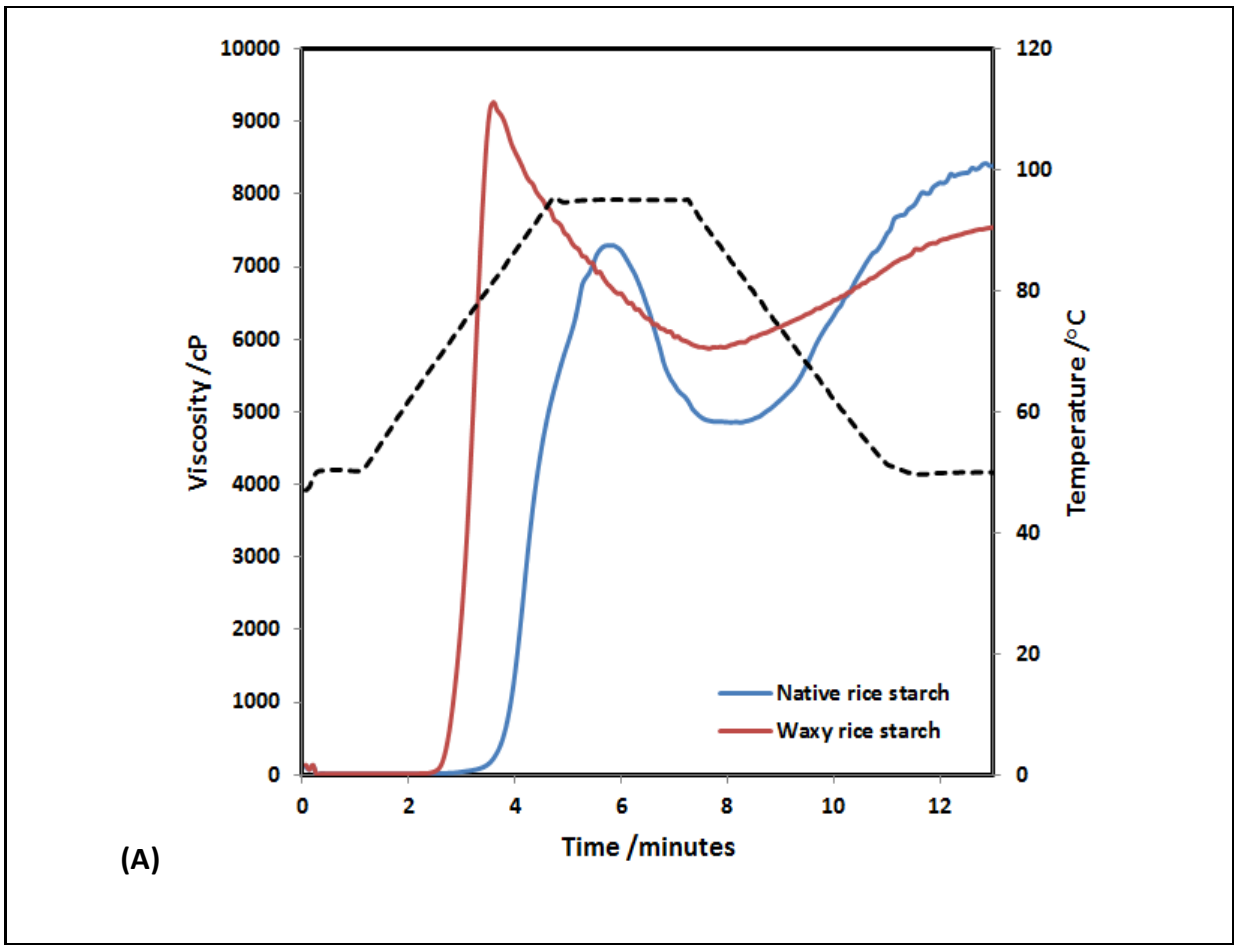

(A)

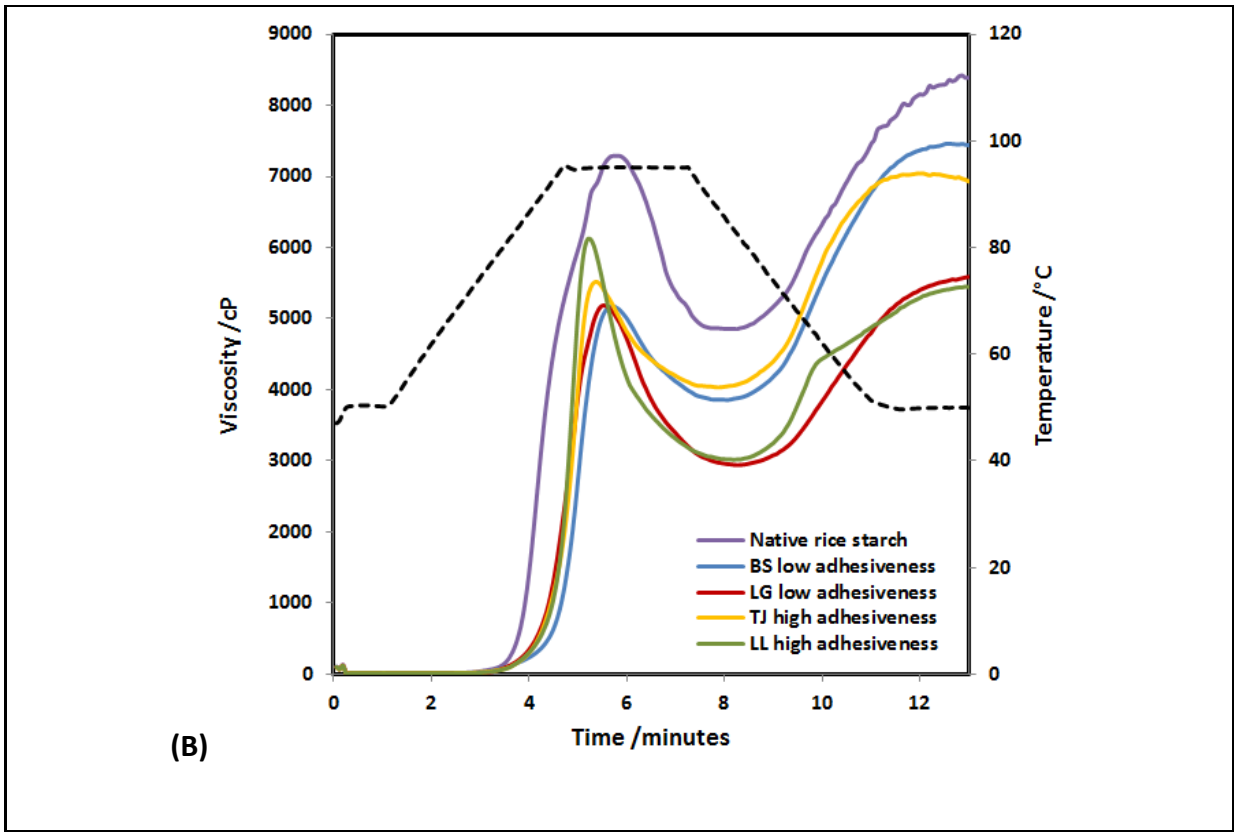

Figure 51. Starch pasting profiles of (A) controls waxy and native rice starch and (B) rice varieties: LA-B1, LA-G2, HA-T3, HA-L4.

Figure 51 shows pasting profiles of (A) controls waxy and native rice starch and (B) rice varieties chosen in this study. Compared to native rice starch, waxy rice starch shows a faster onset of pasting, higher peak viscosity and lower final viscosity. Results of amylose/amylopectin assay shows that waxy rice starch has 98 % amylopectin and 2 % amylose and native has 72.9 % amylopectin and 27.1 % amylose in the starch granule. This means that in any 100 mg of pure waxy rice starch, there is 25.1 g more amylopectin compared to native rice starch granule. Since amylopectin is more soluble in water, the higher amylopectin composition results in a faster swelling of starch granules hence, the faster onset of pasting. The higher concentration of soluble components also results in a more viscous solution,

hence higher peak vicosity. Since there is less amylose (less 25.1 g per 100 g compared to native starch) available to form crystalline structure, or to retrograde, there is less total setback and a lower final viscosity.

Figure 51B shows the RVA profiles of the four rice varieties chosen based on low and high adhesiveness as determined by texture analyser. Apart from LA-B1, the other 3 varieties LA-G2, HA-T3 and HA-L4 have similar onset of pasting time. This can be explained as LA-B1 has the lowest amylopectin content (73.1 %), making it least soluble in hot water. Compared to low adhesive varieities LA-B1 and LA-G2, high adhesive rice varieities HA-T3 and HA-L4 have higher peak viscosity, which reflects their relatively higher amylopectin contents (80.7 % and 85 % respectively). HA-L4 shows the most granule breakdown, lowest total setback and lowest final viscosity while LA-B1 shows the least granule breakdown, highest total setback and highest final viscosity. This can be explained as HA-L4 has the most crystalline region (relative starch crystallinity = 39.2 % and order of starch = 0.70) while LA-B1 has the least crystalline region (relative starch crystallinity = 35.1 % and order of starch = 0.65).

Heating starch in water destroyes the crystalline structure of starch and there is more crystalline region in HA-L4. HA-L4 also has least amount of amylose present for amylopectin to reassociate for retrogradation, hence, the total setback and final viscosity is lowest. On the contrary, LA-B1 has the least crystalline structure to breakdown and contains most amount of amylose to reassociate with amylopectin during retrogradation, resulting in having the highest total setback and final viscosity.

5.5. PROTEIN CONTENT

5.5.1. BICINCHONINIC ACID (BCA) ASSAY: TOTAL PROTEIN ANALYSIS

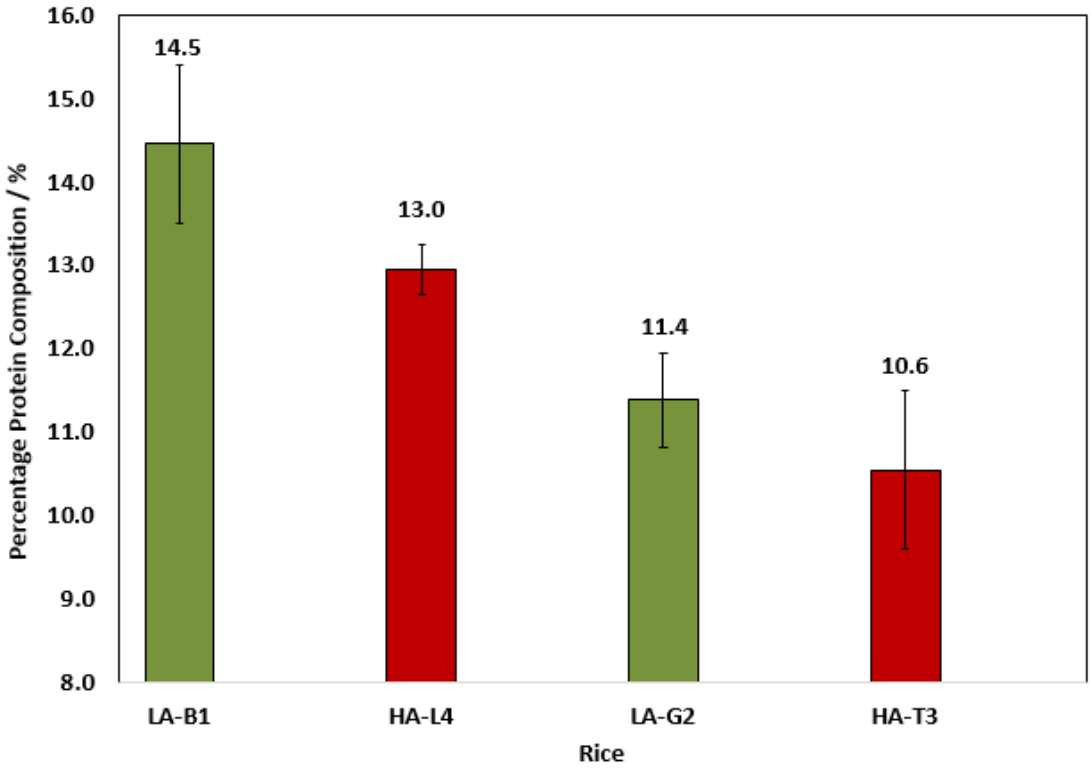

Figure 52. Graph showing percentage protein composition /% of rice samples rice varieties: LA-B1, LA-G2, HA-T3, HA-L4, as measured by Bicinchoninic Assay (BCA).

Figure 52 shows the protein composition of the rice samples used, analysed using BCA protein assay as described in **3.6.4. Bovine serum protein kit**. It can be observed that the protein composition of the samples range between 10.6 % and 14.5 %. BeMiller and Whistler (2009) reported that typical protein content of milled rice is between 6 – 13 %. A high protein result is expected as the total starch content (80.4 – 85.4 %) for the rice samples are relatively high.

The bar graph shows that highest protein content is found in LA-B1 (14.5 %), followed by HA-L4 (13.0 %), LA-G2 (11.4 %) and HA-T3 (10.6 %). There was no significant difference between the low adhesive (LA-B1, LA-G2) and high adhesive samples (HA-L4, HA-T3). Similar trends were observed in starch analysis. From the results of total protein content in this study, it can be concluded that for the samples chosen, there was no correlation between protein content of rice and final cooked rice texture. It may be worth investigating role of different protein types present.

5.5.2. ATTENUATED TOTAL REFLECTANCE-FOURIER TRANSFORM INFRARED (ATR-FTIR) AMIDE PEAKS

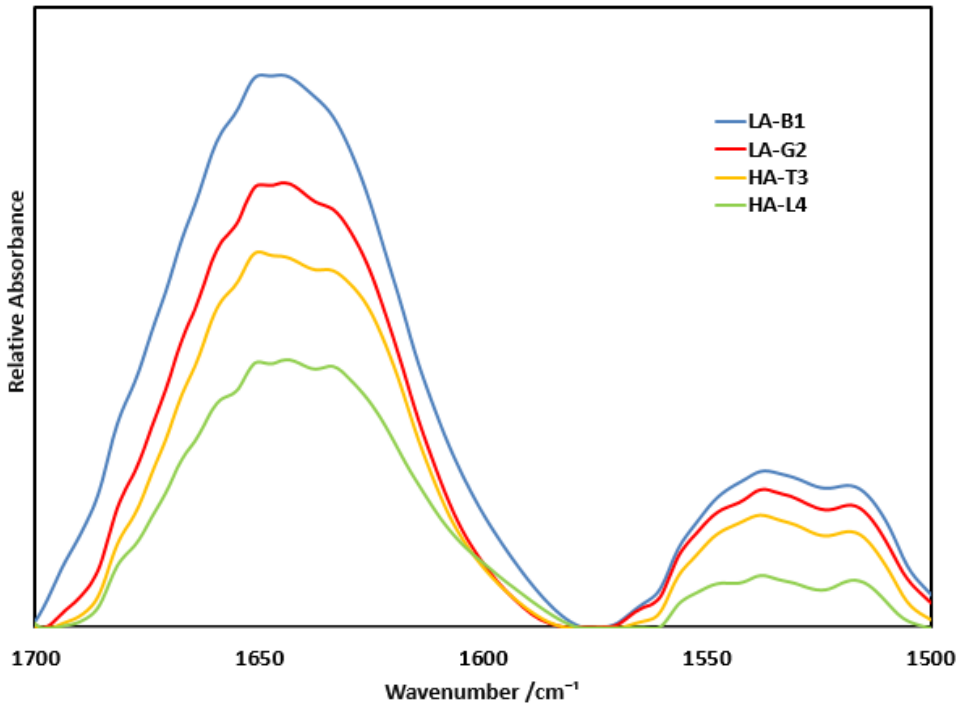

Figure 53. ATR-FTIR showing amide peaks of rice varieties: LA-B1, LA-G2, HA-T3, HA-L4 in the region between 1700 cm^{-1} and 1580 cm^{-1}, and 1580 cm^{-1} and 1480 cm^{-1}.

All four samples showed the presence of amide peaks, amide I (between 1700 cm^{-1} and 1580 cm^{-1}) and amide II (1580 cm^{-1} and 1480 cm^{-1}) peaks. It can be observed that compared to the low adhesive rice samples LA-B1, LA-G2, high adhesive rice samples HA-L4, HA-T3 have lower amide peaks, both amide I and amide II. This shows how ATR-FTIR can be used as a potential rapid detection method for protein in rice.

5.6. LIPID CONTENT

5.6.1. SOLVENT EVAPORATION

Table 13. Lipid content of rice varieties: LA-B1, LA-G2, HA-T3, HA-L4.

Rice Sample	Low adhesive LA-B1	Low adhesive LA-G2	High adhesive HA-T3	High adhesive HA-L4
Percentage Lipid /%	**1.2 ± 0.1**	**0.6 ± 0.2**	**0.5 ± 0.1**	**0.3 ± 0.1**

Table 13 shows results of **3.6.5. Lipids Extraction**. The percentage of lipid obtained from this study is between 0.3 % and 1.2 %. This is low compared to Vidal and Juliano, 1967 where the crude fat from rice samples was between 2.2 and 2.9 % but acceptable compared to BeMiller and Whistler, 2009 who reported that typical lipid content of milled rice is 0.3 – 0.6 % crude fat. In addition, packaging on the commercial rice shows lipid composition between 0.6 % and 1.5 %. Therefore, these results are valid. High adhesive rice (0.3 - 0.5 % lipid) has lower lipid content compared to low adhesive rice (0.9 - 1.2 % lipid).

5.6.2. ATTENUATED TOTAL REFLECTANCE-FOURIER TRANSFORM INFRARED (ATR-FTIR) LIPID ESTER PEAK

According to Lam, Proctor & Meullenet, 2001, ATR-FTIR peaks 1746 cm^{-1} (ester C=O) and 1714 cm^{-1} (fatty acid C=O) correlated well (R^2=0.93) with chemical analysis data. All of the four samples show presence of lipid ester peaks. High adhesive HA-L4 had the lowest lipid ester peak, followed by LA-G2, HA-T3 and LA-B1. This corresponds well to results of lipid composition in the present study. Therefore, this shows the potential of using ATR-FTIR as a rapid detection method for presence and quantification of lipid.

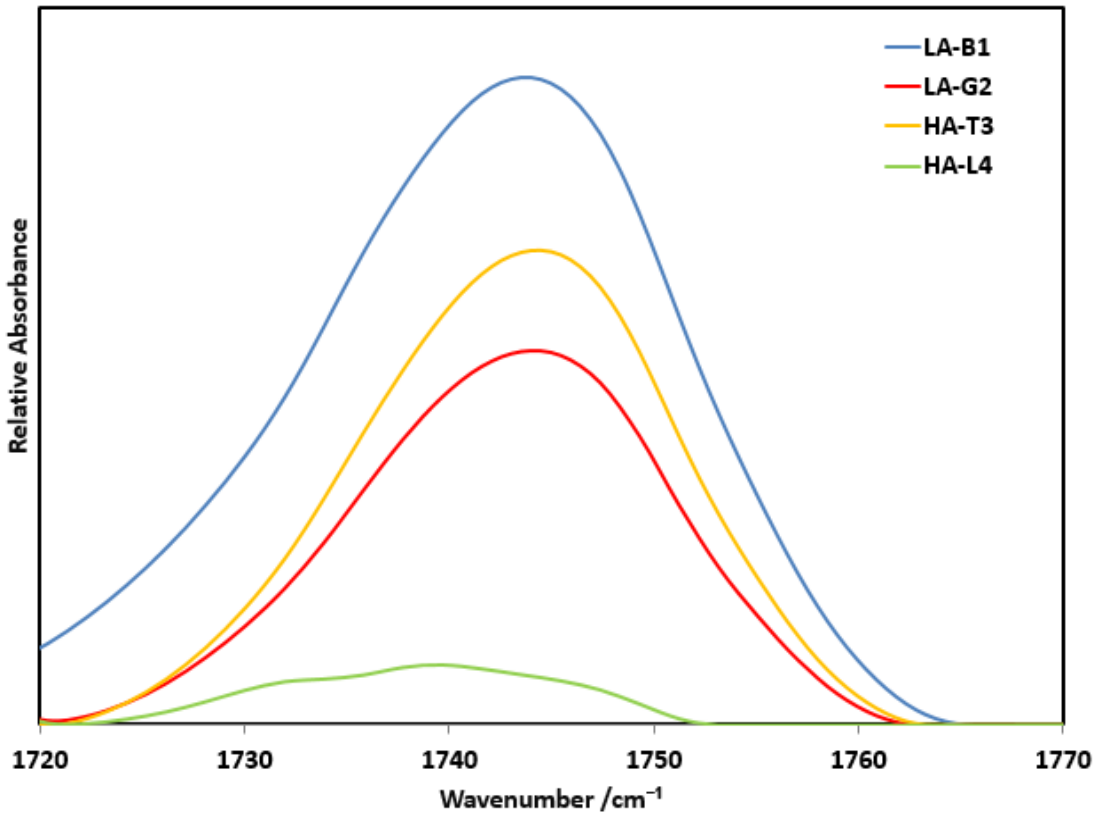

Figure 54. Ester lipid peaks of rice varieties: LA-B1, LA-G2, HA-T3, HA-L4 as shown in ATR-FTIR.

5.6.3. X-RAY DIFFRACTION (XRD) LIPID ESTER PEAK

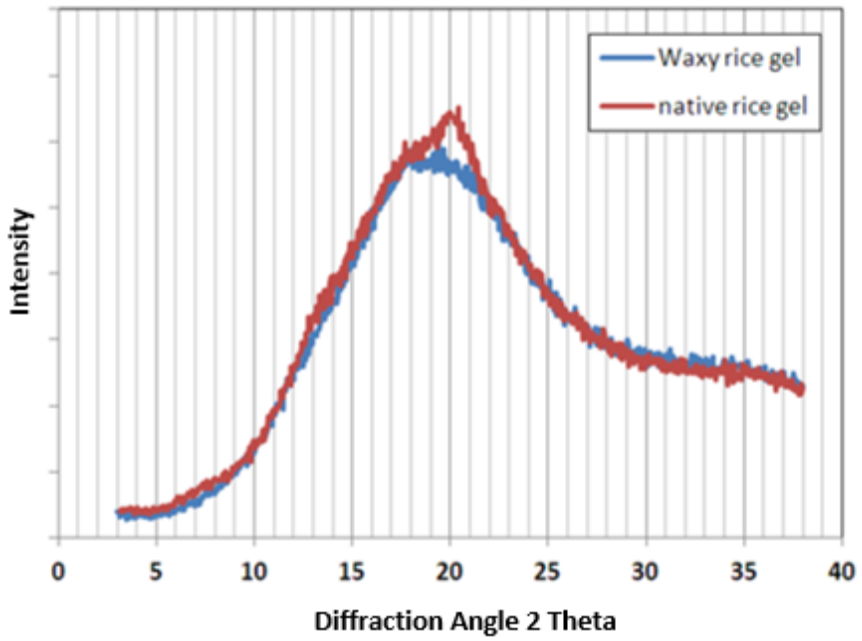

Figure 55. Amorphous samples of pure native and waxy rice starches.

Figure 55 shows amorphous samples of **Figure 38** that are used in this study. Lopez-Rubio *et al*, 2008 commented that the 20^{o} peak is not included in relative crystallinity studies as it could be attributed to the amylose-complex and may not be not part of relative crystallinity. **Figure 55** clearly showed that there was no peak at 20^{o} for waxy rice even though it is highly crystalline while there was a peak for native starch (less crystalline). Even after gelatinisation where starch crystalline structure is broken down completely, the presence of V-amylose peak is still present in native samples, while none was detected in waxy samples. Since these peaks are already present before gelatinisation or cooking of the rice starches, it can be said that these peaks are already in the raw rice structure and are not formed as a result of the heat treatment or cooking of starch/amylose/amylopectin components.

In this study, V-amylose crystallinity for native and waxy rice starch was 1.56 % and 0.23 % respectively (**Table 14**). Native rice starch has higher V-amylose crystallinity than waxy rice starch. This is also observed in a study by Lopez-Rubio *et al*, 2008 where native rice starch (1.85 %) had significantly higher V-amylose compared to waxy rice starch (0.15 %). Actual crystallinity values are different as both studies did not use sample from the same source. This suggests that not only native rice starch has higher amylose content, it also has higher V-amylose and potentially lipid-amylose complex.

Table 14. V-amylose crystallinity of pure rice starch obtained from this study and by Lopez-Rubio *et al*, 2008.

	This study	**Lopez Rubio *et al*, 2008**
Native rice starch /%	1.56 ± 0.3	1.85 ± 0.12
Waxy rice starch /%	0.23 ± 0.1	0.15 ± 0.02

Table 15 shows that V-amylose crystallinity calculated from this study is between 1.26 and 1.63 %. Although there is no observable correlation between V-amylose crystallinity /% and rice adhesiveness, it is to be noted that low adhesive rice LA-B1 has significantly high V-amylose crystallinity compared to the other 3 rice types.

Table 15. V-amylose crystallinitY/% of rice varieties: LA-B1, LA-G2, HA-T3, HA-L4.

Rice Sample	**Low adhesive LA-B1**	**Low adhesive LA-G2**	**High adhesive HA-T3**	**High adhesive HA-L4**
V-amylose crystallinity /%	1.63 ± 0.08	1.26 ± 0.05	1.20 ± 0.05	1.22 ± 0.05

5.6.4. NUCLEAR MAGNETIC RESONANCE (NMR) LIPID ESTER PEAK

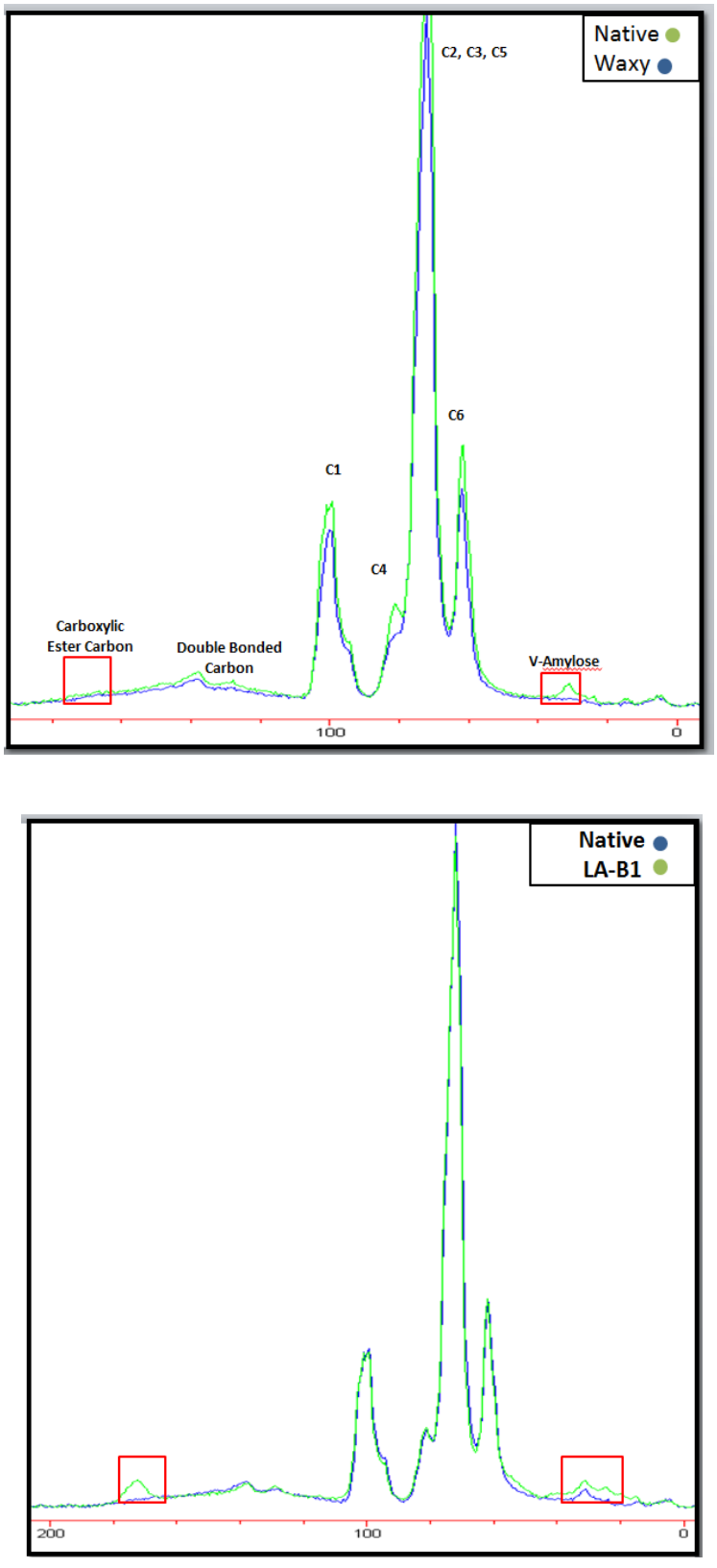

Figure 56. NMR spectra of (i) native and waxy rice starches and (ii) LA-B1 rice grain.

Figure 56 shows results of **3.5.6. CP-MAS nuclear magnetic resonance**. Waxy rice starch lacks V-amylose and carboxylic ester carbon peaks, which was observed in both XRD and FTIR results respectively. Native rice starch showed the V-amylose peak, which was observed in XRD, but the absence of carboxylic ester carbon peak, which was observed in ATR-FTIR spectroscopy. Meanwhile, milled rice powder showed both V-amylose and carboxylic ester carbon peaks that were observed in both XRD and ATR-FTIR spectroscopy respectively.

NMR spectroscopy was trialled because Lopez-Rubio *et al*, 2008 confirmed the correlation between starch relative crystallinity in X-Ray Diffraction studies and in Nuclear Magnetic Resonance studies. This result further justifies the presence and trend of V-amylose peak and crystallinity. However, due to time constraints, calculation of crystallinity was not pursued. This study simply justifies the potential use of ATR-FTIR and XRD as rapid detection methods for lipid ester and V-amylose crystallinity respectively.

5.7. SUMMARY AND CONCLUSION OF CHAPTER

In conclusion, high adhesive rice grains has:

- **Higher** percentage of **amylopectin content**
- **Higher** percentage of **starch crystallinity**
- **Higher order of starch** ratio
- **Lower total lipid** content
- **Lower lipid ester** content

There is no conclusive scientific evidence showing correlation between rice adhesiveness and total starch content, total protein content and V-amylose crystallinity in this project. However, the internal and external regions of rice were not taken into consideration. It is suggested that the next steps should investigate (i) if there are differences in the basic composition in the centre and the surface of rice grains and (ii) if they were any, how this may affect cooked rice texture.

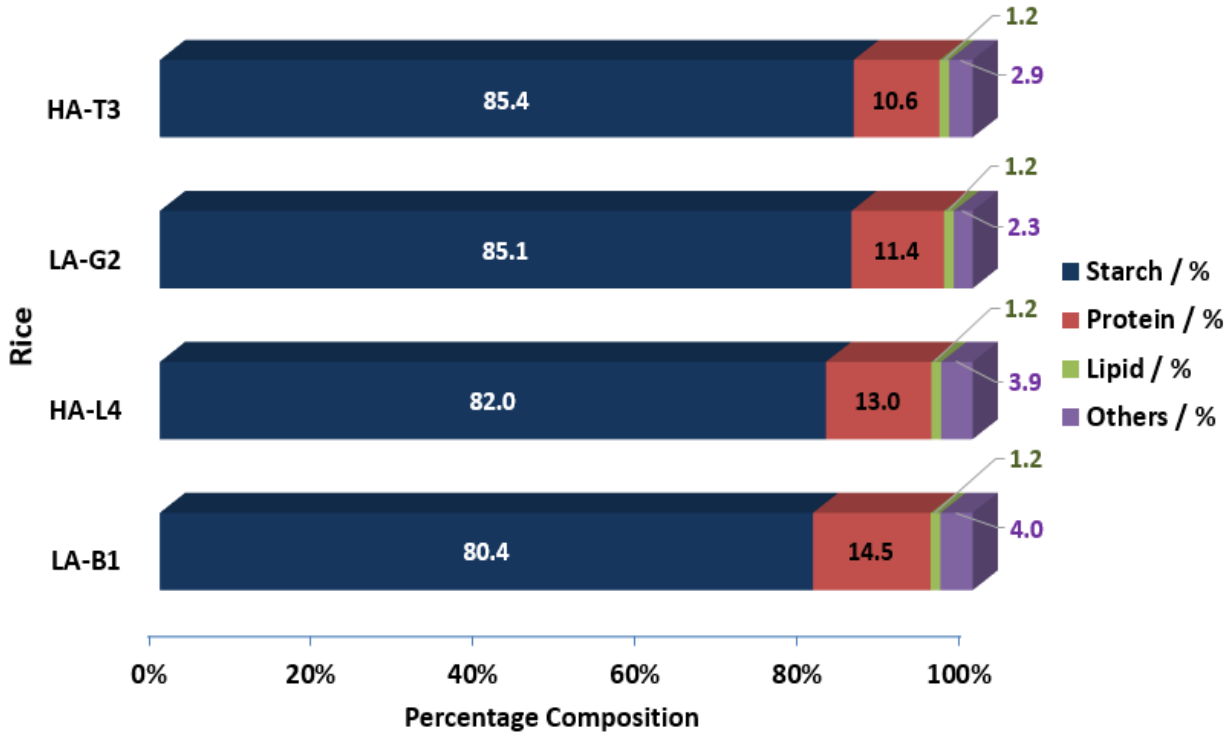

Figure 57. Total composition of starch, protein and lipid of the selected milled rice grains.

6. GROSS LOCALISATION OF COMPONENTS OF RICE GRAINS

The previous chapter shows basic content and composition of the selected rice varieties. However, the localization of components of raw rice grains was not studied. This chapter aims to investigate if there is a difference in the composition of the internal and external structure of uncooked rice and to observe whether this structural property contributes to the adhesive property of cooked rice. Chapter 6 starts with the development of methods to analyse the internal and external structure of uncooked rice grain without physically affecting structures, followed by an analysis of the crystalline structure and lipid and protein components of internal and external regions and concluding whether structural differences have any correlation with rice texture.

6.1. METHOD DEVELOPMENT

6.1.1. SEPARATION OF REGIONS

Table 16 explains the considerations taken to determine whether to separate the internal and external region of rice kernels or to analyse kernels as a whole. Not separating rice kernels is beneficial as the process does not incur any physical damage to the rice grains. However, apart from using imaging equipment, conducting chemical and instrumental analysis is difficult to undertake using whole rice kernels. Despite being time-consuming and the possibility of physical damage, physical separation of internal and external rice structures allows more options for experimental analysis.

Therefore this project physically separated the external and internal parts of rice grains for further analysis.

Table 16. Considerations taken before separating internal and external regions of rice grain kernels.

	Advantages	Disadvantages
Physical Separation of Structures	More different options to analyse results.	Physical damage. Time-consuming.
Whole Grain Analysis	No physical damage – more reliable results. Fast – direct method.	Limited method of analysis.

To demonstrate the difficulty in using whole rice grains for analysis of external and internal regions, ATR-FTIR was used. Individual rice grains were placed onto ATR placeholders and placed a certain amount of pressure was applied (**Figure 58**). One of the main issues incurred was the difficulty to regulate the amount of torque set onto the rice grains. Too little torque results in some rice grains breaking while too much torque results in insufficient contact between the surface of rice grains and diamond crystal which yield inadequate and noisy data signal. Since the amount of pressure needs to be constant, rice grains of similar circumference height were selected which was very tedious and difficult. Moreover, the results were not reproducible as the curvature and shape of each individual rice grain was different. Therefore, this method was not pursued as there was a high risk of unreliability of results. Hence, it was better to separate the structures to get a more reproducible reading.

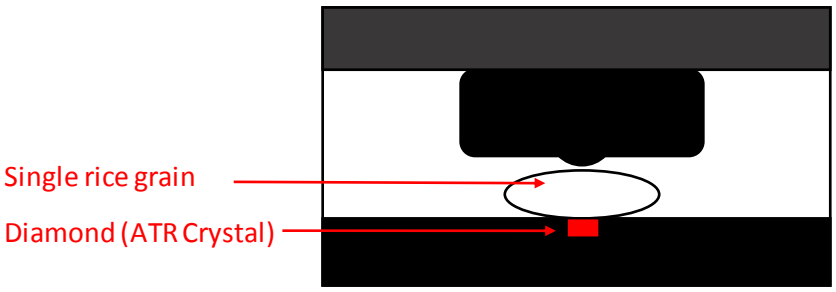

Figure 58. Single rice grain placed directly onto ATR-FTIR placeholder.

Initial studies started by just removing the surface of the rice by rubbing it with sandpaper and observing if there is any difference between the internal regions and rice flour. Results showed significant differences between the internal samples and the whole ground rice (which is mixture of internal and external samples). Therefore, this provoked an investigation of the surface of the rice kernels. Hence, to proceed, there was a need to pain-stakingly scrape hundreds rice grains in order to yield enough sample size for analysis. The dimensions of the internal and external structure finalized in this study has been described in **3.3.1. Cutting of rice**. However, there was great difficulty in (a) obtaining the surface from large quantities of rice grains, with (b) the same repeatable 'external dimensions' and (c) defining this 'surface dimensions'

6.1.2. DETERMINATION OF SURFACE AND CENTRE REGIONS

After deciding that the procedure was worth following up, there was a need to establish standard operating procedures on how to obtain samples. Steps to obtain internal and external region of raw rice grains used in this project were as follows:

(1) First the external regions were cut off (shown as white dotted region in **Figure 59**, collected and milled for further analysis.

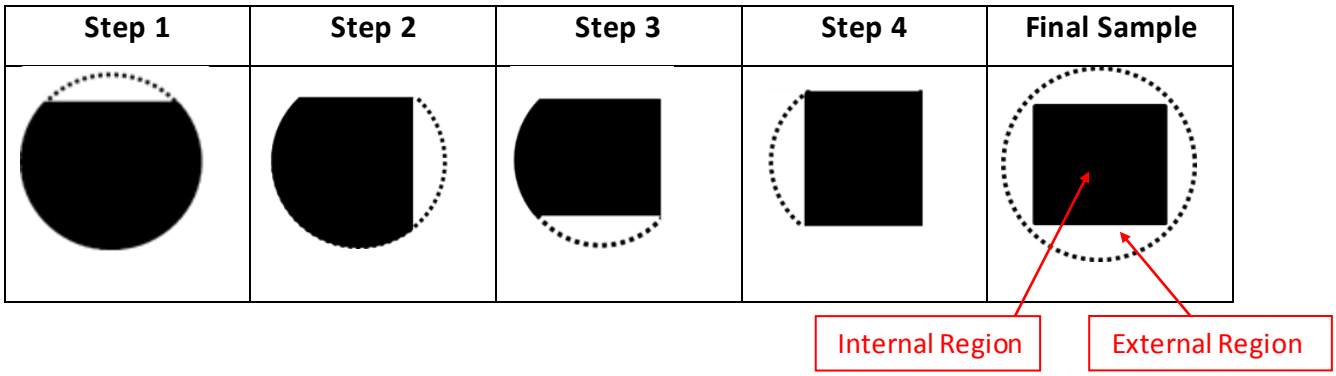

Figure 59. Steps 1-5 involved in cutting individual rice grains and to obtain external rice samples (shown as dotted lines ◌) and internal rice samples (shown as black ■) for analysis.

(2) Second, to reduce the likelihood of external region from mixing with internal region, one layer of about 0.1 mm was scraped off each rice grain surface before proceeding to collection of internal region. This was performed by either lightly scraping with a sharp blade or lightly rubbed on sandpaper.

(3) Thirdly, the internal regions (shown as black region in **Figure 59**) were collected and milled for further analysis.

6.2. GROSS LOCALISATION OF STARCH COMPONENT

6.2.1. ATTENUATED TOTAL REFLECTANCE-FOURIER TRANSFORM INFRARED,ATR-FTIR

Figure 60 shows the spectra of the external and internal regions of LA-B1. Upon first glance of raw data, compared to the internal regions, the external regions have higher lipid (2850 - 2950 cm^{-1}), amide I (1650 cm^{-1}), amide II (1550 cm^{-1}), polysaccharide peaks (1200 - 800 cm^{-1}) and the presence of 1738 cm^{-1} (lipid ester) peak. **Figure 61** shows spectrum of external regions of the four rice varieties. Low adhesive LA-B1 had the highest lipid (2950 - 2850 cm^{-1}), amide I (1650 cm^{-1}), amide II (1550 cm^{-1}), polysaccharide peaks (1200 - 800 cm^{-1}) and the presence of 1738 cm^{-1} (lipid ester) peak, followed by low adhesive LA-G2 and High Adhesive HA-T3 and HA-L4.

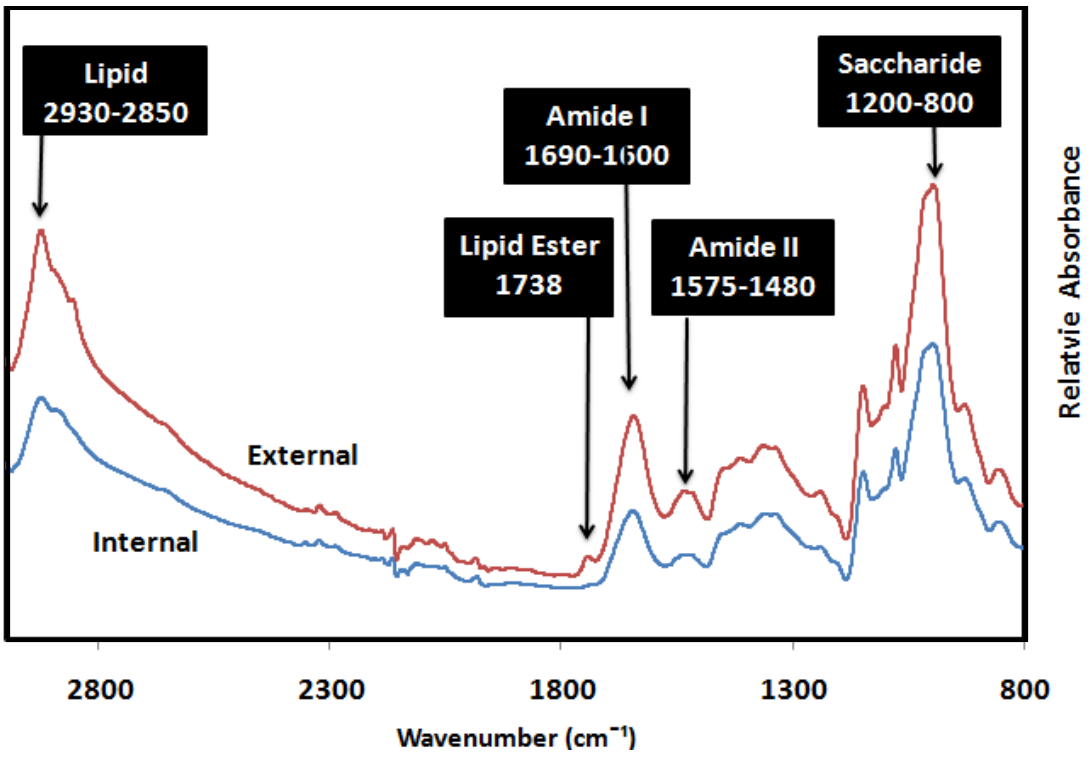

Figure 60. ATR-FTIR spectra of external and internal regions of LA-B1 rice grain.

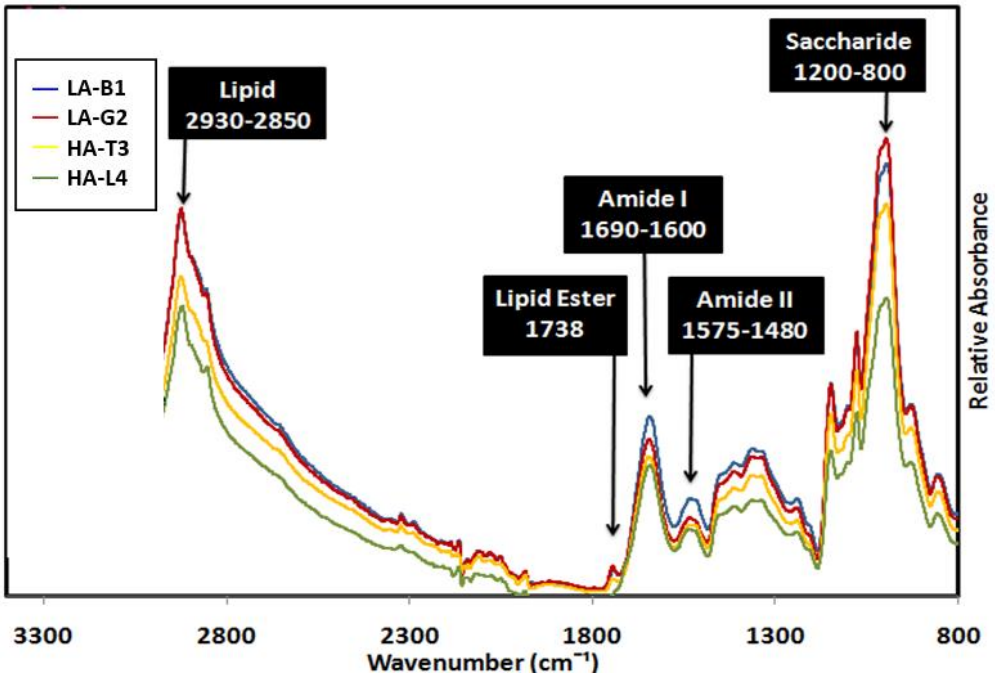

Figure 61. ATR-FTIR spectra of external regions of rice: LA-B1, LA-G2, HA-T3, HA-L4.

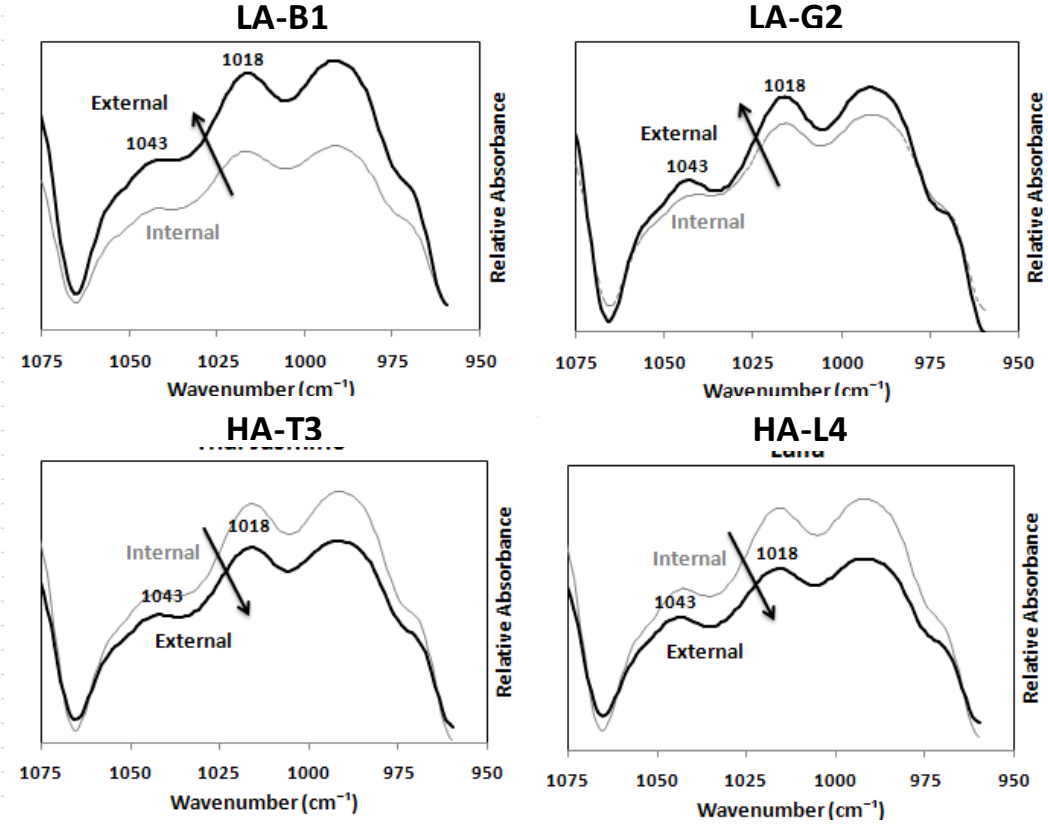

Figure 62. ATR-FTIR spectra of the external and internal regions of rice varieties: LA-B1, LA-G2, HA-T3, HA-L4.

Figure 62 shows ATR-FTIR spectra of the external and internal regions and **Table 17** shows calculation of their intensity ratio of 1045 cm^{-1} to 1018 cm^{-1} bands of the different varieties of rice grains. For all the varieties, absorbance ratio value of milled whole rice grains was halfway between the absorbance values for external and internal regions of raw rice grains. This ensures the reliability of absorbance ratio where whole milled sample was a mixture of external and internal rice grains flour. The external region of low adhesive rice varieties LA-B1 and LA-G2 (0.64 and 0.64 respectively) was less ordered than its internal region (0.66 and 0.66 respectively). Meanwhile for high adhesive rice varieties HA-T3 and HA-L4, their external region (0.68 and 0.73 respectively) is more ordered compared to its centre (0.66 and 0.67 respectively).

Table 17. Intensity ratio of 1045 cm^{-1} to 1018 cm^{-1} of rice varieties: LA-B1, LA-G2, HA-T3, HA-L4.

Rice variety	Section of rice grain	Ratio 1045/1022	Ratio External /Internal
LA-B1	Whole	0.65±0.01	0.97±0.01
	External	0.64±0.01[a]	
	Internal	0.66±0.01[a]	
LA-G2	Whole	0.65±0.01[a]	0.97±0.01
	External	0.64±0.01[a]	
	Internal	0.66±0.01[a]	
HA-T3	Whole	0.67±0.01[a]	1.03±0.01
	External	0.68±0.01[a]	
	Internal	0.66±0.01[a]	
HA-L4	Whole	0.70±0.01[a]	1.09±0.01
	External	0.73±0.01 [a]	
	Internal	0.67±0.01 [a]	

[a]The values shown are means ± SD of three replicates.

6.2.2. X-RAY DIFFRACTION (XRD) CRYSTALLINITY

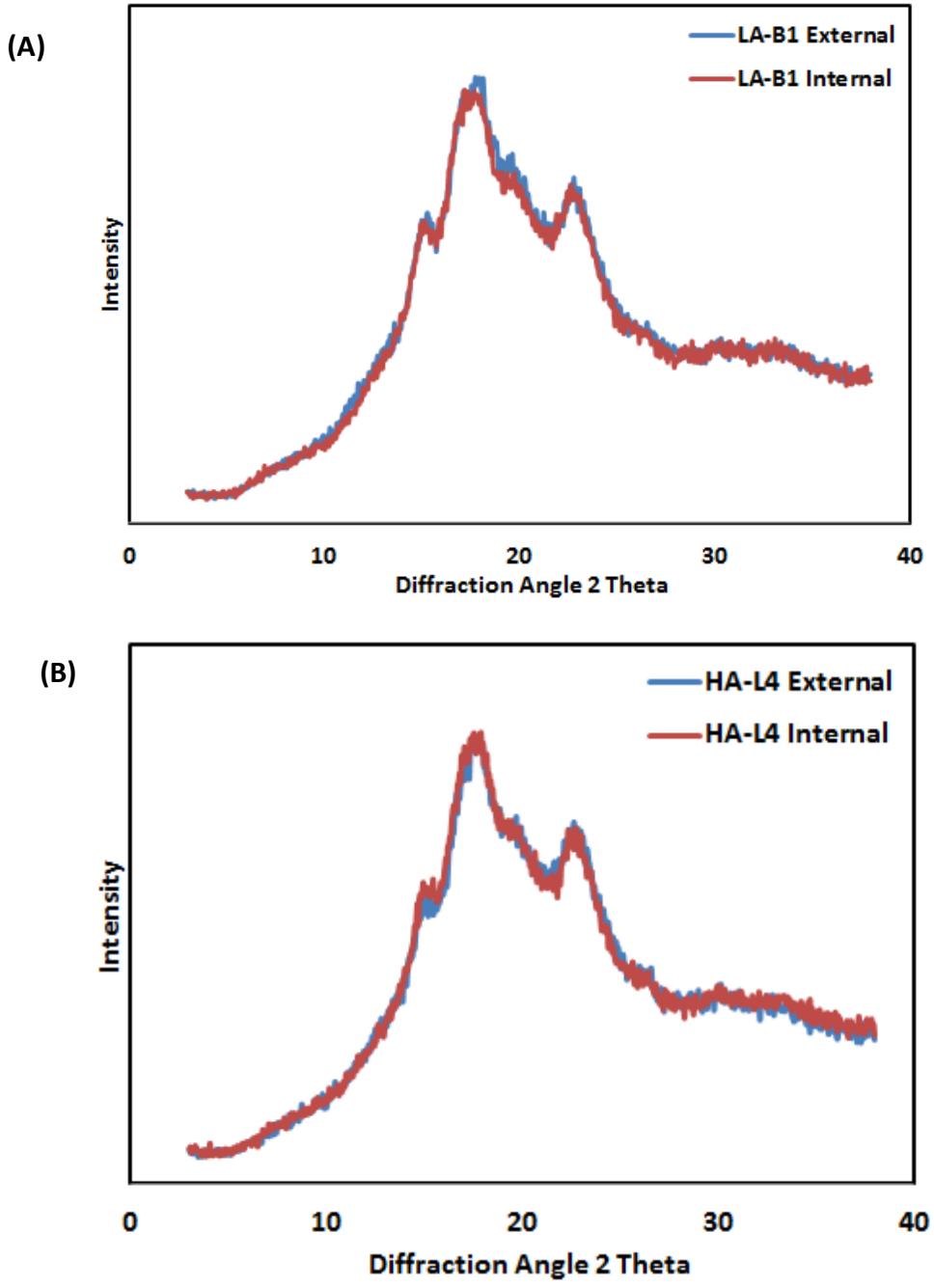

Figure 63. XRD spectra of external and internal regions of (A) LA-B1and (B) HA-L4 rice.

Table 18 shows the calculation of relative crystallinity (XRD) of ground whole grain, external and internal structures of four different varieties of rice grains. As observed by order of starch value in ATR-FTIR results, relative crystallinity value of all milled whole rice grains is halfway between the relative crystallinity value for external and internal regions of raw rice grains. This ensures the reliability of relative crystallinity value of external and internal regions. The external region of low adhesive rice varieties LA-B1 and LA-G2 (34.1 % and 32.1 % respectively) has significantly lower relative crystallinity compared to its internal regions (37.8 % and 37.6 % respectively). Meanwhile for high adhesive rice varieties HA-T3 and HA-L4, the external region (40.1 % and 40.1 % respectively) is more crystalline at its centre (38.6 % and 37.2 % respectively). This trend was also observed with order of starch.

Table 18. Relative crystallinity of rice flours: LA-B1, LA-G2, HA-T3, HA-L4.

Rice	Section of rice grain	Relative crystallinity (%)	Ratio External/Internal
LA-B1	Whole	35.1±0.1 [a]	0.90±0.01
	External	34.1±0.1 [a]	
	Internal	37.8±0.1 [a]	
LA-G2	Whole	34.5±0.1 [a]	0.85±0.01
	External	32.1±0.1 [a]	
	Internal	37.6±0.1 [a]	
HA-T3	Whole	38.3±0.3 [a]	1.03±0.01
	External	40.1±0.1 [a]	
	Internal	38.6±0.1 [a]	
HA-L4	Whole	39.2±0.3 [a]	1.07±0.01
	External	40.1±0.1 [a]	
	Internal	37.2±0.1 [a]	

[a]The values shown are means ± SD of three replicates

6.3. CORRELATION BETWEEN CRYSTALLINITY LOCALISATION AND RICE ADHESIVENESS

Figure 64 shows the correlation between adhesiveness of cooked rice (g.sec) and the ratio of relative crystallinity of external to internal region determined by XRD, and the ratio of the order of starch of external to internal region determined by ATR-FTIR. There is a positive correlation between the sticky behaviour of cooked rice and the relative crystallinity and order of starch of the surface of rice grains. The starch crystallinity (R^2=0.684) has a weaker correlation compared to the order of starch (R^2=0.908).

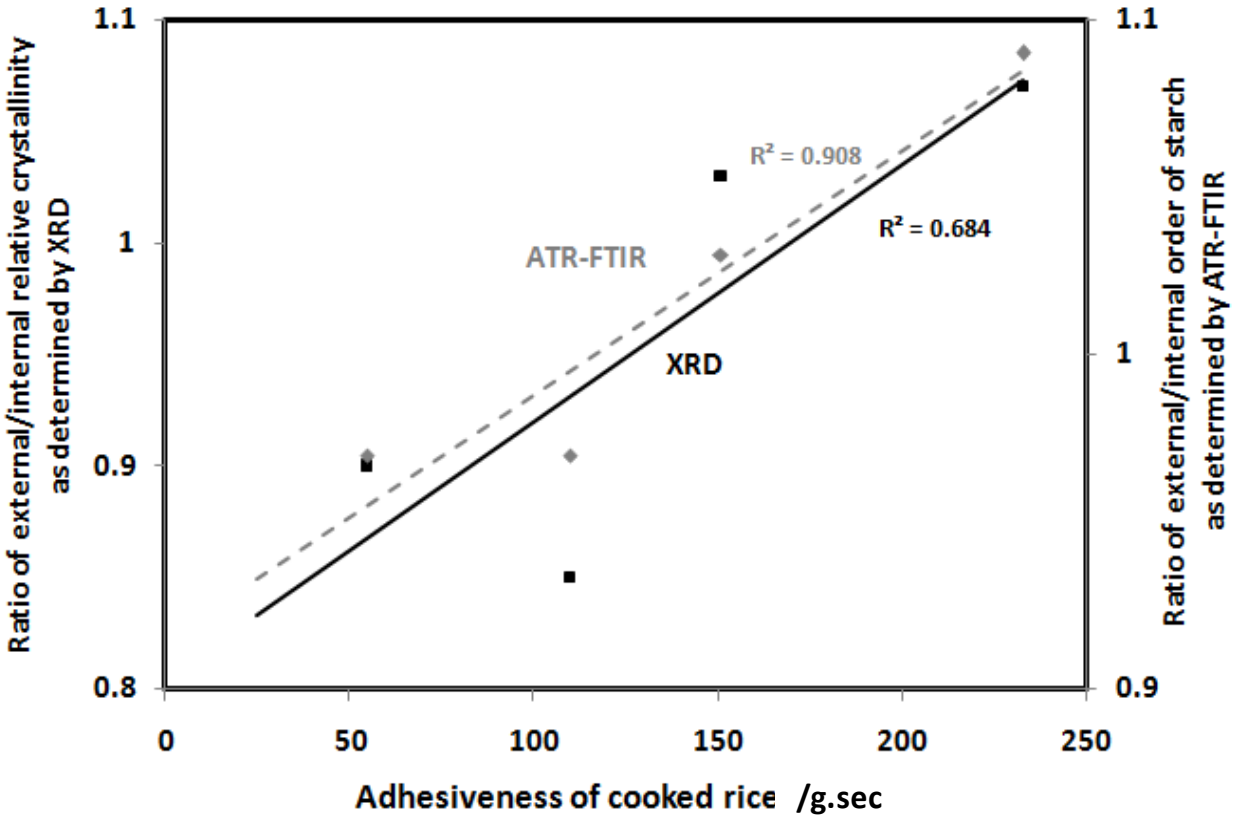

Figure 64. Correlation between adhesiveness of cooked rice (g.sec) and the ratio of relative crystallinity of external to internal region determined by XRD, and the ratio of the order of starch of external to internal region determined by ATR-FTIR.

6.4. LOCALISATION OF PROTEIN

6.4.1. BICINCHONINIC ACID (BCA) ASSAY TOTAL PROTEIN

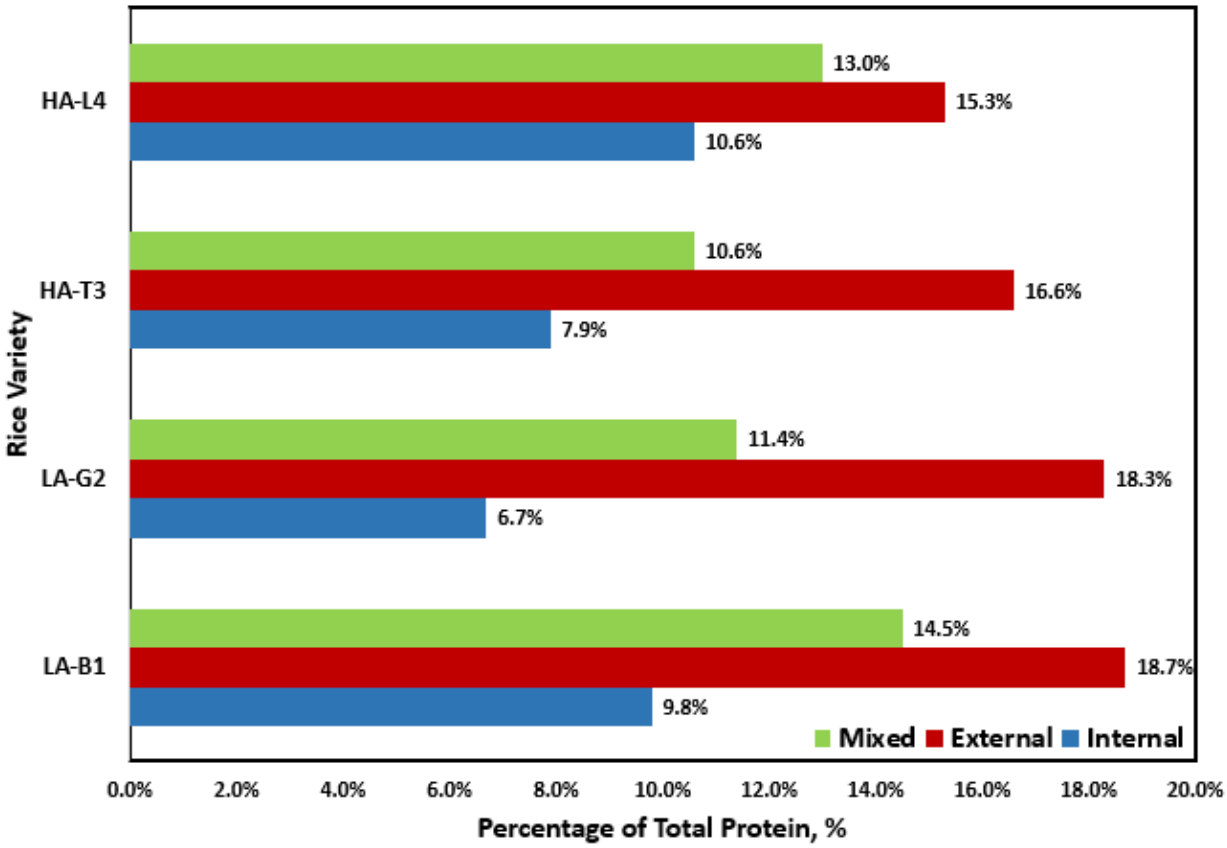

Figure 65. Percentage of total rice protein, % in the external and internal rice grains of rice varieties: LA-B1, LA-G2, HA-T3, HA-L4 chosen in this study.

Figure 65 shows the results of BCA analysis showing percentage of total rice protein, % in the external and internal regions rice grains. Percentage of external protein composition range from 15.3 % to 18.7 % while percentage of internal

protein percentage range from 6.7 % to 10.6 %. It can observed for all the rice varieties, both low and high adhesive samples exhibit higher protein content on the surface of rice compared to the central regions.

Table 19. Bicinchoninic Acid, BCA analysis result of milled external and internal regions of rice, and whole rice grains: LA-B1, LA-G2, HA-T3, HA-L4.

Rice Variety	Whole	Internal	External	Average Internal, External	Ratio External/Internal
LA-B1	14.5 %	9.8 %	18.7 %	14.25 %	1.91
LA-G2	11.4 %	6.7 %	18.3 %	12.5 %	2.73
HA-T3	10.6 %	7.9 %	16.6 %	12.2 %	2.10
HA-L4	13.0 %	10.6 %	15.3 %	13.0 %	1.44

Table 19 shows total protein content of whole kernels, external regions only and internal regions only of rice varieties LA-B1, LA-G2, HA-T3, HA-L4. There is concern that the protein content value of the external and internal regions of the rice grains may not be accurate as it is difficult to be consistent on the amount of surface material removed from each individual grain. However, **table 19** has shown that the total protein content value of whole milled rice flour is roughly the average of the protein content values of internal and internal protein content values if they were to be mixed. This indicates reliability in the physical separation method used to separate the surface and the internal regions of rice grains in this project.

There is no trend in the ratio of amount of protein present in the external and internal region of rice grains between low and high adhesive rice. There is also no trend in the internal protein composition. However, there is negative correlation between external protein composition of rice grains and cooked rice adhesiveness (**Figure 66**). Low adhesive rice grains LA-B1 and LA-G2 have a higher protein composition on their external regions (18.7 % and 18.3 % respectively) compared to external regions of high adhesive rice HA-T3 and HA-L4 (16.6 % and 15.3 % respectively).

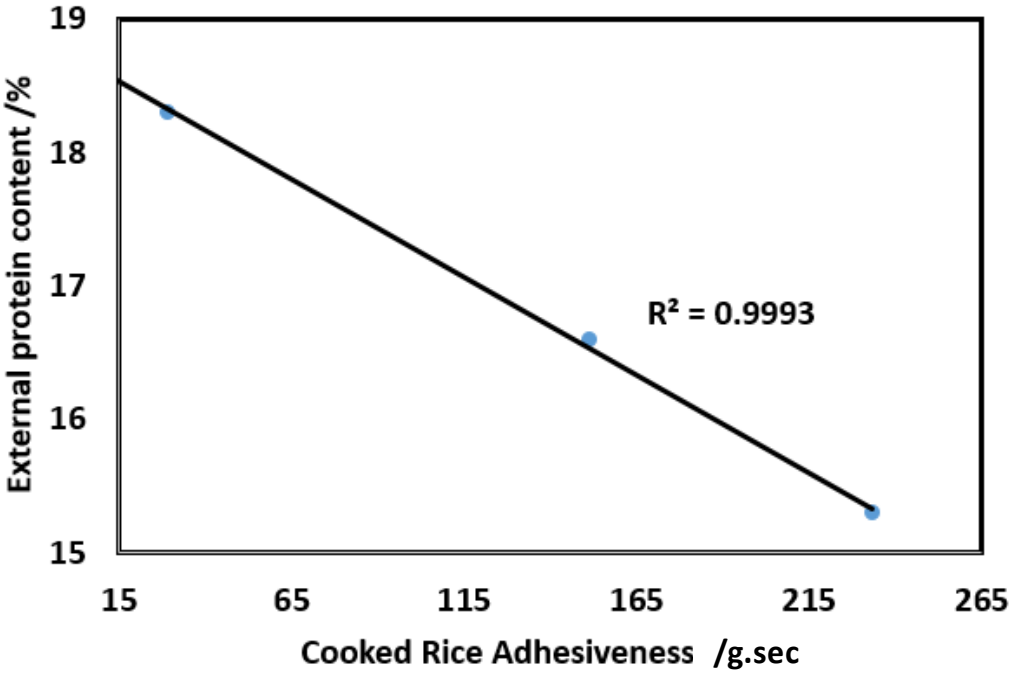

Figure 66. Correlation between external protein content /% and cooked rice adhesiveness /g.sec.

6.4.2. FOURIER TRANSFORM INFRARED AMIDE PEAK

(A)

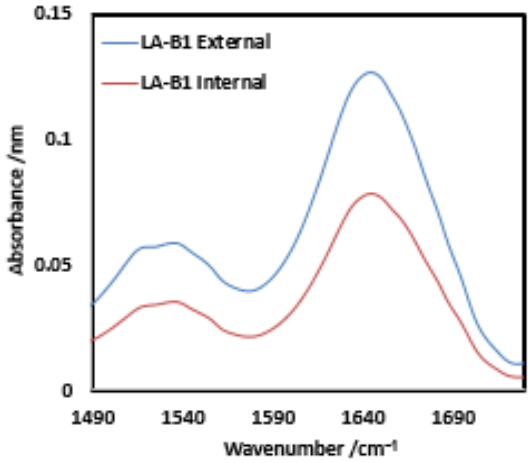

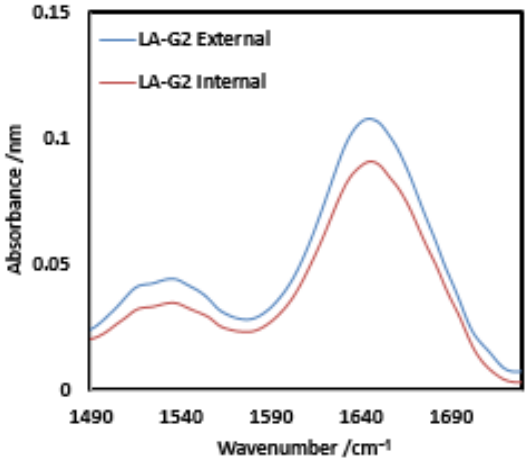

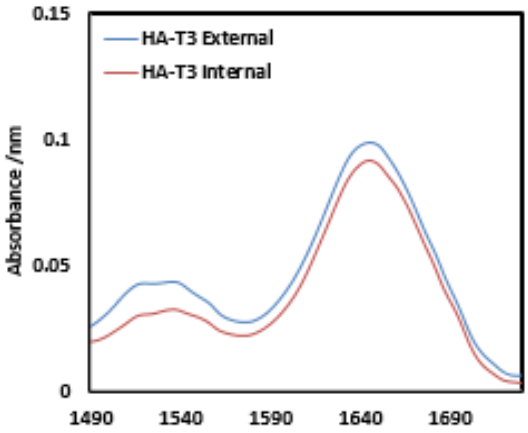

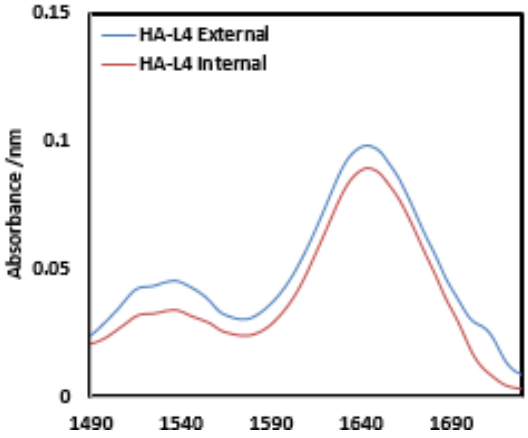

(B)

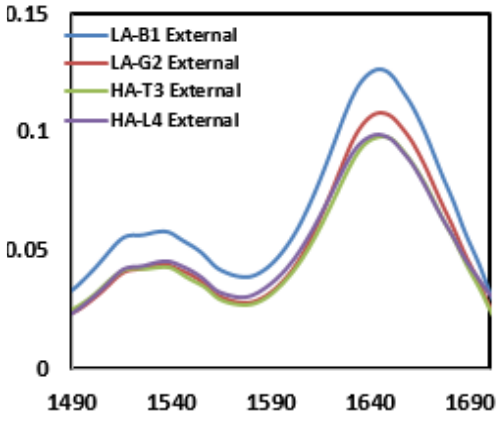

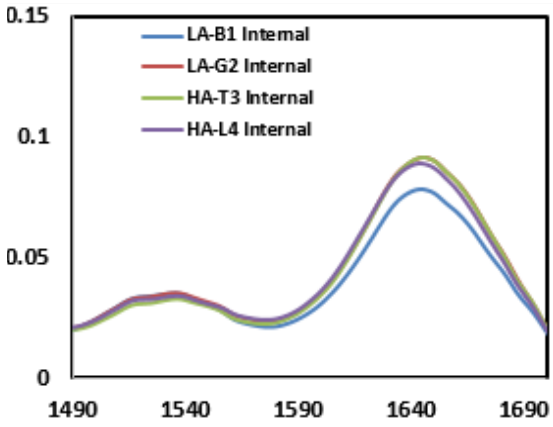

Figure 67. Amide I and amide II ATR-FTIR peaks of external and internal regions of low and high adhesiveness rice varieties: LA-B1, LA-G2, HA-T3, HA-L4; (A) individual spectrum of each variety, (B) cumulative spectra of internal and external regions.

From **Figure 67**, it can be observed that for all 4 rice varieties, both low and high adhesive groups exhibit higher amide I and amide II peaks for their external regions compared to their internal region. In addition, the external region of low adhesive rice have higher amide I and amide II peaks compared to the external region of high adhesive rice. This is also reflected in total protein content where external region of low adhesive rice have higher protein content than high adhesive rice. This also shows relative quantification of protein content in rice flour using ATR-FTIR. Therefore, it can be concluded that there is more protein present on the surface of low adhesive rice grains compared to high adhesive rice grain.

6.4.3. FOURIER TRANSFORM INFRARED (FTIR) MICROSCOPE AMIDE PEAK

In-order to further justify that there is a significant difference between the external and internal regions of the rice grain as observed by ATR-FTIR, FTIR microspectroscopy is used to investigate the distribution of amide spectra across the cross-section of a rice grain. **Figure 68A** shows a photograph taken of a cross-section of a LA-B1 rice grain using FTIR microscope (**3.5.3. FTIR microscope**). The dimensions are different horizontally and vertically. In this case, horizontal dimensions are approximately 1500 µm and vertically 1700 µm. Two methods were used to investigate the distribution of spectra per 100 µm layer of the sample. The first method (**Figure 68B**) involves the acquisition of IR spectra horizontally across the rice grain (in this case 12 selected

positions) while the second method (**Figure 68C**) was achieved by IR measurements taken vertically (in this case 12 selected positions). Both methods were performed on the four varieties of rice per 100 µm layer of the sample.

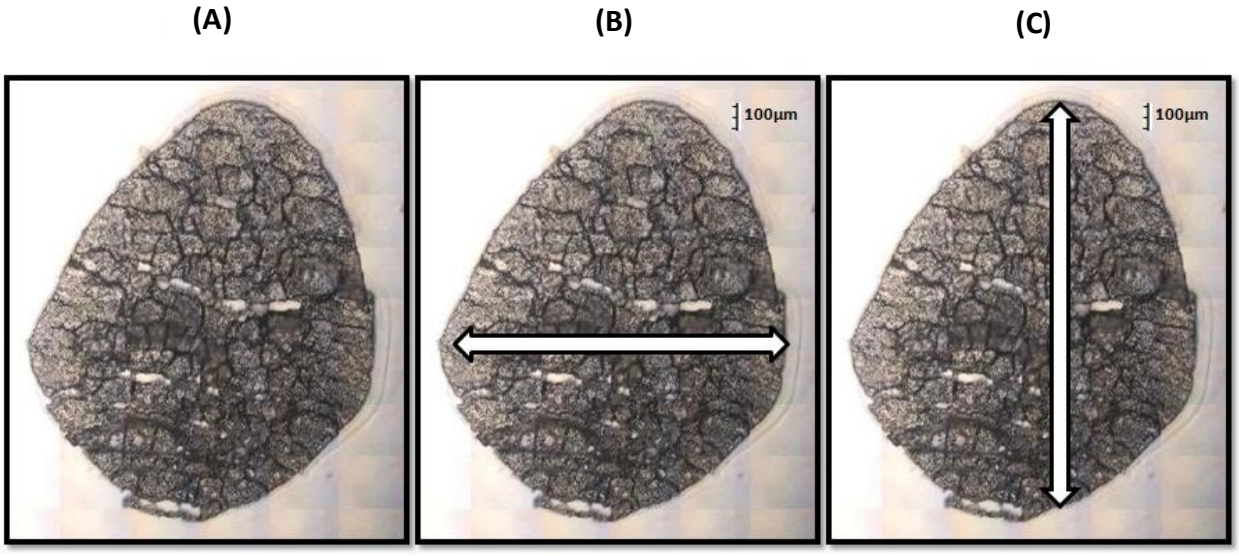

Figure 68. Snapshots taken using FTIR microscope (A) 10 µm cross-section of a LA-B1 rice grain (dried in P_20_5 for 48 hours) and FTIR measurements along (B) horizontally and (C) vertically.

Figure 69 shows the average distribution of the amide I (1650 cm^{-1}) and amide II (1550 cm^{-1}) peaks along the cross-section of low adhesive LA-B1 (**Figure 69A**) and High Adhesive HA-T3 (**Figure 69B**) rice grains using both of the methods described. For Low Adhesive LA-B1, it can be clearly observed that the distribution of amide bands is not uniform within the rice grain. There is a high absorbance at the surface of raw rice (points 0 - 2) which decreases gradually towards the centre (point 6) and increases again towards the surface (points 10 - 12). However, for High Adhesive HA-T3, there was no significant difference in the spectra of amide peaks along its cross-section.

(A)

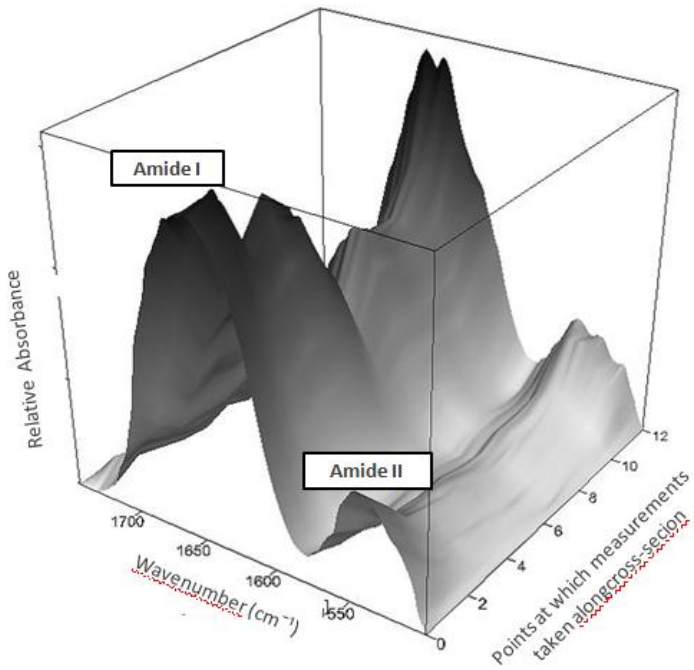

(B)

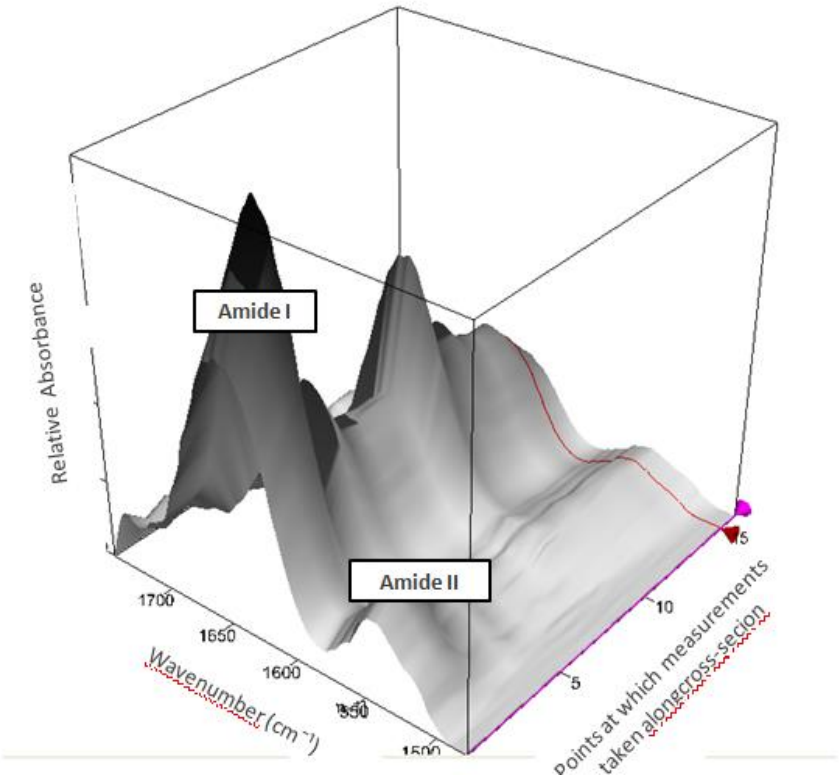

Figure 69. The distribution of amide I (1650 cm-¹) and amide II (1550 cm-¹) along the cross-section of (A) low adhesiveness LA-B1 (B) high adhesiveness HA-L4 rice grain.

6.5. LOCALISATION OF LIPID ESTER

6.5.1. ATTENUATED TOTAL REFLECTANCE-FOURIER TRANSFORM INFRARED (ATR-FTIR) LIPID ESTER

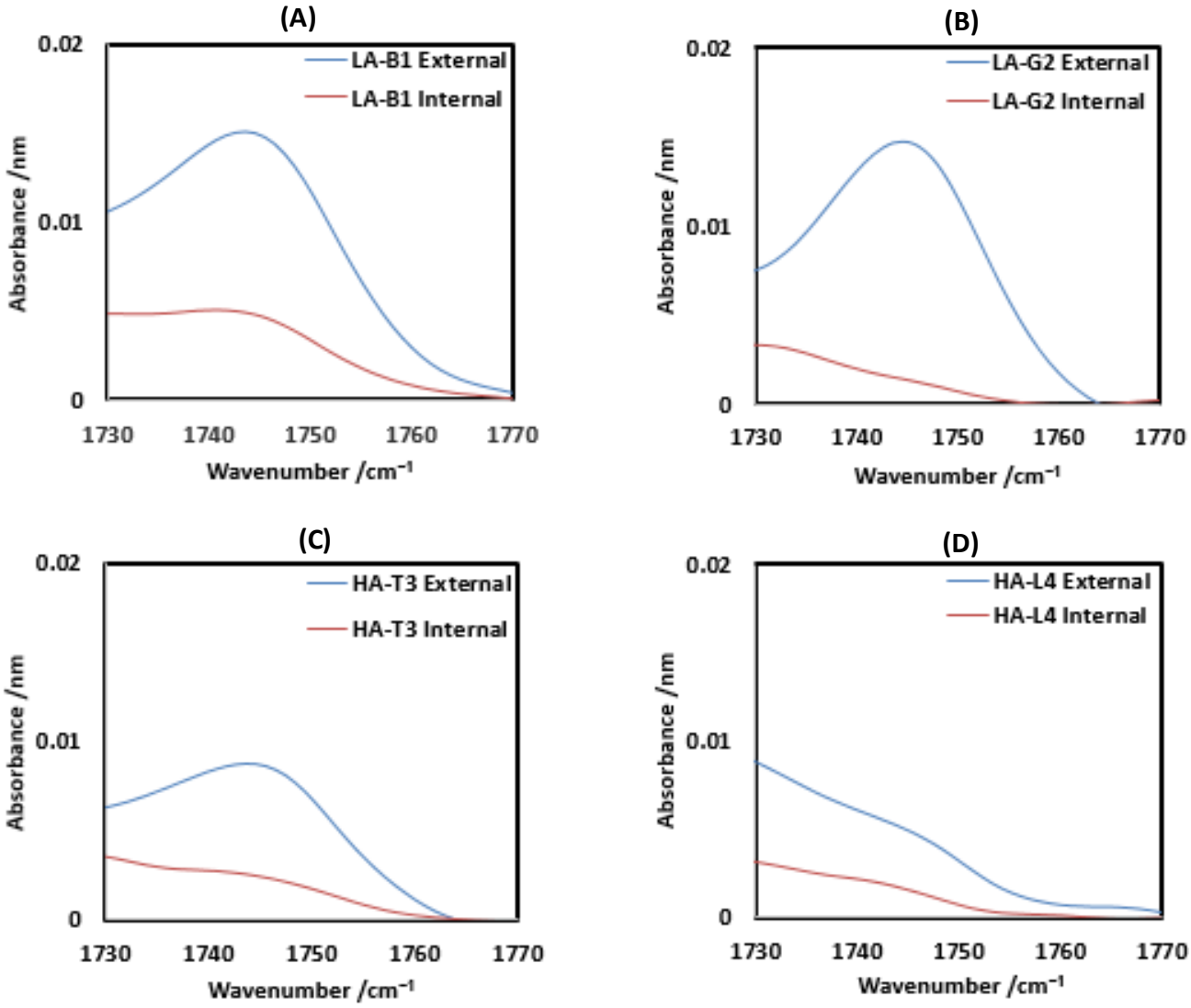

Figure 70. Ester lipid peaks of external and internal regions of low and high adhesiveness rice varieties: (A) LA-B1, (B) LA-G2, (C) HA-T3, (D) HA-L4.

Figure 70 shows that for all four rice varieties, external ester lipid peak is higher than its internal lipid peak. It can also be observed that external region of low adhesive rice varieties LA-B1 and LA-G2 have higher ester lipid peaks compared to external region of high adhesive rice varieties HA-T2 and HA-L4. Previous chapter shows that ester lipid peaks in ATR-FTIR can be used to determine relative quantification of lipid contents in rice starch and rice flour. Therefore from this result, it can be suggested that there is more amount of lipid present in the surface of low adhesive rice compared to high adhesive rice. It can be concluded that lipid content on the surface of raw rice grains can contribute to the texture of cooked rice.

6.6. CORRELATION BETWEEN SURFACE PROTEIN, SURFACE LIPID AND RICE ADHESIVENESS.

The sticky texture of rice is negatively correlated to the external protein and lipid content and lipid peaks in ATR-FTIR. This indicates that the higher amount of protein and lipid present on the surface of raw rice grains results in less adhesive and less sticky rice when cooked. This correlates with the results by Ramesh *et al*, 2000 who reported that high protein content in the outer layers of rice contributes to reduced stickiness after cooking and vice versa.

6.7. SUMMARY AND CONCLUSION OF CHAPTER

This chapter shows that there is indeed a significant difference between the internal and external components of raw rice grains. There is a significant difference in amide and lipid peaks and order of starch between the centre of rice grains and the external regions. This is important to highlight that in previous studies; only whole structures of rice grains are considered. Based on preliminary subjective assessment of stickiness, it was also observed that the sticky texture of rice is negatively correlated to the external amide and lipid content whereas the correlation to the relative crystallinity and order of starch was shown to be positive.

This highlights the importance of a surface study when considering rice stickiness. It is important to consider both the basic composition of whole rice grains as well as the localisation of the components when correlating the results with rice texture data. It was decided that it would be interesting to study the removal and addition of protein and lipid components from the surfaces of rice grains to investigate any differences in cooked rice stickiness when the surfaces are altered in Chapter 7.

7. SURFACE ALTERATION

The previous chapter has shown that surface properties of raw rice grains play a role in the texture of cooked rice. It was concluded that the protein and lipid content on the surface of rice grains is negatively correlated to stickiness of cooked rice. Low adhesive rice had more protein and lipid on the surface of its grains. From this, it was hypothesized that the removal or reduction of protein and lipid from the surface of rice grains can result in a more adhesive cooked rice texture. This chapter aims to physically alter the surface components of raw rice grains and to test this hypothesis whereby a reduction of surface protein and lipid increases the adhesiveness texture of cooked rice. The chapter starts with the development of efficient removal of protein and lipid components from rice flour with minimal disruption of rice starch, followed by the removal of protein and lipid components from surface of rice grains and ends with a conclusion on whether a reduction in the surface protein and lipid components has any effect on cooked rice texture.

7.1. METHOD DEVELOPMENT: REMOVAL OF PROTEIN

Prior to the removal of protein components from the surface of rice grains, the efficiency of protein removal was first tested on rice flour. To provide the most reliable comparison, rice flour with the highest external protein content is used. Previous chapters have shown that LA-B1 had the highest protein composition as a whole rice grain (14.5 %) and on its surface region (18.7 %).

7.1.1. EFFICIENCY OF PROTEIN EXTRACTION:

Lim *et al*, 1999 reported successful protein removal methods using alkaline solvents, surfactants and protein hydrolyzing enzymes. This includes sodium hydroxide (NaOH), sodium dodecyl sulfate (SDS) and pronase enzyme treatment. **3.4.2 Washing of proteins** shows steps used in alkaline protein removal, which involves up to 3 hours and 3 rounds of extraction and the efficiency of each alkaline solvent is tabulated in **Table 20**. Concentrations 1.2 % SDS, 0.1 % NaOH, 0.2% NaOH are used as performed by Lim *et al*, 1999.

Table 20. Protein contents of LA-B1 after 3 rounds of treatments with alkaline solvents 1.2 % SDS, 0.1 % NaOH and 0.2 % NaOH.

	Pre-treatment	**1.2 % SDS**	**0.1 % NaOH**	**0.2 % NaOH**
Protein Content /%	14.5 ± 0.1 %	3.2 ± 0.1 %	4.0 ± 0.1 %	3.1 ± 0.1 %
Protein removed /%	-	78.0 ± 0.1 %	72.0 ± 0.1 %	79.0 ± 0.1 %

LA-B1 rice flour treated with all alkaline solvents shows a decrease in protein content /% after treatment. Alkaline solvents 1.2 % SDS, 0.1 % NaOH and 0.2 % NaOH reduced protein content of untreated LA-B1 rice flour from 14.5 % composition down to 3.1 – 4.0 %. This indicates protein removal efficiency of 72.0 – 79.0 % of total rice protein. Lim *et al*, 1999 reported similar results where protein removal efficiency is approximately 80 %. Amongst the three solvents, the most efficient protein removal is 0.2 % NaOH (79.0 % efficiency), followed by 1.2 % SDS (78.0 % efficiency while least

efficient alkaline solvent is 0.1 % NaOH (72.0 % efficiency). Since 80 % of rice protein is alkaline-soluble glutelin, it can be suggested that 0.2 % NaOH is able to fully remove glutelin protein from rice flour. Therefore, for the rest of alkaline soluble protein removal studies, 0.2 % NaOH is used. To investigate whether other types of rice proteins contribute to rice texture, methods to remove them is also developed.

7.1.2. REMOVAL OF DIFFERENT TYPES OF RICE PROTEIN: ATTENUATED TOTAL REFLECTANCE-FOURIER TRANSFORM INFRARED (ATR-FTIR).

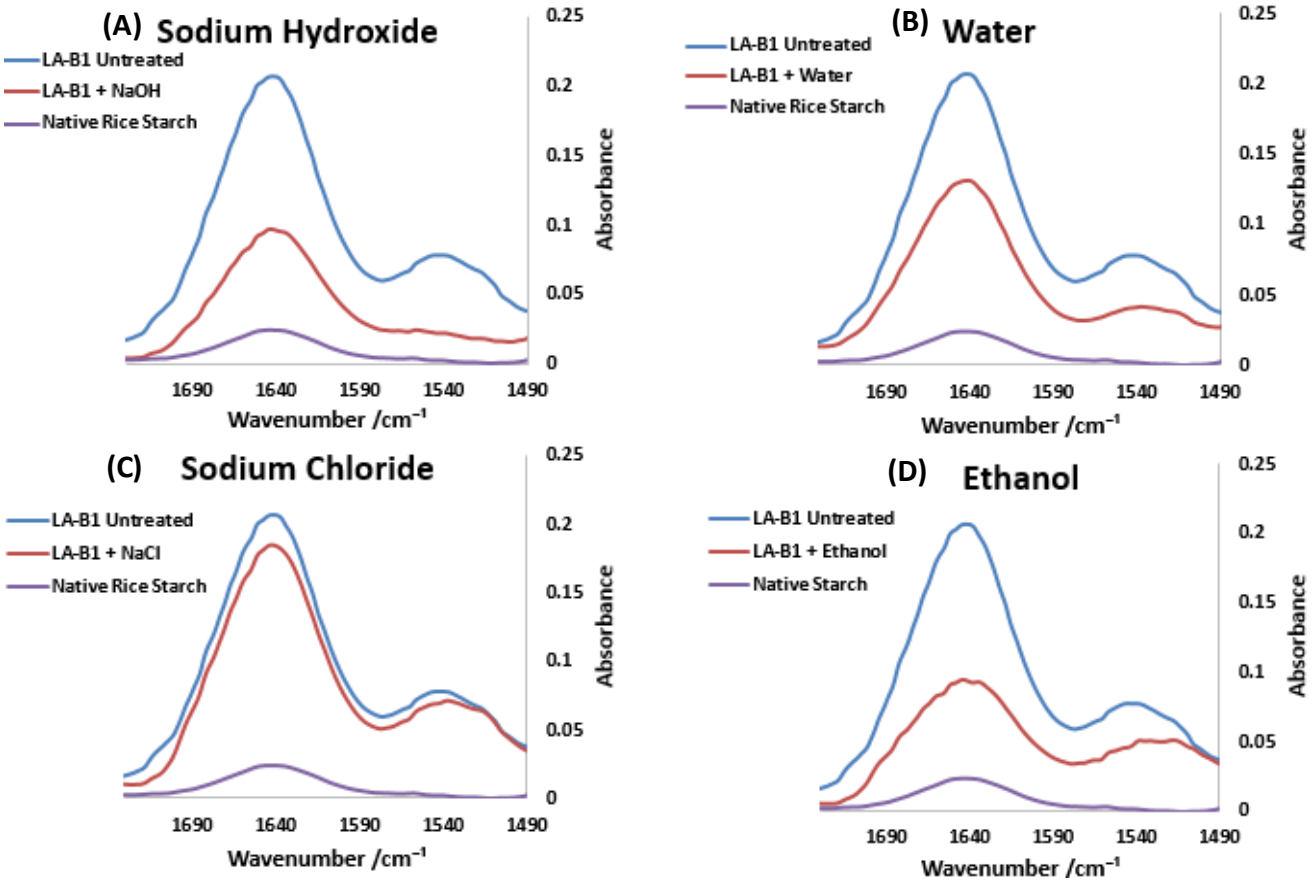

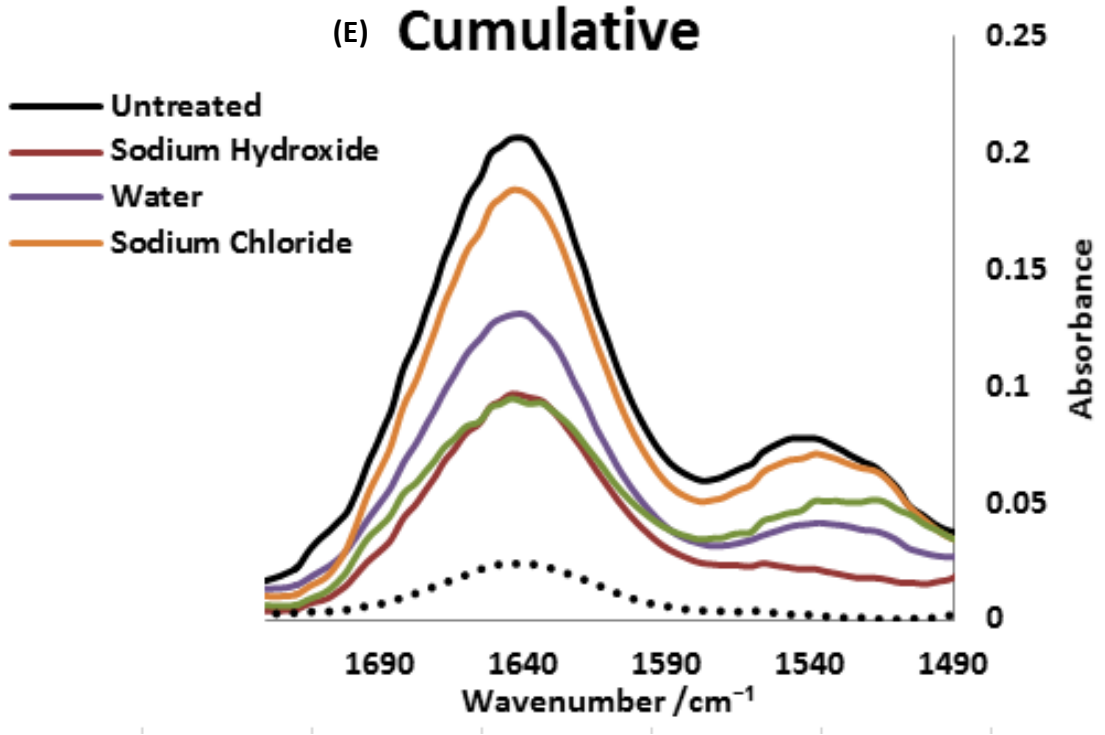

Figure 71. ATR-FTIR amide I and amide II peaks of LA-B1 before and after one treatment with different protein removal solutions: (A) sodium hydroxide, (B) water, (C) sodium chloride, (D) ethanol and (E) cumulative spectra.

Figure 71 showing removal of different types of protein in LA-B1. All four types of proteins removal solutions/solvents show a decrease in amide I and amide II peaks. For amide I peak (1690 – 1600 cm^{-1}), treatment with sodium hydroxide and ethanol shows most decrease followed by treatment with water and little change when treated with sodium chloride. For amide II peak (1575 - 1490 cm^{-1}), treatment with sodium hydroxide shows most decrease, followed by treatment with water and ethanol, and little change when treated with sodium chloride.

In theory, sodium hydroxide removes alkali soluble globulins (80 % of rice protein), aater removes water soluble albumin (9 - 11 % of rice protein), sodium chloride removes salt soluble glutelins (7 – 15 %) and ethanol removes alcohol soluble prolamins (2 - 4 %). Results of amide peaks can be explained by the relative protein contents of rice flour where the highest contents of protein type extracted was by NaOH, followed by NaCl and water. However, results of ethanol spectra shows too much protein removal, hence not suitable for this study. Therefore, ethanol will not be used further in this study.

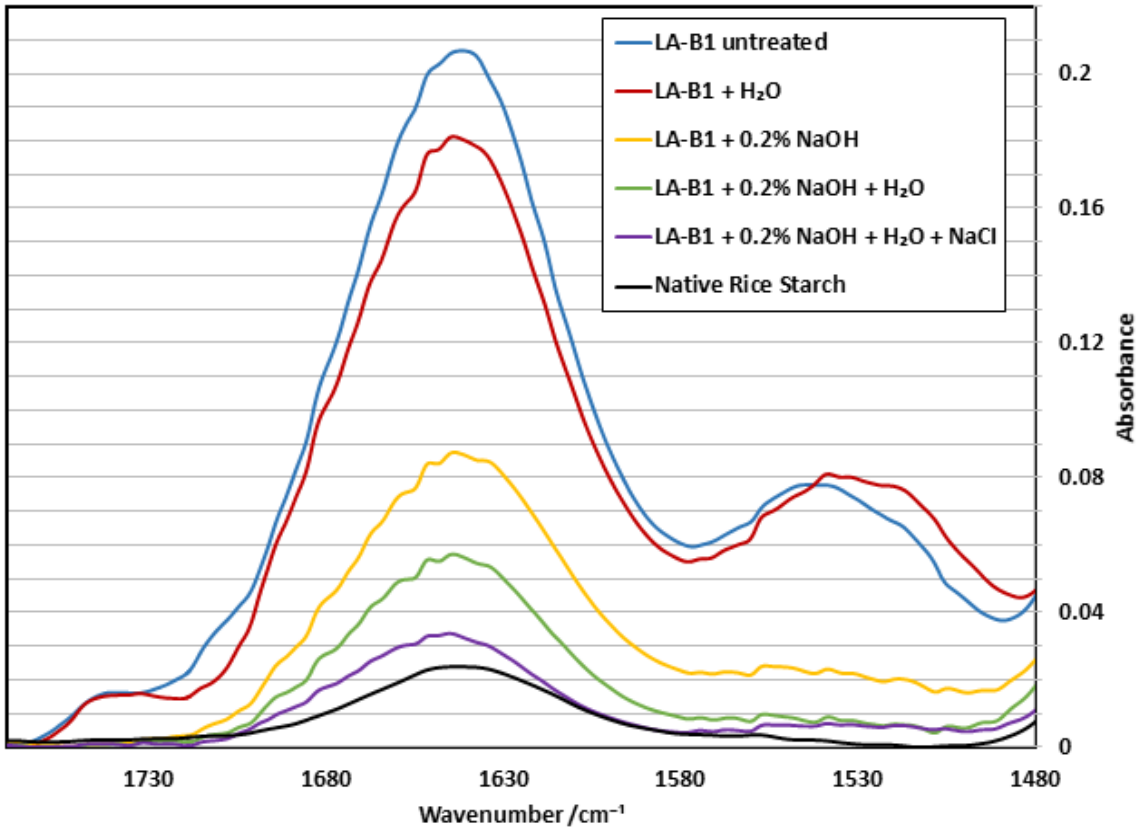

Figure 72. ATR-FTIR amide I and amide II peaks of LA-B1 rice flour after treatment with 0.2 % NaOH, H_2O and NaCl.

Figure 72 shows ATR-FTIR amide peaks of LA-B1 after 4 rounds of treatment with (i) H_2O only, (ii) 0.2 % NaOH only, (iii) 0.2 % NaOH + H_2O and (iv) 0.2 % NaOH + H_2O + NaCl. Spectra shows highest amide I and amide II peaks for (1) untreated LA-B1, followed by (2) treatment with only H_2O (control), (3) treatment with only 0.2 % NaOH, (4) treatment with 0.2 % NaOH and H_2O, (5) treatment with 0.2 % NaOH, H_2O and NaCl and (5) native rice starch, with peak values tabulated in **Table 21**. **Figure 72** clearly demonstrates gradual breaking of amide bonds firstly by alkali soluble glutelin rice protein (using 0.2 % NaOH), followed by water soluble albumin rice protein (using H_2O) and lastly by salt soluble globulin rice protein (using NaCl) until peak values almost reaches amide peak values of rice starch.

A trend can be observed in peak values of amide I peaks and the relative decrease in amide peak value is calculated relative to LA-B1 and native rice starch (**Table 21**). It is interesting to note that the decrease in amide peaks corresponds to estimated amount of rice protein type. It can be predicted that the removal of glutelin, albumin, and globulin will approximately remove 80 %, 10 % and 10 % of amide bonds respectively. Therefore, the predicted cumulative amide bonds broken after sequential treatments with 0.2 % NaOH, H_20 and finally NaCl is 80 %, 90 % and 98 %. **Table 21** shows that in this study, the removal of glutelin, albumin and globulin shows relative decrease in amide peak by 65.3 %, 81.8 % and 94.6 %. This highlights the potential use of ATR-FTIR for detection of gradual protein removal.

Table 21. Amide I and amide II peak absorbance values of LA-B1 after treatments with H_2O, 0.2 % NaOH and NaCl.

Peak Absorbance	LA-B1	LA-B1 + H_2O	LA-B1 + 0.2 % NaOH	LA-B1 + 0.2 % NaOH + H_2O	LA-B1 + 0.2 % NaOH + H_2O + NaCl	Native Rice Starch
Amide I	0.207	0.181	0.0875	0.0572	0.0337	0.0239
Relative decrease in Amide peak	-	14.2 %	65.3 %	81.8 %	94.6 %	-

7.1.3. GRADUAL BREAKING OF AMIDE BONDS: ATTENUATED TOTAL REFLECTANCE-FOURIER TRANSFORM INFRARED (ATR-FTIR)

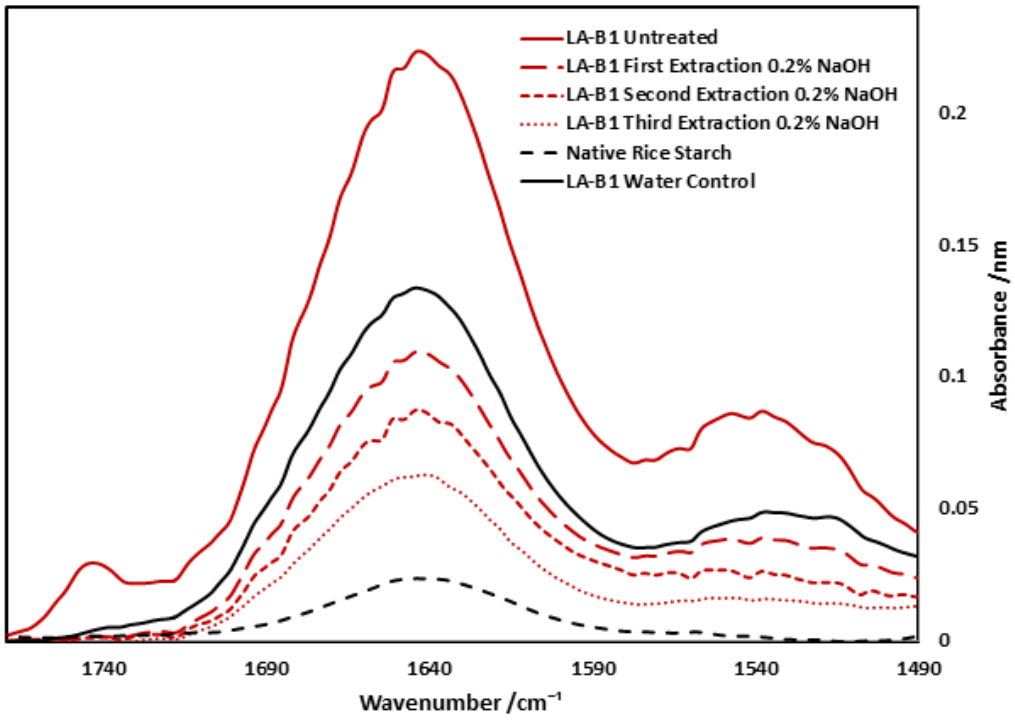

Figure 73. ATR-FTIR spectra of first, second and third round of protein extraction with 0.2 % NaOH from LA-B1, as observed by amide I and amide II peaks.

Figure 73 shows gradual breaking of amide peaks of low adhesive rice LA-B1 when treated with 0.2 % NaOH. This clearly shows gradual decrease of amide I and amide II peaks from first to third extraction. This again highlight the potential of ATR-FTIR to be used to monitor changes in amide bonds during protein removal studies.

7.2. MONITORING LOSS OF STARCH

7.2.1. POST REMOVAL DIFFERENT TYPES OF RICE PROTEIN: X-RAY DIFFRACTION

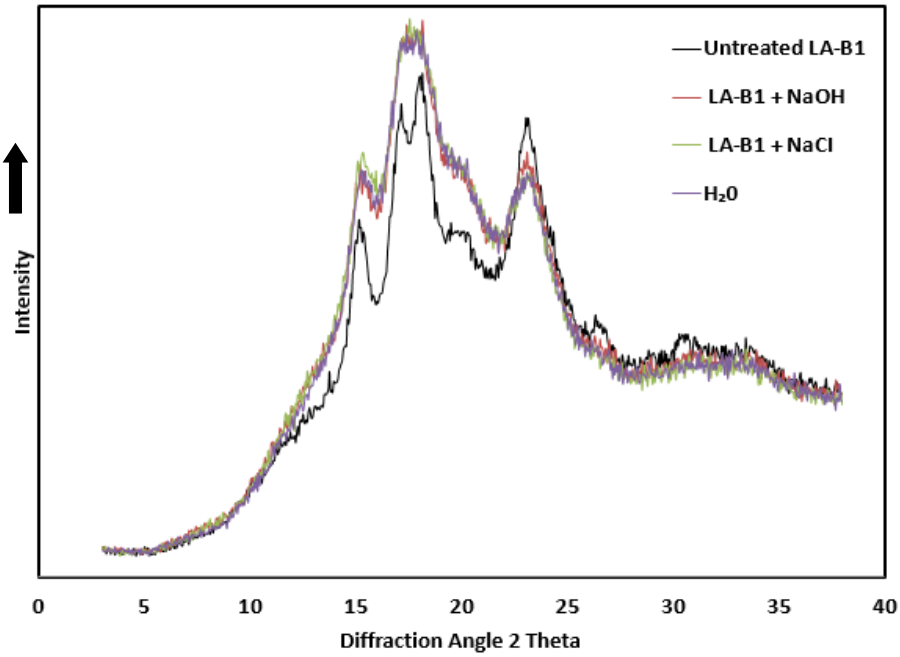

Figure 74. X-Ray Diffraction (XRD) pattern when LA-B1 is treated with 0.2 % NaOH, H_2O, NaCl and ethanol.

Figure 74 shows XRD pattern when LA-B1 has undergone treatment with NaOH, H_2O, NaCl and ethanol while **Table 22** shows starch crystallinity values. Treatment with NaOH, H_2O, NaCl and ethanol did not have a significant effect on relative starch crytallinity, therefore, samples can be used for further analysis. All the solvents can be

used for protein removal method without affecting starch granule, hence, studies on rice texture can be performed.

Table 22. Relative crystallinity /% of LA-B1 after treatment with 0.2 % NaOH, NaCl and ethanol.

	LA-B1 + H_2O	LA-B1 + 0.2 % NaOH	LA-B1 + NaCl	LA-B1 + Ethanol
Relative crystallinity /%	32.6 ± 0.4	29.8 ± 0.1	29.8 ± 0.2	30.4 ± 0.02

7.3. EFFECT OF REMOVAL OF PROTEIN ON RICE PASTING PROPERTIES.

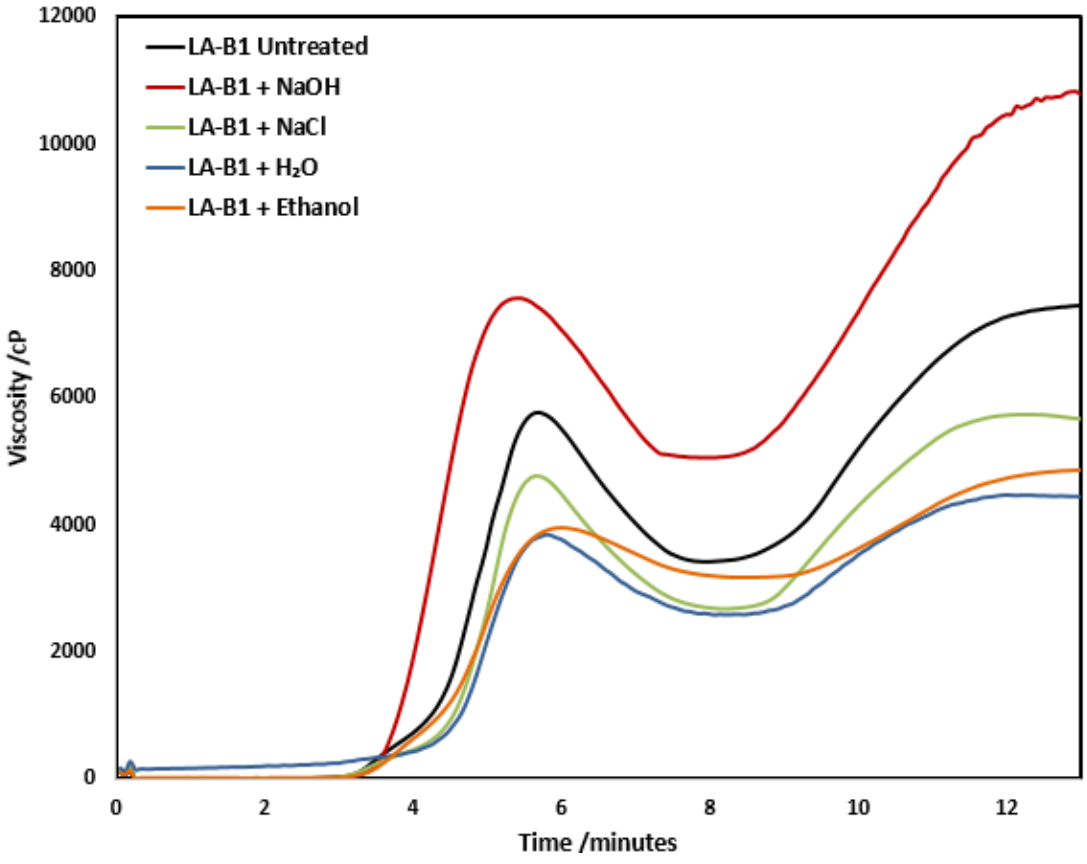

Figure 75. Behaviour of LA-B1 rice powder after removal of different types of rice proteins: treatment with 0.2 % sodium hydroxide, sodium chloride, water and ethanol.

Figure 75 shows starch pasting properties of LA-B1 after removal of different types of rice proteins with 0.2 % sodium hydroxide, sodium chloride, water and ethanol. Treatment with 0.2 % NaOH resulted in a faster pasting time, higher peak viscosity and higher final viscosity compared to untreated LA-B1. On the other hand, treatment with NaCl, water and ethanol results in a delayed onset of pasting time but results in a lower peak viscosity and lower final viscosity. This correponds to study by Marshall *et al*, 1990 where removal of rice protein had a measurable effect on starch gelatinisation.

7.4. REMOVAL OF SURFACE PROTEINS

7.4.1. METHOD DEVELOPMENT

Successful removal of rice proteins from rice grains led to attempts to remove rice proteins from the surface of raw rice grains. **Figure 71** shows ATR-FTIR results showing external, internal regions of LA-B1 whole kernel rice grains after treatment with 0.2 % NaOH, water and NaCl, with LA-B1 rice flour as controls. Both external and internal regions shows absence of amide II peak and decreased level of amide I peak. However, in theory internal regions of LA-B1 should not be affected when only the surface of rice grains is exposed to the alkaline solvent.

It is interesting to note that when rice flour was treated with 0.2 % NaOH, water and NaCl, there was absence of ester lipid bonds (also observed in **7.1.3, Figure 68**).

However, when whole rice kernels were treated with 0.2 % NaOH, water and NaCl, the surface region of the rice kernels still show presence of lipid and ester lipid peaks (**Figure 76**). This indicates that lipids bonds were not broken if whole rice kernels were treated with 0.2 % NaOH but lipid bonds were broken when the rice kernels are milled into flour. It can be suggested that the milling process might slightly physically damage rice flour, facilitating breaking of lipid bonds. This shows successful removal of proteins from surface of rice grains.

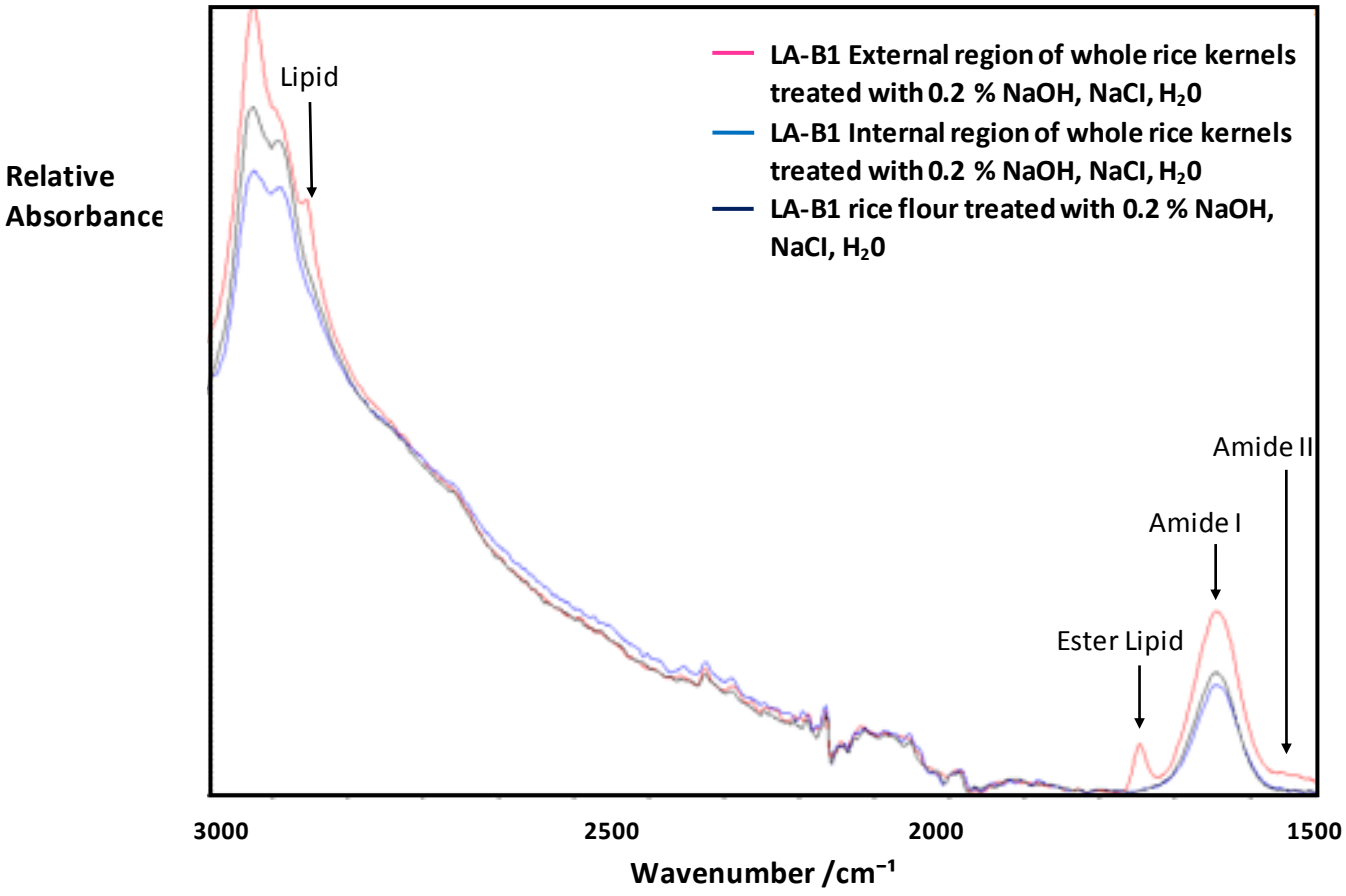

Figure 76. External and internal regions of LA-B1 after treatment with 0.2 % NaOH, water and NaCl, with rice flours as controls.

7.4.2. EFFECT ON COOKED RICE TEXTURE

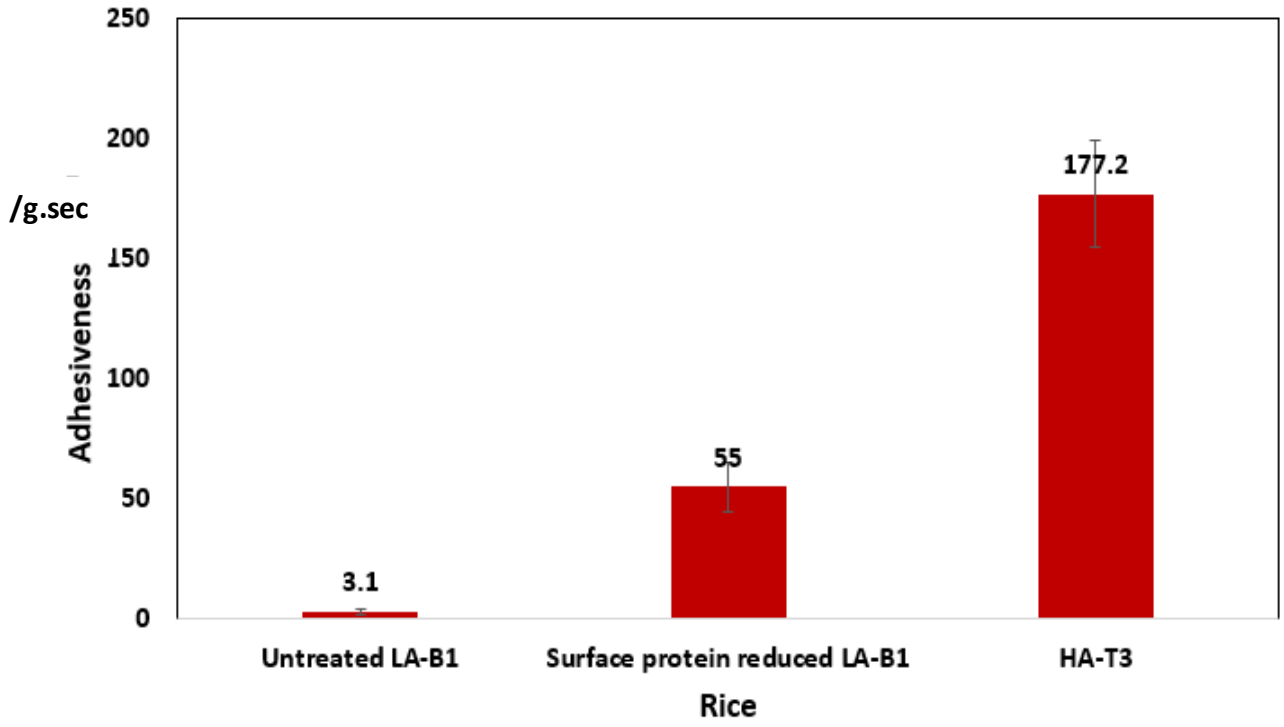

Figure 77. Texture analysis of surface protein reduced LA-B1.

Figure 77 shows texture analysis results of LA-B1 rice grains when their surface protein is reduced. Compared with untreated LA-B1 (3.1 g.sec), adhesiveness of surface protein reduced LA-B1 is significantly higher (55.0 g.sec). However, compared with untreated high adhesive rice variety HA-T3 (177.2 g.sec), the adhesiveness of surface protein reduced LA-B1 is still significantly lower. This further justifies that protein content on the surface of rice grains have a contribution to the textural properties of cooked rice.

Removing protein from the surface of raw rice grains increase its adhesiveness texture when cooked. This corresponds with study by Hamaker and Griffin, 1990 where

adhesiveness of cooked rice increased when rice is cooked in water containing dithiothreitol, a compound known to disrupt protein. Although the adhesiveness value of surface reduced protein is not as high as that of high adhesive HA-T3 which has naturally lower protein on its external regions, this either indicates that surface protein alone do not contribute to cooked rice texture, or there is not enough protein removed from the surface of rice. Due to time constraints, the protein content of the rice surface is not conducted.

7.5. REMOVAL OF RICE LIPIDS

After treatment with chloroform, hexanal, water saturated butanol and hexane, this project has concluded that the most efficient lipid removal is using 2:1 chloroform:methanol.

7.5.1. EFFICIENCY OF LIPID ESTER REMOVAL.

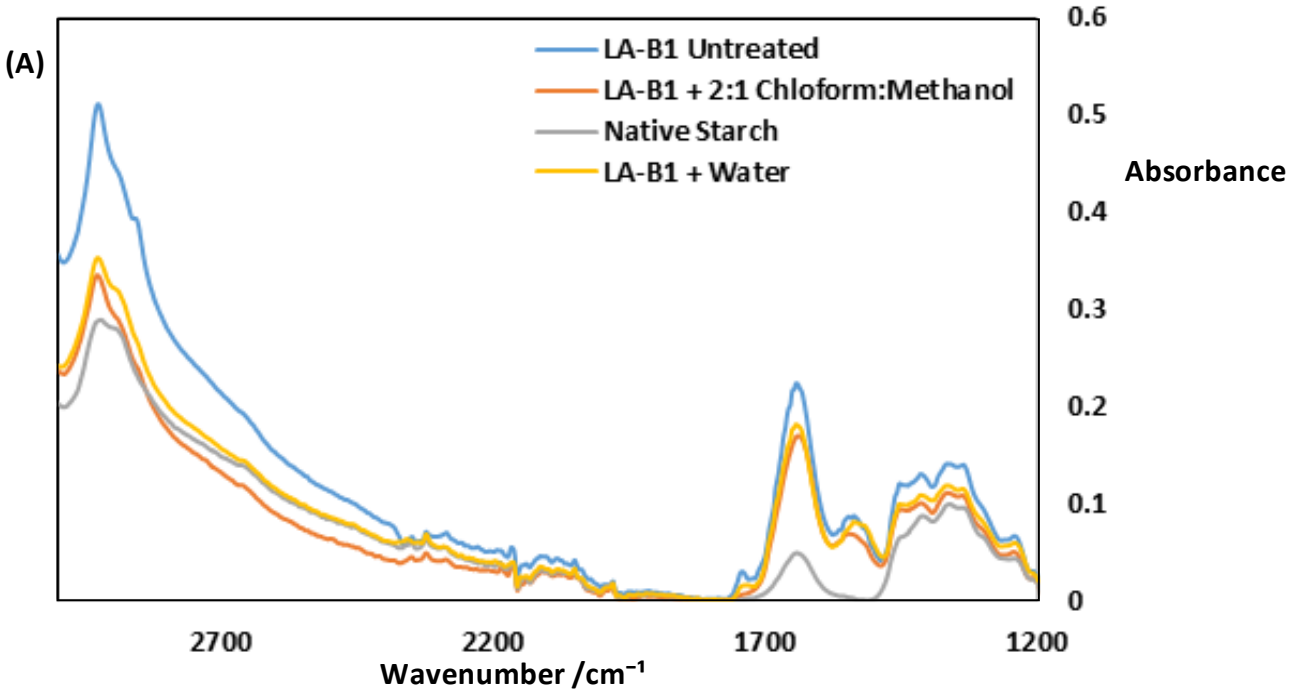

(B)

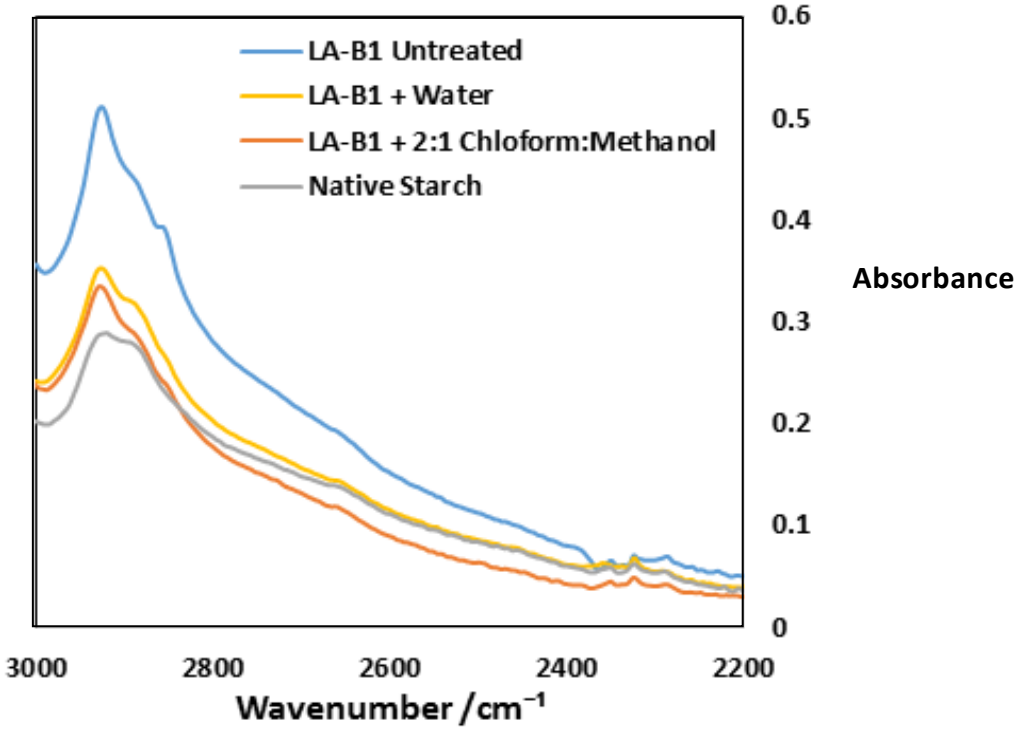
LA-B1 Untreated
LA-B1 + Water
LA-B1 + 2:1 Chloform:Methanol
Native Starch
0.6
0.5
0.4
0.3
0.2
0.1
0
Absorbance
3000
2800
2600
2400
2200
Wavenumber /cm⁻¹

(C)

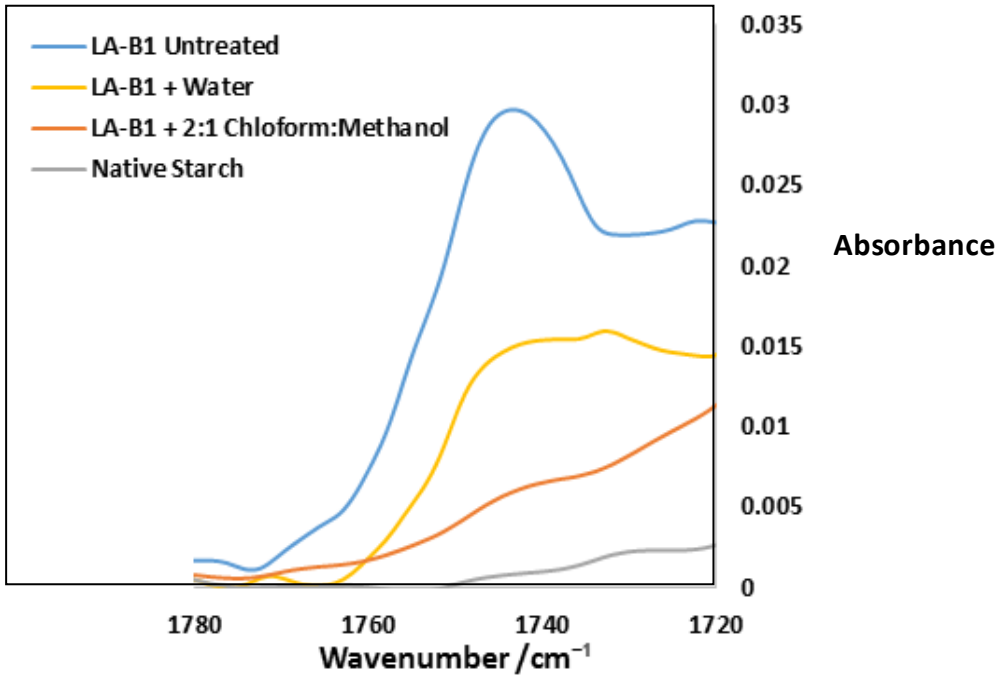
LA-B1 Untreated
LA-B1 + Water
LA-B1 + 2:1 Chloform:Methanol
Native Starch
0.035
0.03
0.025
0.02
0.015
0.01
0.005
0
Absorbance
1780
1760
1740
1720
Wavenumber /cm⁻¹

Figure 78. ATR-FTIR lipid ester peak of LA-B1 rice flour after treatment with 2:1 chloroform: methanol; (A) absorbance range 1200-3000 cm^{-1}, (B) absorbance range 2200-3000 cm^{-1}, (C) absorbance range 1720-1780 cm^{-1}.

Figure 78 shows ATR-FTIR lipid ester peak of LA-B1 before and after treatment with 2:1 chloroform:methanol. Chloroform:methanol treated LA-B1 shows decrease in lipid peaks and absence of lipid ester peak. This indicates successful extraction of lipids form surface of LA-B1 rice grains.

7.5.2. LIPID ISOLATED: ATTENUATED TOTAL REFLECTANCE-FOURIER TRANSFORM INFRARED (ATR-FTIR)

(A)

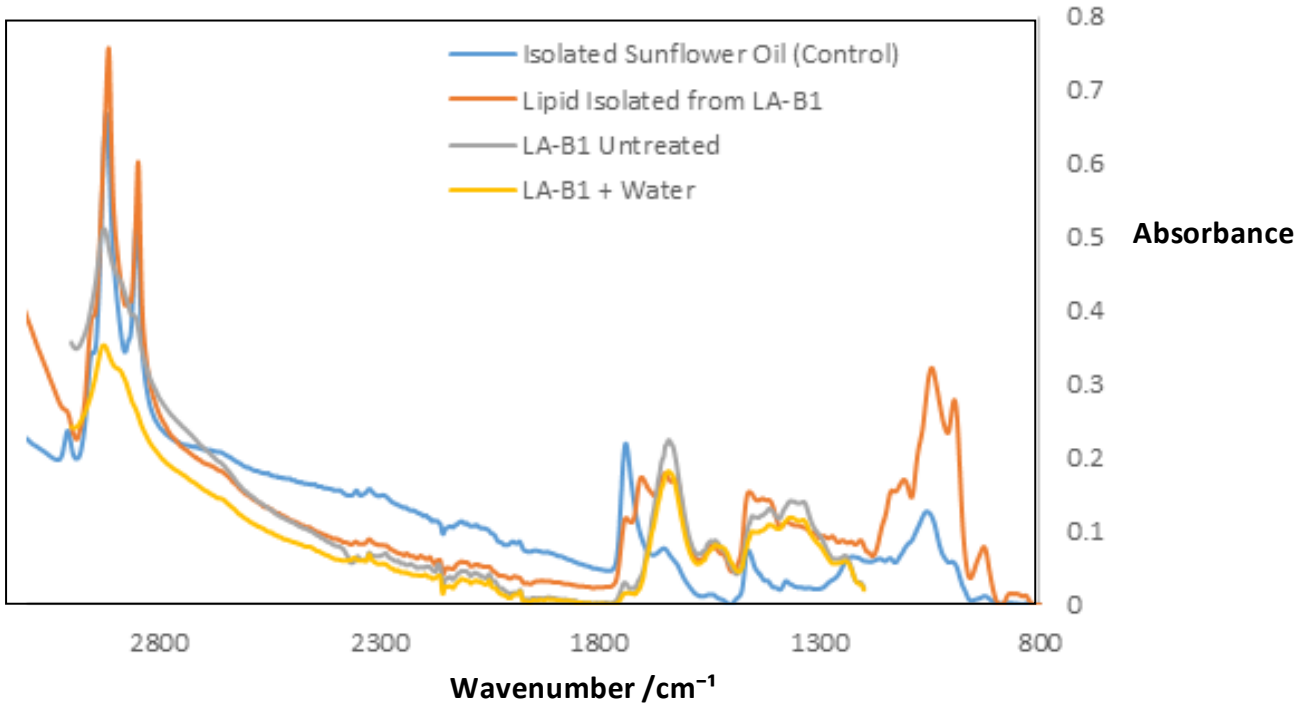

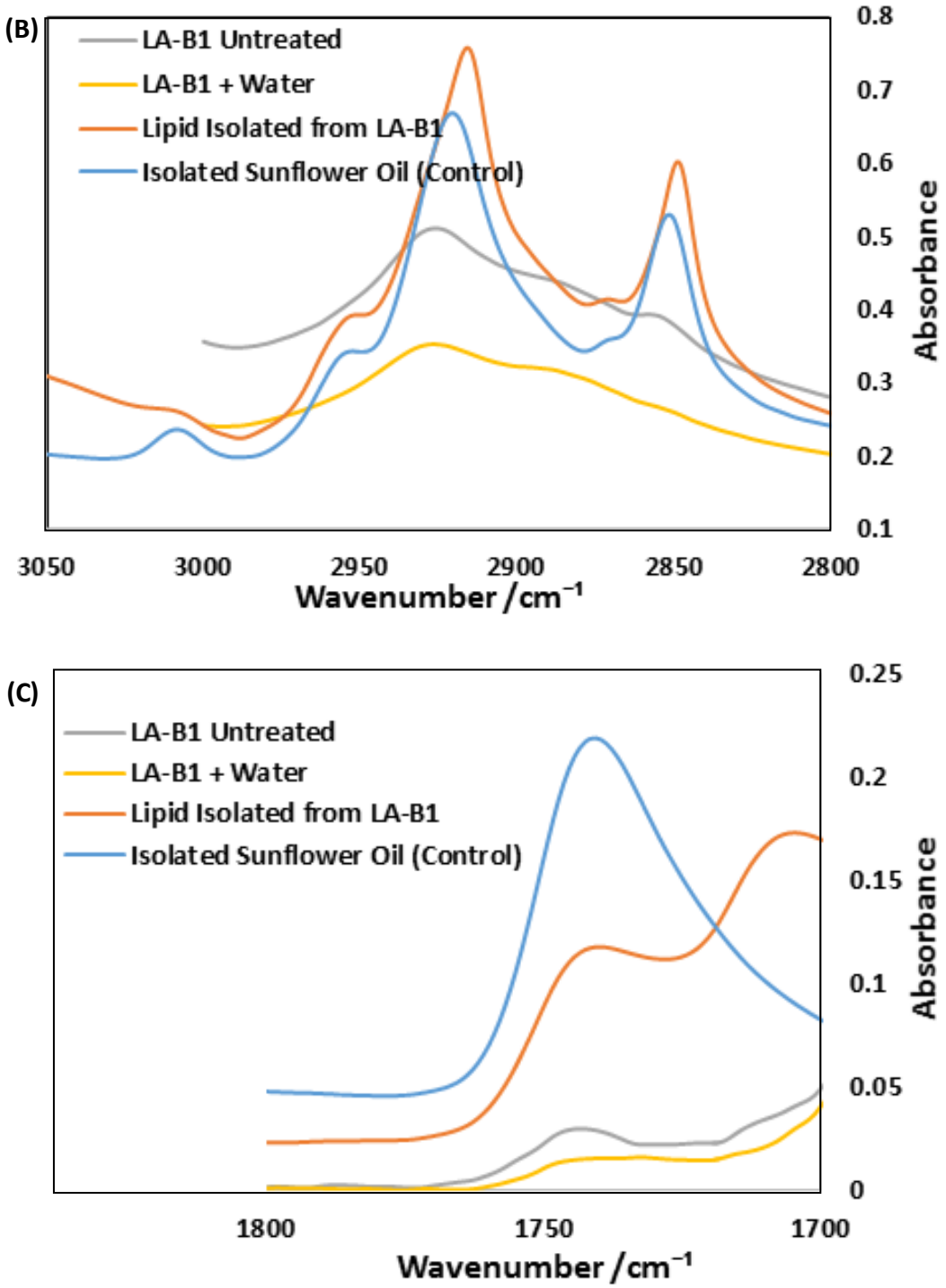

Figure 79. Ester lipid and lipid peaks of untreated LA-B1, LA-B1 with water (control), Isolated lipid from LA-B1 after extraction, isolated lipid from sunflower oil (control); (A)

absorbance range 800-3000 cm^{-1}, (B) absorbance range 1700 – 1800 cm^{-1}, (C) absorbance range 1700 – 1800 cm^{-1}

Figure 79 shows comparison between ester lipid and lipid peaks of LA-B1 before lipid extraction, and isolated lipid from LA-B1 with isolated lipid from sunflower oil as control. Lipid isolated from LA-B1 has similar sharp peaks compared to lipid isolated from sunflower oil. This indicates successful isolation of surface lipid from LA-B1 rice.

7.5.3. MONITORING LOSS OF PROTEIN

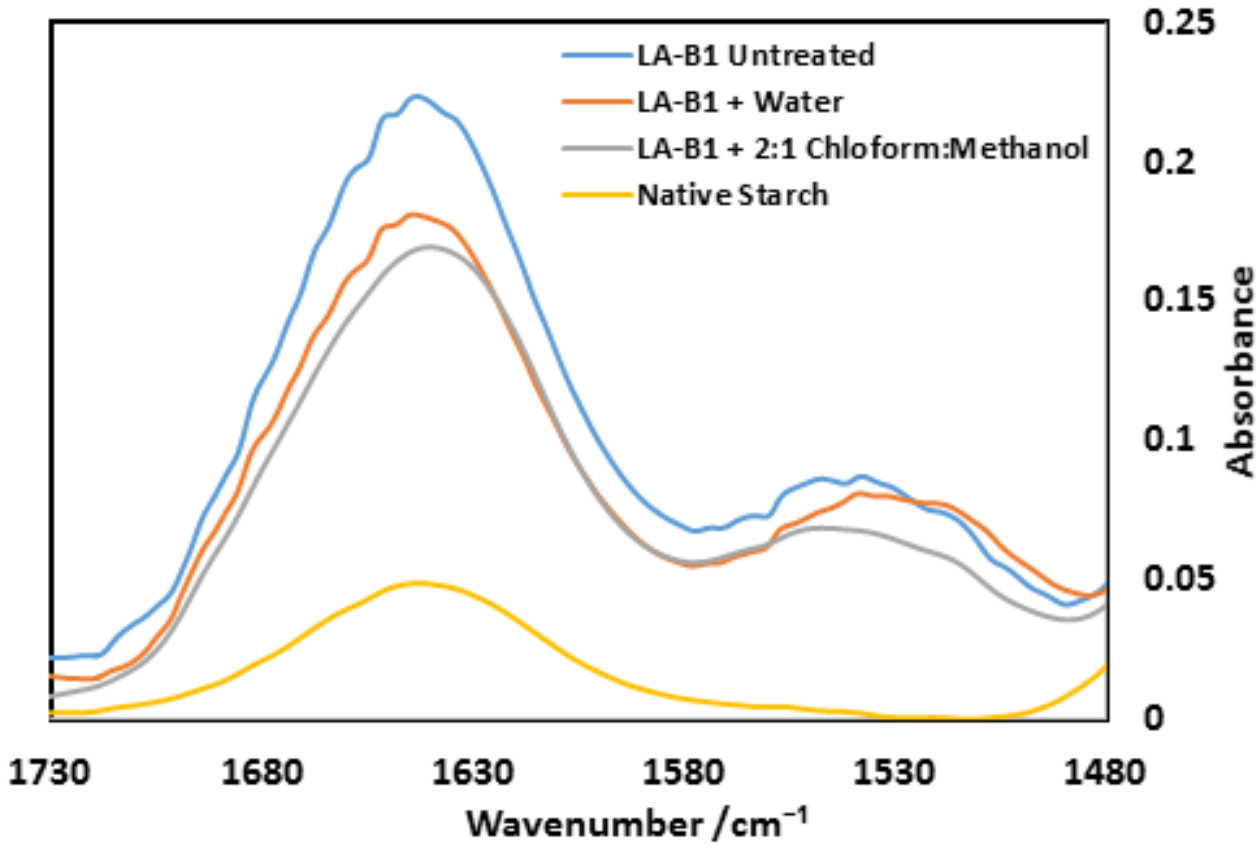

Figure 80. LA-B1 amide peaks before and after treatment with chloroform: methanol.

Figure 80 shows that no change in amide peaks after treatment with chloroform:methanol.

7.6. REMOVAL OF SURFACE ESTER LIPIDS

Although results show successful removal of lipids from rice flour, it is not possible to cook rice grains due to the low boiling point of chloroform and methanol. Boiling point of chloroform and methanol is 61.2 ^{o}C and 64.7 ^{o}C respectively and mixture of chloroform and methanol is positive azeotrope where their boiling point will be less than its constituents. Therefore, it is dangerous to attempt cooking the surface lipid removed rice grains despite using water at lowest heat as possible. It is important to note that even after several washing of rice flour to remove chloroform:methanol residue, there was strong smell of chemicals from rice flour. This also renders any successful cooking of rice to be unsuitable for human consumption.

On the other hand, Monsor and Proctor (2002) found that simple water washing significantly reduced rice surface lipid and free fatty acids (via Soxhlet extraction and subsequent acid/base titration). Saleh and Meullenet (2007) found that soaking of rice kernels significantly decreased the Surface Lipid Content (SLC) of rice kernels (via Soxtec system).

Figure 81 shows ATR-FTIR peaks of external regions of LA-B1 rice grains when LA-B1 was soaked in water for 60 minutes. Surface of LA-B1 soaked in water show similar peaks to surface of unsoaked rice grains apart from loss in lipid and lipid ester peaks. However, solids leached as a result of the soaked rice grain contains high lipid, lipid ester and amide peaks. This indicated some leaching of water soluble albumin surface protein and a substantial leaching of surface lipids. Since there was little loss of amide

peaks and substantial loss of lipid peaks from surface of LA-B1 rice grains, LA-B1 soaked in water can be used for reduced surface lipid texture studies.

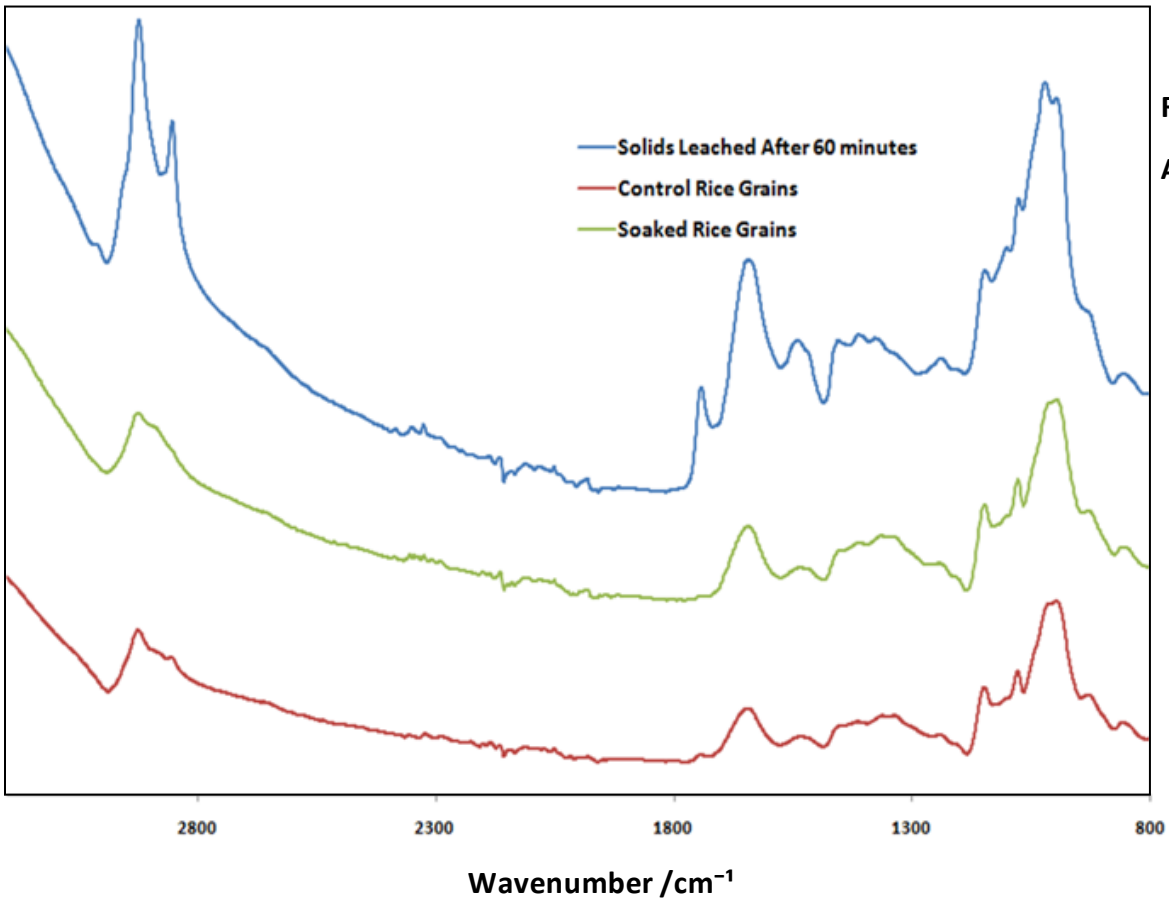

Figure 81. ATR-FTIR peaks of external regions of LA-B1 rice grains before and after being soaked in water for 60 minutes, and of solids leached from LA-B1 after 60 minutes of soaking.

7.6.1. LEACHED SOLIDS

Traditionally rice is soaked for 30 - 60 minutes before cooking. This helps the water to penetrate samples to the centre quickly and hence facilitate the cooking of rice. If rice is not soaked, the outer layer cooks faster than the centre of the rice. If rice is soaked, the centre of the rice gelatinises at a similar rate to the external layer, hence producing a more homogenous fluffly rice. Horigane, Suzuki and Yoshida, 2013 studied the moisture distribution of soaked rice grains by NMR and they showed that when polished rice kernels are soaked in water, water penetrates the grains either from the surface of rice or from the embryo and at 60 minutes, fills the rice grains completely.

From ATR-FTIR results, we know that when rice is soaked for 60 minutes, there is loss of some surface protein and substantial loss of surface lipid. Before analysis any further, it is important to understand what happens when rice is submerged in water. **Figure 82A** shows solids leached from surface of rice grains from 0 - 60 minutes while **Figure 82B** shows water absorption of rice grains when rice is soaked in water. It can be observed that the longer soaking time for rice kernel, the more solids are leached.

(A)

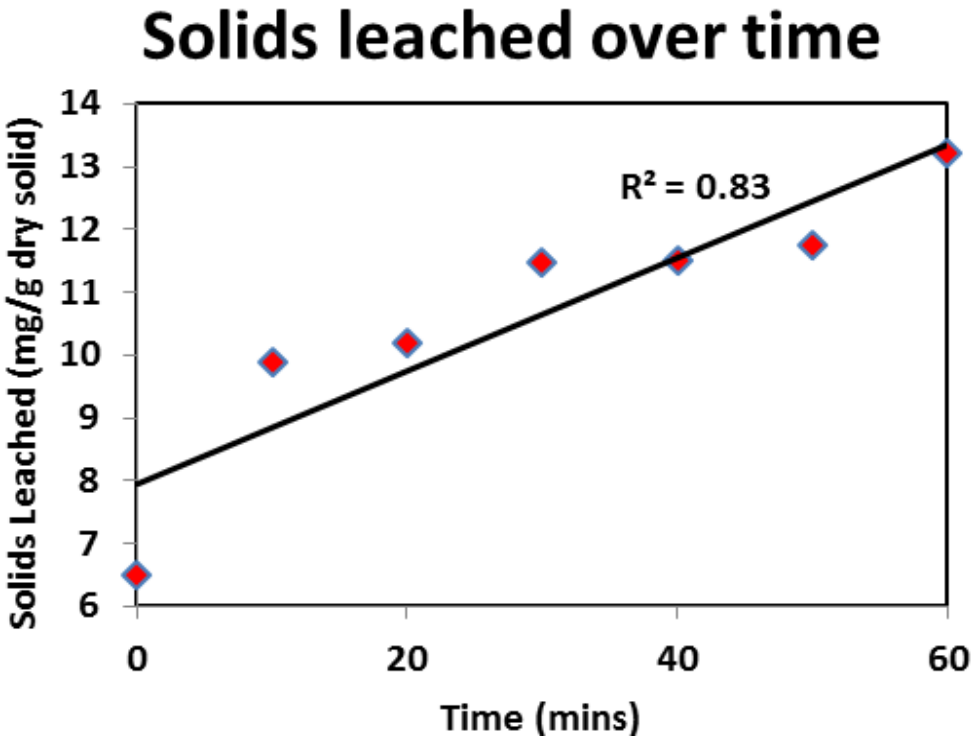

(B)

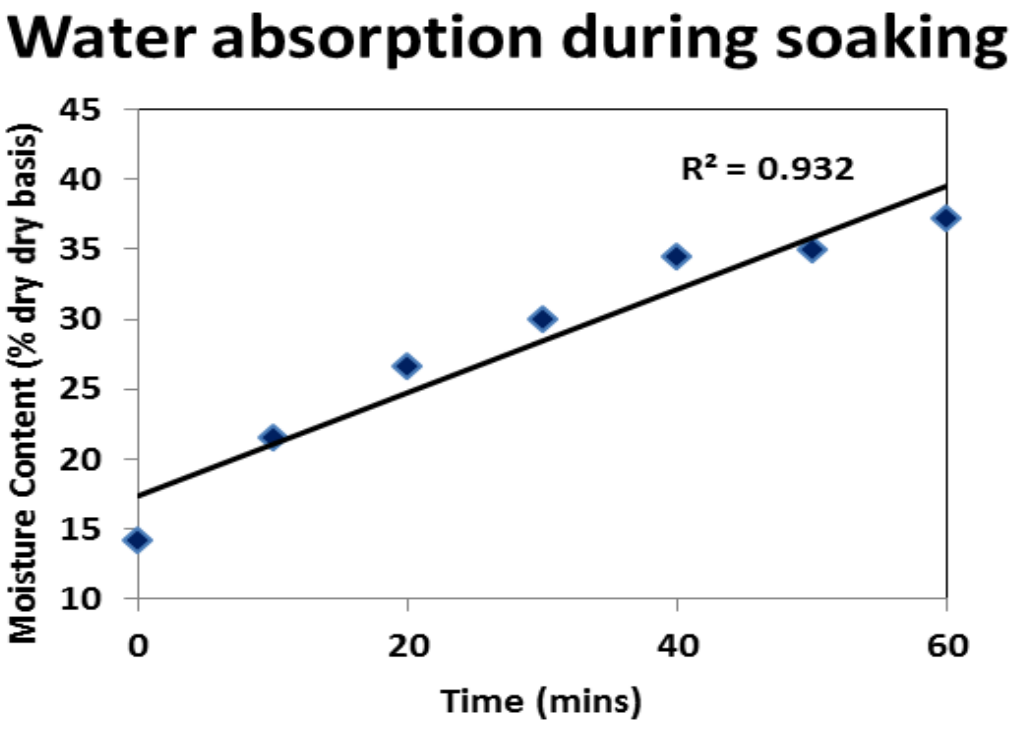

Figure 82. Solids leached over time (A), and water absorbed during soaking (B).

7.6.2. RICE FLOUR PASTING PROPERTIES

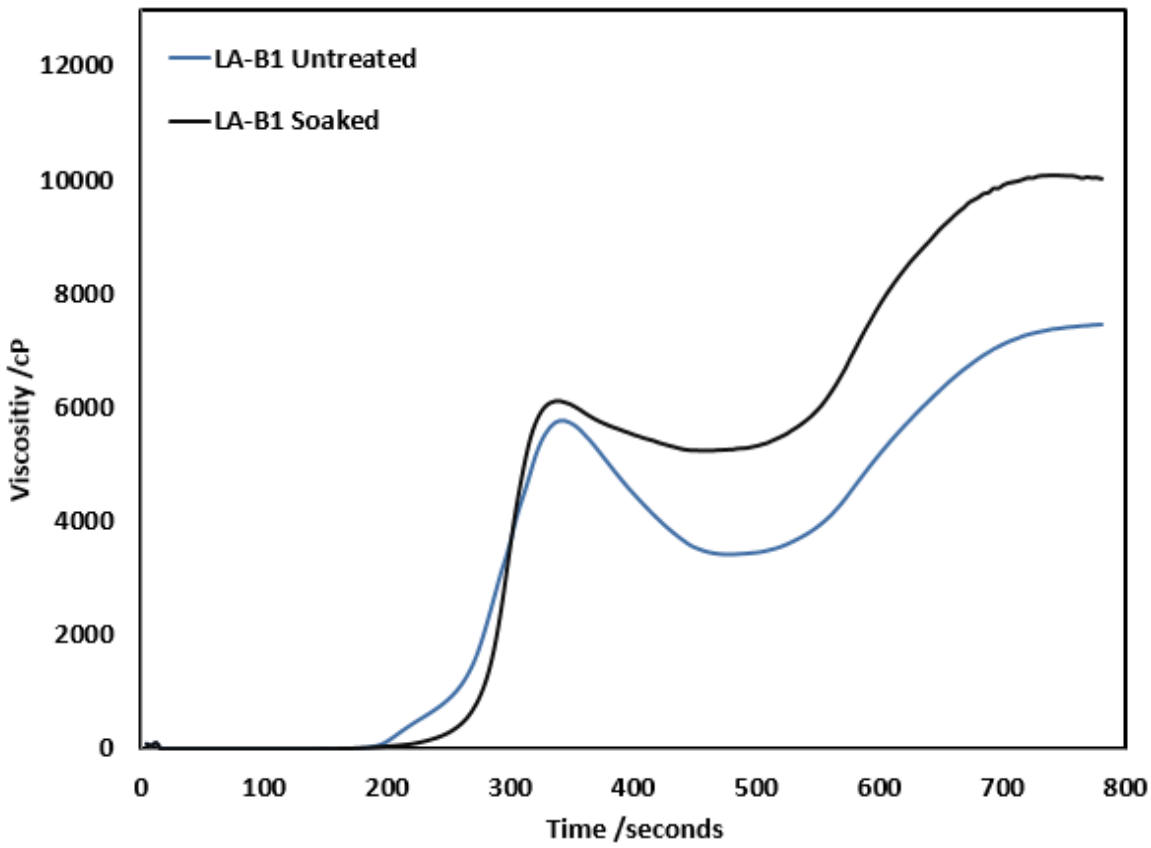

Figure 83. RVA result of LA-B1 rice flour untreated and soaked in distilled water.

Figure 83 shows rice pasting properties of LA-B1 rice flour after soaking in water for 60 minutes. Soaking LA-B1 delays onset of pasting slightly, less breakdown of starch granule and higher setback viscosity. This correponds to study by Marshall *et al*, 1990 where removal of rice lipid have a measurable effect on starch gelatinisation. It was also reported that starch gelatinisation curves measured by differential scanning calorimetry for rice soaked in water for 30 minutes resembled curves for lipid-solvent treated kernels. Therefore, it can be hypothesized that this is the same result expected if 2:1 chloroform:methanol treated rice is to be cooked in RVA.

7.7. EFFECT OF SURFACE LIPID REMOVAL ON COOKED RICE TEXTURE.

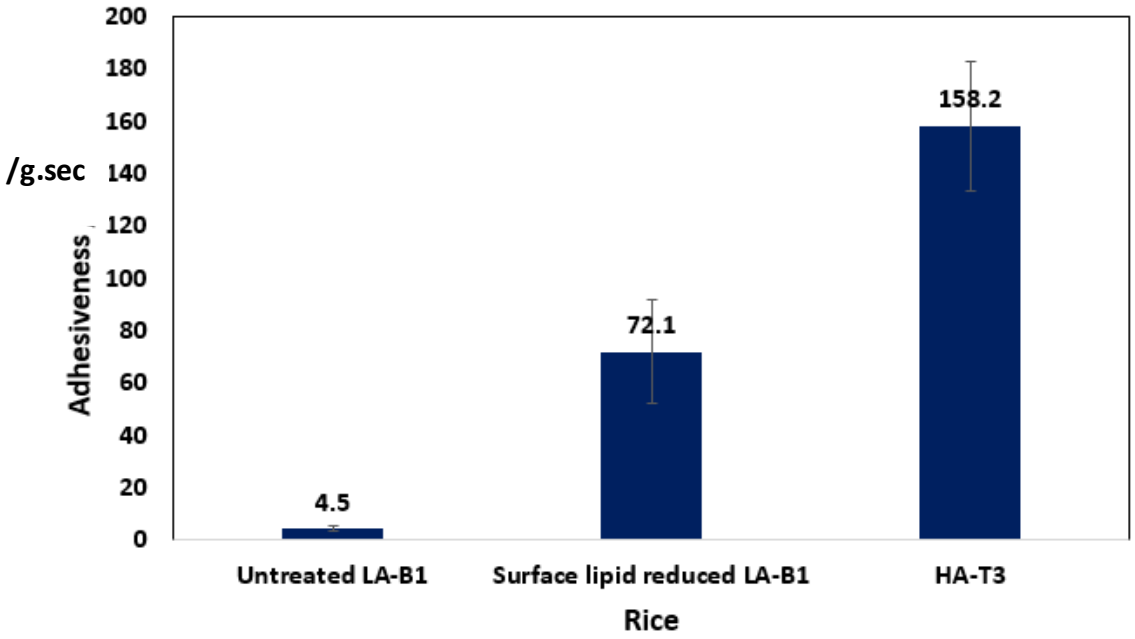

Figure 84. Texture analysis of surface lipid reduced LA-B1 rice grains.

Figure 84 shows texture analysis results of LA-B1 rice grains when their surface lipid is reduced. Compared with untreated LA-B1 (4.5 g.sec), adhesiveness of surface lipid reduced LA-B1 is significantly higher (72.1 g.sec). However, compared with untreated high adhesive rice variety HA-T3 (158.2 g.sec), the adhesiveness of surface lipid reduced LA-B1 is still significantly lower.

This further justifies that lipid content on the surface of rice grains have a contribution to the textural properties of cooked rice. Removing lipid from the surface of raw rice grains increase its adhesiveness texture when cooked. It can be suggested that adding lipid to the surface of cooked rice decreases its adhesive properties. This corresponds to studies by Juliano, 1983 where milled rice surface cooked with high lipid products such as ghee results in a reduced cooked rice stickiness. Although the adhesiveness

value is not similar to high adhesive HA-T3 which has naturally low lipid on its external regions, this indicates that surface lipid alone do not contribute to cooked rice texture.

7.8. SUMMARY AND CONCLUSION OF CHAPTER

In-order to justify that surface structure of rice grains has any effect on rice texture, it is important to test the hypothesis that the elimination of surface components can affect rice texture. This chapter has shown successful removal of native rice protein and lipid from rice flour and successful removal of native protein and lipid form the surface of rice grains. It has been shown that reducing the surface protein and lipid of raw rice grains increases the adhesiveness of rice when cooked.

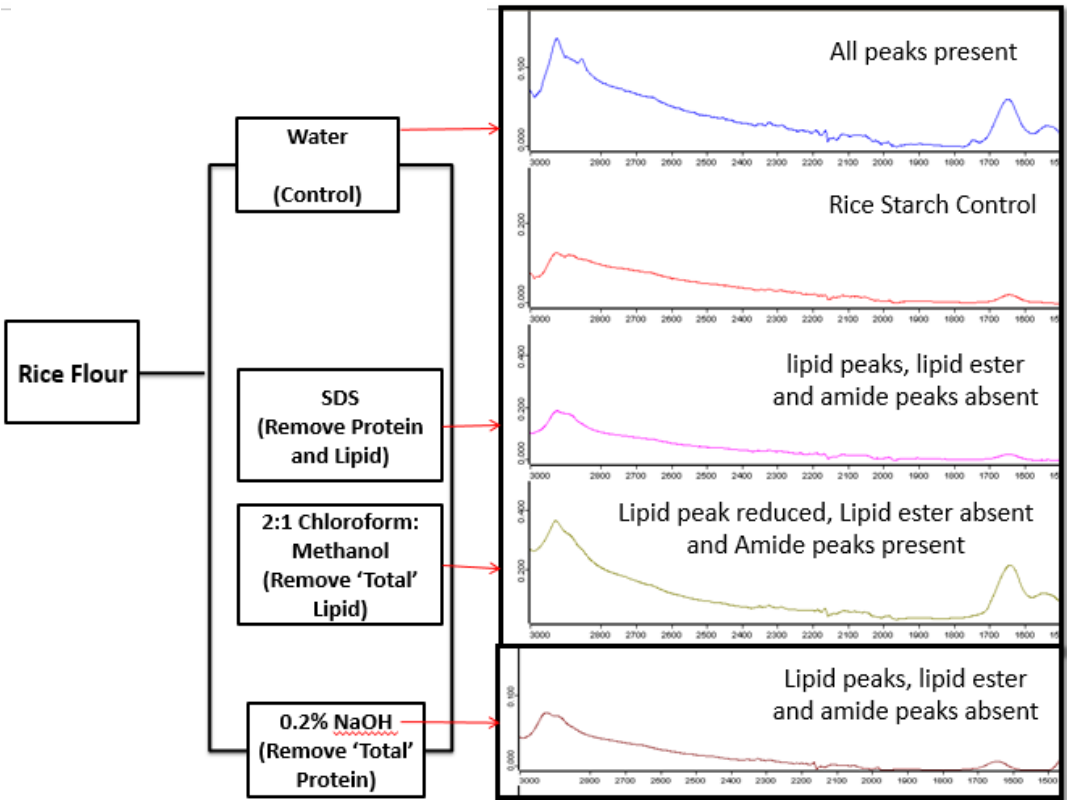

Figure 85. Summary of ATR-FTIR spectra of LA-B1 rice flour treated with different solvents; SDS, 2:1 chloroform methanol and 0.2 % NaOH.

8. GENERAL DISCUSSION AND CONCLUSION

8.1. SUMMARY AND GENERAL DISCUSSION

As a summary, **Chapter 4 – Evaluation of cooked rice texture** selected rice varieties with desired high and low adhesiveness texture behavior which is used throughout this project. **Chapter 5 – Basic rice composition** provided an analysis of the composition of whole rice grains in terms of starch, lipid and protein composition. It was concluded that high adhesive rice varieties possess (i) higher percentage of amylopectin, (ii) higher percentage of starch crystallinity and (iii) higher order of starch ratio, compared to low adhesive rice.

Chapter 6 – Gross localisation demonstrates that there is localisation of components in the internal and external structure of raw rice grains in terms of starch crystallinity, order of starch, protein and lipid composition. This is important to highlight the importance of considering the surface regions when performing cooked rice texture studies. In addition, protein and lipid composition on the surface of raw rice grains show a negative correlation with adhesive texture of cooked rice grains, while the correlation with starch crystallinity and order of starch is positive. This is justified further in **Chapter 7 – Surface alteration** where the removal of surface protein and lipid resulted in a more adhesive cooked rice texture.

8.2. DISCUSSION

Rice kernels are about 80 % starch, 15 % protein and 1 % lipid. Although the major component is starch, studies on rice texture should not heavily focus only on starch and its relative composition only, in which most studies are doing. The small amount of protein and lipid has potential impact on the final cooked rice texture.

In addition, most studies only analyse how individual components of rice kernels of rice grains contribute to its texture. This includes starch, amylose/amylopectin, protein and lipid. Majority of studies isolates individual components and correlate each of the component to the rice texture and do not relate the whole kernel as a whole. It is essential to study all the components of rice grains together and understand how each of the components play a role and work together to contribute to a certain rice texture. It is not wise to assume only one component, starch granule contribute to texture.

This project shows that non-sticky rice varieties shows lower starch crystalline, high protein and V-amylose on its external structure compared to sticky rice. It can be hypothesized that the presence of protein and V-amylose (lipid complex) restricts/restrains starch granules and acts a barrier for the swelling of starch granule on the surface of non-sticky rice.

Lower starch crystalline indicates low amylopectin content on the surface of non-sticky rice. Since amylopectin is more hot water soluble than amylose and low amylopectin

content is believed to contribute to less amylopectin leaching from the surface of non-sticky rice. In addition to this, Reddy *et al,* 1993 published that amylopectin component of high amylose rice, or low amylopectin rice has more β chains on the amylopectin surface. It was also suggested that these longer amylopectin chains can from interactions with protein or V-amylose (lipid complex) structures. Therefore, in addition to having more protein and V-amylose (lipid complex) structures, the availability of longer amylopectin β chains to interact with these components enhances the less swelling, less amylopectin leaching and thus, non-sticky behavior of rice.

In the absence (or lower proportion) of protein and lipid components in the surface of sticky rice creates space for the starch granule to swell more and therefore, burst and leach into solution. There is less amount of protein and lipid components that restrict the swelling of starch granule. Reddy *et al,* 1993 also reported that amylopectin component of low amylose rice, or high amylopectin rice has less amount of long β chains and high amount of short chains on the amylopectin surface. Therefore the lack of long chains to form interactions with less amount of protein and V-amylose lipid components results in a more brittle surface, however it is more starch crystalline.

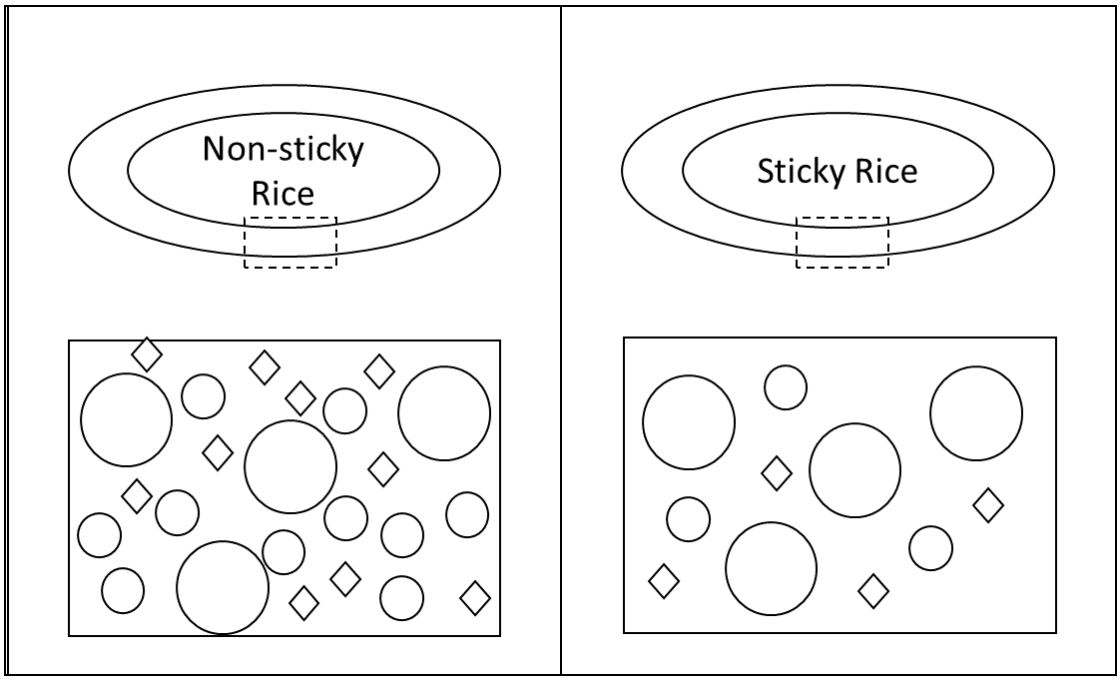

Figure 86. Schematic representation of non-sticky rice with more protein and V-amylose (lipid complex) and sticky rice with less protein and V-amylose (lipid complex).

This is clearly demonstrated in starch pasting profiles in this study whereby rice flour and rice starch has unexpected pasting profiles if results are only explained in terms of their amylose and amylopectin ratios. Rice starch has almost absence of proteins and V-amylose lipid while rice flour shows clear presence of proteins and V-amylose lipid. This is shown in ATR-FTIR pattern of the native rice starch and rice flour used in this project, in **figure 43 (page 89).**

The results of pasting profiles of rice flour can be explained better when the presence of proteins and V-amylose in rice flour is taken into account. In **figure 51 (page 101)**, the presence of proteins and V-amylose in rice flour delays the onset of pasting and decreases peak viscosity. This supports the theory whereby the presence of more

protein and V-amylose restricts the swelling of the starch granules, which result in slower pasting and less swelling of starch granules.

The removal of protein from rice flour in **chapter 7: Surface alteration** shows a faster onset of pasting and increase in peak viscosity. This further justifies whereby the absence of protein provokes faster and more swelling of starch granules, in which the hypothesis is that there is less barrier/restrains for the starch granules to swell when there is less protein components available.

Ayabe *et al*, 2009 reported that sticky rice varieties contains more amylopectin on its cooked rice surface, compared to non-sticky rice varieties. The raw surface/internal components of rice grains were not studied and only the whole rice grain amylose and amylopectin content was analysed. It was not known whether the sticky rice grains already has more amylopectin on the surface prior to cooking, or there is a migration of amylopectin from the internal structures to the external structures during cooking.

Based on the rice varieties chosen in this project, raw sticky rice varieties already has more amylopectin (based on crystallinity results) on its surface. It can be hypothesized that there was no migration of amylopectin components from the central regions to the surface regions during cooking of rice, but simply the amylopectin components is already present prior to cooking. This also can be hypothesized to apply to non-sticky rice whereby the surface of non-sticky already has less amylopectin on its surface prior to cooking which explains the low amylopectin content in the surface of cooked non-sticky rice observed by Ayabe *et al*, 2009.

This project shows that more V-amylose lipid on the surface of non-sticky rice contribute to the less sticky texture. This is also reflected on the study of parboiled rice. In western part of the world, most rice varieties are parboiled and these rice are called easy-cook rice. Most studies on parboiled rice shows that there is more V-amylose present, and some suggests that V-amylose is produced as a result of parboiling. Parboiling of rice results in a less sticky and more separated rice texture which is desired by westerners. Therefore, it can suggested that the presence of V-amylose contributes to a less sticky rice texture and the absence, or reduction of V-amylose component will result in a more sticky rice texture.

This project shows that the presence of V-amylose on the external structure results in a less sticky rice texture while the absence of V-amylose on the external structure results in a more sticky rice texture. This result correlates with parboiling studies that the presence of V-amylose contributes to a less sticky rice texture and the absence, or reduction of V-amylose component will result in a more sticky rice texture. In addition to this, easy-cook versions of the rice samples used in this study has a less sticky texture and a higher V-amylose crystallinity peaks compared to normal varieties (preliminary results not shown).

In my opinion, it is not only the starch, protein or lipid components that contribute to the final cooked rice texture, but each of the component play a role with each other. It can be suggested that the texture is largely most contributed by starch and its swelling

and the swelling is partially controlled by the other available components, protein and lipid.

Based on these studies, it can suggested that the removal of protein and lipid components results in a more sticky rice texture, which is the desired texture of Bruneians and several Asian countries, including Japan and Thailand. Therefore, it can be suggested that post-harvest modification of rice kernels, which is treatment with sodium hydroxide and sodium chloride can yield rice of stickier texture.

Other studies published that brown rice (before milling) contains more surface lipid and similar protein contents compared to milled white rice (post-milling). This suggests that more milling is enough to remove a substantial amount of surface lipid. Salleh and Meullenet (2007) also reported that increased milling of rice grains results in a decrease in surface lipids and also a sticky rice texture. Therefore, it can be concluded that a non-sticky rice rough rice exposed to more degree of milling to remove more surface lipid plus sodium hydroxide, sodium chloride and water to remove more surface protein will produce a more sticky milled rice.

8.3. LIMITATIONS OF STUDY

The following were not performed:

Building on this study I would:

- Justification of instrumental texture analysis with sensory texture analysis
- Study on localization of rice components during and after cooking

- Study on addition of protein and lipid components onto rice surface
- Using more rice varieties to further justify conclusions
- Understand how storage, parboiling and milling degree play a role in rice grain external/internal structure whereby storage and parboiling decreases stickiness of rice and increased milling degree increases stickiness of rice.

8.4. FUTURE WORK

It is proposed that if this project were to be followed-up, the following will be recommended, for purposes of further justification of this study further and to uncover new grounds:

8.3.1. SENSORY STUDY

The method used to analyse texture in this study is based simply on instrumental methods. It would be useful to continue the study with sensory analysis as this will strengthen it further, as it will involve real human perception of the rice texture, which involves in-mouth sensation, which includes biting, chewing and sticking to palate and aroma.

8.3.2. LOCALISATION OF COMPONENTS DURING AND AFTER COOKING OF RICE

This study revolves around uncooked rice grains and the results are promising. It would be interesting to investigate how the original localization of components in the raw rice grains plays a role in the cooking process. Is there any possible migration of components? Are there any components which do not play a role directly in the

cooking process, but instead aid the other components? How do they all interact with each other? How do the structures of each component, the amylose, amylopectin, protein, protein complexes, lipid, lipid-complexes play a role behave when they are all heated together and allowed to cool?

8.3.4. UNDERSTANDING PROTEIN COMPOSITION

Since the presence or absence of protein on the surface of rice kernels has an impact on the texture of cooked rice, it is recommended that the composition of the external protein on the external structures of non-sticky rice and sticky rice is studied. It is crucial to investigate and understand further if total protein, a protein components or even merely a bond within a protein complex contributes the texture of cooked rice.

8.4. OVERALL CONCLUSION

In conclusion, this project highlights the importance of studying the surface properties of raw rice grains, which can change during cooking. However, this project invested countless hours on separating the surface of rice grains from the central portion. It is advised to follow-up this project, there needs to be use of better equipment and techniques, such as a rice grain cutter or more successful imager equipment, which were unsuccessful in this project. I believe that there is great potential in analyzing more on the surface properties of rice grains.

REFERENCES

Ascheri, D.P.R., Boeno, J.A., Bassinello, P.Z., Ascheri, J.L.R., 2012. Correlation between grain nutritional content and pasting properties of pre-gelatinised red rice flour. *Food Science and Technology*. 59(1): 16-24.

Ayabe, S., Kasai, M., Ohishi, K., Hatae, K, 2009. Textural properties and structures of starches from Indica and Japonica rice with similar amylose content. *Food. Sci. Technol. Res*. 15(3): 299-306.

Bao., J., Bergman, C.J., 2004. The functionality of rice starch, in: starch in food: structure, function and applications, edited by Eliasson A.C. Cambridge, United Kingdom: Woodhead Publishing limited. CRC Press LLC. Pp 258-294.

Barsby, T.L., Donald, A.M., Frazier, P.J., 2001. Starch: advance in structure and function. Cambridge, United Kingdom: Royal Society of Chemistry. Pp 224.

Bello, M., Tolaba, M.P., Suarez, C., 2004. Factors affecting water uptake of rice grain during soaking. *Lebensmittel-Wissenschaft und-Technologie*. 37(8): 811-816.

BeMiller, J.N., Whistler, R.L., 2009. Starch: chemistry and technology. Third Edition. New York, United States of America: Academic Press. Elsevier. Pp 904.

Bergman, C., Chen, M.H., Delgado, J., Gipson, N., 2009. Rice grain quality. USDA-ARS-Rice research unit rice quality program, accessed 1st May 2016. <https://beaumont.tamu.edu/elibrary/studyricecontest/2006/rice%20grain%20quality.pdf>

Bhattacharya, K.R., Sowbhagya, C.M., Indudhara Swamy, Y.M., 1982. Quality profiles of rice: A tentative scheme for classification. *Food Science*. 47(2): 564-569.

Bhattacharya, K.R., 2001. Rice quality: A guide to rice properties and analysis. Cambridge, United Kingdom: Woodhead Publishing Limited. Pp 608.

Bielinski, D., Pysklo, L., Dul, J., Slusarski, L., Janowska, G., Lewandowicz., 2003. Preliminary studies on the surface layer of starch. *Macromol. Symp*. 194: 233-239.

Biliaderis, G.C., Tonogai, J.R., 1991. Influence of lipids on the thermal and mechanical properties of concentrated starch gels. *J. Agric. Food. Chem*. 39: 833-840.

Biliaderis, C.G., Tonogai, J.R., Perez, C.M., Juliano, B.O., 1993. Thermophysical properties of milled rice starch as influenced by variety and parboiling. *Cereal Chemistry*. 70(5): 512-516.

Brunei Agrifood, 2010. Department of Agriculture and Agrifood. Ministry of Industry and Primary Resources, accessed 1st October 2015. <http://www.agriculture.gov.bn/>

Buleon, A., Gallant, D.J., Bouchet, B., Mouille, G., D'Hulst, C., Kossman, J., Ball, S., 1997. Starches from A to C1. *Chlamydomonas reinhardtii* as a model microbial system to investigate the biosynthesis of the plant amylopectin crystal. *Plant Physiol*. 115: 949-957.

Buleon, A., Colonna, P., Planchot, V., Ball S, 1998. Starch granules: structure and biosynthesis. *Int J Biol Macromol*. 23(2): 85 -112.

Cai, J., Yang, Y., Man, J., Huang, J., Zhang, C., Gu, M., Liu, Q., Wei, C., 2013. Structural and functional properties of alkali treated high amylose rice starch. *Food Chemistry.* 142:245-53.

Cai, J., Man, J., Huang, J, Liu, Q., Wei, W., Wei, C., 2015. Relationship between structure and functional properties of normal rice starches with different amylose contents. *Carbohydrate Polymers*. 125: 35-44.

Callaghan, P.T., 1993. Principles of nuclear magnetic resonance microscopy. New York, United States of America: Oxford University Press Inc. Pp 492.

Cameron, D.K., Wang, Y.J., 2005. A better understanding of factors that affect the hardness and stickiness of long grain rice. *Cereal Chemistry*. 82(2): 113-119.

Champagne, E.T., 1996. Rice starch composition and characteristics. *Cereal Foods World*. 41(11): 833-838.

Champagne, E.T., Bett, K.L., Vinyard, B.T., McClung, A.M., Barton II, F.E., Moldenhauer, K., Linscome, S., McKenzie, K., 1999. Correlation between cooked rice texture and rapid visco analyser. *Cereal Chemistry*. 75(5): 764-771.

Charu, L.M., Ali, S.Z., Bhattacharya, K.R., Mukherjee, P.S., 1989. Nature of starch crystallinity in parboiled rice. *Starch*. 41(5): 171-176.

Chen, N., Xie, L.H, Duan, B.W, 2007. Effect of disulphide bond-containing protein on texture of cooked rice. *Acta Agronomica Sinica*. 2007-01.

Chrastil, J., 1990. Protein-starch interactions in rice grains. Influence of storage on oryzenin and starch. *J. Agric. Food Chem*. 38: 1804-1809.

Chung H.J., Liu, Q., Lee, L., Wei, D., 2011. Relationship between the structure, physicochemical properties and in vitro digestibility of rice starches with different amylose contents. *Food Hydrocolloid*. 25: 968-975.

CIA World Factbook, 2014. Central Intelligence Agency, accessed 1st October 2015. <https://www.cia.gov/library/publications/the-world-factbook/>

Cullity, B.D., 1956. Elements of x-ray diffraction. Second Edition. Minnesota, United States of America: Addison-Wesley Publishing Company Inc. Pp 514.

Donald, A.M., Waigh, T.A., Jenkins, P.J., Debet, M., Smith, A.C., 1997. Internal structure of starch granules revealed by scattering, in: starch: structure and functionality by Frazier, P.J., Donald, A.M., and Richmond, P. London, United Kingdom: The Royal Society of Chemistry. 172-179.

Eliasson, A.C., Krog, N., 1986. Physical properties of amylose monoglyceride complexes. *Cereal Science.* 3(3): 239 – 248.

Eliasson A.C., 2004. Starch in food: structure, function and applications. Cambridge, United Kingdom: Woodhead Publishing limited. CRC Press LLC. Pp 605.

Fitzgerald, M.A., Bergman, C.J., Resurreccion, A.P., Moller, J., Jimenez, R., Reinke, R.F., Martin, M., Blanco, P., Molina, F., Chen, M.H., Kuri, V., Romero, M.V., Habibi, F., Umemoto, T., Jongdee, 2009. Addressing the dilemmas of measuring amylose in rice. *Cereal Chemistry*. 86(5): 492-498.

French, D., 1984. Organisation of starch granules, in: Starch: chemistry and Technology, edited by Whistler, R.L, BeMiller, J.N., and Paschall, E.F. Second edition, New York, United States of America: Academic Press. Elsevier. 183-247.

Frost, K., Kaminski, D., Kirwan, G., Lascaris, E., Shanks, R., 2009. Crystallinity and structure of starch using wide angle X-ray scattering. *Carbohydrate Polymers*. 78: 543-548.

Griffiths, P.R., de Haseth, J.A., 2007. Fourier transform infrared spectrometry. Second Edition. New Jersey, United States of America: John Wiley and Sons. Pp 560.

Hamaker, B.R., Griffin, V.K., 1990. Changing the viscoelastic properties of cooked rice through protein disruption. *Cereal Chemistry*. 67:261.

Hamaker, B.R., Griffin, V.K., 1993. Effect of disulfide bond-containing protein on rice starch gelatinization and pasting. *Cereal Chemistry.* 70(4): 377-381.

Harrick, N.J., 1967. Internal reflection spectroscopy. New York, United States of America: John Wiley and Sons. Pp 327.

Hizukuri, S., 1986. Polymodal distribution of the chain lengths of amylopectins and its significance. *Carbohydrate Polymers*. 147: 342-347.

Horigane, A.K., Suzuki, K., Yoshida, M., 2013. Moisture distribution of soaked rice grains observed by magnetic resonance imaging and physicochemical properties of cooked rice grains. *Cereal Science*. 57(1): 47-55.

International Starch Institute, 2016. Rice, accessed 5th May 2016. <http://www.starch.dk/isi/starch/rice.asp>

Juliano, B.O., Boulter, D., 1976. Extraction and composition of rice endosperm glutelin. *Phytochemistry.* 15: 1601-1606.

Juliano, B.O., Pascual, C.G., 1980. Quality characteristics of milled rice grown in different countries. *IRRI Research Paper Series*. 48: 1-25.

Juliano, B.O., 1983. Lipids in rice and rice processing, in: Lipids in cereal technology. London, United Kingdom: Academic Press. 305-330.

Juliano, B. O., 1985. Rice: Chemistry and Technology. 2nd Edition. St. Paul, United States of America: American Association of Cereal Chemists. Pp 774.

Juliano, B.O., 1993. Rice in human nutrition, in: Food and Nutrition Series (FAO), no 26. Rome, Italy: Food and Agriculture Organisation of the United Nations. Pp 168.

Juliano, B.O., 2005. Overview of rice and rice-based products, in: Rice is life: scientific perspectives for the 21st century. Edited by Toriyama K., Heong, K.L., Hardy, B. Manila, Philippines: International Rice Research Institute.

Kim, S.K., Rhee, C.O., 2004. Analysing and improving the texture of cooked rice, in: Texture in Food. Volume 2: Solid foods. Edited by Kilcast, D. Cambrige, United Kingdom: Woodhead Publishing Limited. CRC Press. Pp 560.

Kong, J., Yu, S., 2007. Fourier transform infrared spectroscopic analysis of protein secondary structures. *Acta Biochimica et Biophysica Sinica*. 39(8): 549-559.

Kulp, L, Ponte, J. G., 2000. Handbook of cereal science and technology. Second Edition. New York, United States of America: Marcel Dekker Inc.

Lam, H.S., Proctor, A., Meullenet, J.F., 2001. Free fatty acid formation and lipid oxidation on milled rice. *JAOCS*. 78(12): 1271 – 1275.

Landers, P.S., Hamaker, B.R., 1994. Antogenic properties of albumin, globulin and protein concentrate fractions from rice bran. *Cereal Chemistry*. 71: 409-411.

Lim, S.T., Lee, J.H., Shin, D.H., Lim, H.S., 1999. Comparison of protein extraction solutions for rice starch isolation and effects of residual protein content on starch pasting properties. *Starch*. 51 (4): 120 – 125.

Lumdubwong, N., Seib, P.A., 2000. Rice isolation by alkaline protease digestion of wet-milled rice flour. *Journal of Cereal Science*. 31(1): 63-74.

Lim, S.T., Lee, J.H., Shin, D.H., Lim, H.S., 1999. Comparison of protein extraction solutions for rice starch isolation and effects of residual protein content on starch pasting properties. *Starch*. 51(4): 120-125.

Lopez-Rubio, A., Flanagan, B.M., Gilbert, E.P., Gidley, M.J., 2008. A novel approach for calculating starch crystallinity and its correlation with double helix content: A combined XRD and NMR study. *Biopolymers*. 89(9): 761-768.

Lyon, B.G., Champagne, E.T., Vinyard, B.T., Windham, W.R., 2000. Sensory and instrumental relationships of texture of cooked rice from selected cultivars and postharvest handling practices. *Cereal Chemistry.* 77(1): 64 -69.

Marshall, W.E., Normand, F.L., Goynes, W.R., 1990. Effects of lipid and protein removal on starch gelatinization in whole grain milled rice. *Cereal Chemistry*. 67(5): 458-463.

Marshall, W.E., Wadsworth, J.I., 1994. Rice science and technology. New York, United States of America: Marcel Dekker Inc.

Megazyme, 2016. Megazyme amylose/amylopectin assay. Megazyme International, Ireland, accessed 1st October 2010. <https://secure.megazyme.com/Amylose-Amylopectin-Assay-Kit>

Megazyme, 2016. Megazyme total starch assay. Megazyme International, Ireland, accessed 1st October 2010. <https://secure.megazyme.com/Total-Starch-Assay-Kit>

Metres, C., Ribeyre, F., Pons, B., Fallet, V., Matencio, F., 2011. Sensory texture of cooked rice is rather linked to chemical than to physical characteristics of raw grain. *Journal of Cereal Science*. 53: 81-89.

Mitchell, C.R., 2009. Rice Starch: production and properties, in: starch: chemistry and technology, edited by BeMiller, J.N., Whistler, R.L. Third Edition. New York, United States of America: Academic Press. Elsevier. 569-578.

Monsor, M.A., Proctor, A., 2002. Effect of water washing on the reduction of surface total lipids and FFA on milled rice. *JAOCS*. 79(9): 867-870.

Morrison, W.R., Milligan, T.P., Azudin, M.N., 1984. A relationship between the amylose and lipid contents of starches from diploid cereals. *Cereal Science.* 2(4): 257 - 271.

Mousia, Z, Farhat, I.A., Pearson, M., Chesters, M.A., Mitchell, J.R., 2001. FTIR microspectroscopy study of composition fluctuations in extruded amylopectin-gelatin blends. *Biopolymers (Biospectroscopy)*. 62: 208-218.

Mutters, R.G., Thompson, J.F., 2009. Rice quality handbook. California, United States of America: University of California Agriculture and Natural Resources. Pp 141.

Obiro, W.C., Ray, S.S., Emmambux, M.N., 2012. V-amylose structural characteristics, methods of preparation, significance and potential applications. *Food Reviews International*. 28(4): 412-438.

Okabe, M., 1979. Texture measurement of cooked rice and its relationship to the eating quality. *Journal of Texture studies.* 10(2): 131-152.

Ong, M.H., Blanshard, J.M., 2006. The significance of starch polymorphism in commercially produced parboiled rice. *Starch*. 47(1): 7-13.

Ottenhof, M.A., Hill, S.E, Farhat, I.A., 2005. Comparative study of the retrogradation of intermediate water content waxy maize, wheat and potato starches. *J. Agric. Food. Chem.* 53(3): 631-638.

Patindol, J., Gu, X., Wang, Y.J., 2010. Chemometric analysis of cooked rice texture in relation to starch fine structure and leaching characteristics. *Starch.* 62(3-4): 188-197.

Qin, F.L., Man, J.M., Cai, C.H., Xu, B., Gu, M.H., Zhu, L.J, Shi, Y.C, Liu, Q.Q., Wei, C.X., 2012. Physicochemical properties of high-amylose rice starches during kernel Development. *Carbohydrate Polymers*. 88: 690– 698.

Ramesh, M., Zakiuddin Ali, S., Bhattacharya, 1999. Structure of rice starch and its relation to cooked-rice texture. *Carbohydrate Polymers*. 38 (4): 337 – 347.

Ramesh, M., Bhattacharya, K.R., Mitchell, J.R., 2000. Developments in understanding the basis of cooked-rice texture. *Critical reviews in Food Science and Nutrition*. 40(6): 449-460.

Reddy, K.R., Ali, S.Z., Bhattacharya, K.R., 1993. The fine structure of rice-starch amylopectin and its relation to the texture of cooked rice. *Carbohydrate Polymers*. 22: 267-275.

Robin, J.P., Mercier, F., Duprat, R., Charbonniere, R., and Guilbot, A., 1975. Amidons lintnearises. *Starch.* 2: 36-45.

Saleh, M., I., Meullenet, J.F., 2007. Effect of protein disruption using proteolytic treatment on cooked rice texture properties. *Journal of texture studies*. 38(4): 423-437.

Saleh, M., I., Meullenet, J.F., 2007. Effect of moisture content at harvest and degree of milling (based on surface lipid content) on the texture properties of cooked long-grain rice. *Cereal Chemistry*. 84(2): 119-124.

Saleh, M., Meullenet, J.F., 2013. Contour presentation of long grain rice degree of milling and instrumental texture during cooking. *International Food Research Journal.* 20(3): 1337-1344.

Sevenou, O., Hill, S.E., Farhat, I.A., Mitchell, J.R., 2002. Organisation of the external region of the starch granule as determined by infrared spectroscopy. *International Journal of Biological Macromolecules.* 31: 79-85.

Shelton, D.R., Lee, W.J., 2000. Cereal Carbohydrates, in: Kulp, L., Ponte, J.G. Handbook of cereal science and technology. Second Edition. New York, United States of America: Marcel Dekker Inc.

Shibuya, N., Iwasaki, T., 1982. Effect of the enzymatic removal of endosperm cell wall on the gelatinisation properties of aged and un-aged rice flours. *Starch*. 34: 300-303.

Smith, B. C., 1996. Fundamentals of fourier transform infrared. Florida, United States of America: CRC Press.

Smith, C.W., Dilday, R.H., 2003. Rice: origin, history, technology and production. New Jersey, United States of America: John Wiley & Sons. Pp. 626.

Stuart, B., 2004. Infrared spectroscopy: fundamentals and applications. West Sussex, United Kingdom: John Wiley and Sons Ltd. Pp 242.

Suryanarayana, C., Grant Norton, M., 1998. X-ray diffraction: A practical approach. New York, United States of America: Springer sciences and business media. Pp 273.

Szczesniak, A.S., 2015. Stable micro systems Ltd, accessed 1st October 2015. <http://www.stablemicrosystems.com>

Stable micro system, 2015. Stable micro systems Ltd, accessed 1st October 2015. <http://www.stablemicrosystems.com>

Tanaka, Y., Resurreccion, A.P., Juliano, B.O., Bechtel, D.B., 1978. Properties of whole and undigested fraction of protein bodies of milled rice. *Agric. Bol. Chem*. 42: 2015 - 2033.

Tanaka, K., Sugimoto, T., Ogawa, M., Kasai, Z., 1980. Isolation and characterization of two types of protein bodies the rice endosperm. *Agric. Biol. Chem*. 44: 1633 – 1639.

The report: Brunei Darussalam 2009. Prime Minister's Office, Brunei Darussalam. Brunei: Oxford Business Group. Pp 220.

Thermofisher, 2016. Pierce BCA protein assay kit, accessed 1st May 2016. https://tools.thermofisher.com/content/sfs/manuals/MAN0011430_Pierce_BCA_Protein_Asy_UG.pdf

Tomasik, P., 2003. Chemical and functional properties of food saccharides. Florida, United States of America: CRC Press. Pp 440.

USDA, 2015. Oryza. Brunei targets 60% self-sufficiency in rice production by 2015, accessed 1st October, 2015. <http://www.oryza.com/>

Van Soest, J.J.G., Dewit, D., Tournois, H., Vliegenthart, J.F.G., 1994. The influence of glycerol on structural-changes in waxy maize starch as studied by fourier transform infrared spectroscopy. *Polymer*. 35(22): 4722-4727.

Van Soest, J.J.G., Tournois, H., Wit, D., Vliegenthart, J.F.G., 1995. Short-range structure in (partially) crystalline potato starch determined with attenuated total reflectance fourier-transform IR spectroscopy. *Carbohydrate Research*. 279: 201-214.

Van Soest, J.J.G., Dewit, D., Tournois, H., Vliegenthart, J.F.G., 1999. Retrogradation of potato starch as studied by fourier transform infrared spectroscopy. *Starch*. 46(12): 453-457.

Vidal, A. J., Juliano, B.O., 1967. Comparative composition of waxy and non-waxy rice. *Cereal Chemistry*. 44: 86-91.

Wang, L, Wang, Y., 2001. Structures and physicochemical properties of acid-thinned corn, potato and rice starches. *Starch*. 53(11): 570-576.

Wawasan Brunei 2035, 2008. Brunei Darussalam long-term development plan. Brunei: Wawasan Brunei 2035. Pp 263.

Whistler, R.L, BeMiller, J.N., Paschall, E.F., 2012. Starch: chemistry and technology. Second Edition. London, United Kingdom: Academic Press. Pp 589.

Yu, S, Ma, Y., Sun, D., 2009. Impact of amylose content on starch retrogradation and texture of cooked milled rice during storage. *Journal of Cereal Science*. 50(2): 139-144.

Zhou, Z., Robards, L, Helliwell, S., Blanchard, C., 2002. Ageing of stored rice: changes in chemical and physical attributes. *Journal of Cereal Science*. 35(1): 65-78.

Zhu, T., Jackson, D.S., Wehling, R.L., Geera, B., 2008. Comparison of amylose determination methods and the development of a dual wavelength iodine binding method. *Cereal Chemistry*. 85: 51-58.

Zhu, L.J., Liu, Q.Q., Wilson, J.D., Gu, M.H., Shi, Y.C., 2011. Digestibility and physiochemical properties of rice (Oryza sativa L.) flours and starches differing in amylose content. *Carbohydrate Polymers*. 86 (4): 1751-1759.